LONG-TERM ENVIRONMENTAL MONITORING PROGRAM

RESULTS AND INTERPRETATIONS FROM SAMPLING, 2008-2012

James R. Payne, Ph.D.
William B. Driskell
Mark G. Carls
Marie L. Larsen
Larry G. Holland

August 2013

PWSRCAC Contract No. 951.10.01

TABLE OF CONTENTS

List of Figures

List of Tables

Cover image - view from the mussel community at Disk Island, PWS, July 2013; logistics provided by Northwind Aviation, Homer. Photo by Bill Driskell.

ABBREVIATIONS

Stations:

AMT	Alyeska Marine Terminal, Port Valdez
AIB	Aialik Bay, west of Seward
COH	Constantine Harbor, Hinchinbrook Entrance, PWS
DII	Disk Island, Knight Island Group, western PWS
GOC	Gold Creek, Port Valdez
KNH	Knowles Head, eastern PWS
SHB	Sheep Bay, eastern PWS
SHH	Shuyak Harbor, Kodiak
SLB	Sleepy Bay, Latouche Island, western PWS
WIB	Windy Bay, Outer Kenai Peninsula
ZAB	Zaikof Bay, Montague Island, central PWS

ABL	NOAA/NMFS Auke Bay Laboratory, Juneau AK
AHC	aliphatic hydrocarbons (same as saturated hydrocarbons – SHC)
ANS	Alaskan North Slope
BWTF	Alyeska Terminal's Ballast Water Treatment Facility
DSI	Dissolved Signal Index
DW	Dry Weight
EVOS	*Exxon Valdez* oil spill
EVTHD	*Exxon Valdez* Trustees Hydrocarbon Database
EMAP	US EPA Environmental Monitoring and Assessment Program
GC/FID	gas chromatography/flame ionization detector
GC/MS	gas chromatography/mass spectrometry
GERG	Geochemical and Environmental Research Group, Texas A&M University
KLI	Kinnetic Laboratories, Inc., Anchorage AK
MDL	analytic method detection limit
NIST	National Institute of Standards and Technology
NMFS	National Marine Fisheries Service
NOAA	National Oceanographic and Atmospheric Administration
PAH	polycyclic (or polynuclear) aromatic hydrocarbons
PECI	Payne Environmental Consultants, Inc., Encinitas, CA
PGS	particle grain size
PSI	Particulate Signal Index
PWS	Prince William Sound
RCAC	Regional Citizens' Advisory Council
SAC	Scientific Advisory Committee for PWSRCAC
SCAT	Shoreline Cleanup Assessment Team
SHC	saturated hydrocarbons (same as AHC: n-alkanes + pristane and phytane)
SIM	selected ion monitoring
SRM	NIST standard reference material
TAHC	total AHC
TIC	total inorganic carbon
TOC	total organic carbon
TPAH	total PAH
TSHC	total saturated hydrocarbons (same as total alkanes)
UCM	unresolved complex mixture

1

REPORT FOR LTEMP 2008-2012

ABSTRACT

Petrogenic hydrocarbon inputs from the Alyeska Marine Terminal (AMT) and tanker operations are declining in mussels and sediments. The decrease likely reflects a combination of reduced ballast-water-treatment-facility (BTWF) discharge volumes from decreased North Slope oil production, the transition to double-hulled tankers with segregated ballast tanks, and improved BWTF efficiency at removing particulate/oil-phase polycyclic aromatic hydrocarbons (PAH) but also reflects an apparent regional decline evident in Knowles Head mussels. Composition is shifting away from petrogenic to pyrogenic in mussels and sediments; even the sediments at the terminal are beginning to look more like the background-reference, pyrogenic profiles at Gold Creek (GOC). Low levels of ANS oil are evident in Port sediments based on biomarkers; concentrations of these recalcitrant, source-specific indicators are seven times higher at AMT than GOC. Beyond Port Valdez, replicates at each of the seven remote sites show remarkable site fidelity in both PAH and saturated hydrocarbon (SHC) patterns, even at trace levels. Compared to 2004-05 West Coast Mussel Watch data and the more recent Alaskan Mussel Watch sites, LTEMP results for the Prince William Sound (PWS) and Gulf of Alaska (GOA) sites demonstrate that the region is exceptionally clean.

INTRODUCTION

In July 2008 and April 2009, all ten LTEMP stations (Figure 1) were visited in a sampling scheme designed, in part, to monitor for lingering impacts from the Exxon Valdez oil spill (EVOS). In subsequent years, the “grand round” sampling was reduced to only once every five years, and in Port Valdez and Knowles Head, the spring and fall collections were discontinued. Annual summer collections continued at the Port and nearby Knowles Head sites specifically monitoring terminal and tanker operations. This report summarizes findings for July 2008 through July 2012, a period comprising the previous contract’s final year (2008-2009) for visiting all sites plus years 1-4 of the current 5-year monitoring cycle. As appropriate, the results are presented with the overall perspective/trend analysis from the inception of the program. Next year’s report will cover the recently completed July 2013 visit to all sites and summarize the program’s results and findings since 1993. Some of these data have been previously presented in a 2011 interim data report (Driskell and Payne 2011).

METHODS

Collection and analytical methods have been described in previous LTEMP reports (Payne et al., 2008a, 2010a). Briefly, three replicates of mussels are collected by hand at each site while triplicate sediment samples are collected from two locations within the Port using a modified Van Veen grab. Sampling protocols have remained constant, and the NMFS Auke Bay Laboratory has continued with the analytical chemistry measurements using their Standard Operating Procedures (SOPs) as detailed in our previous reports.

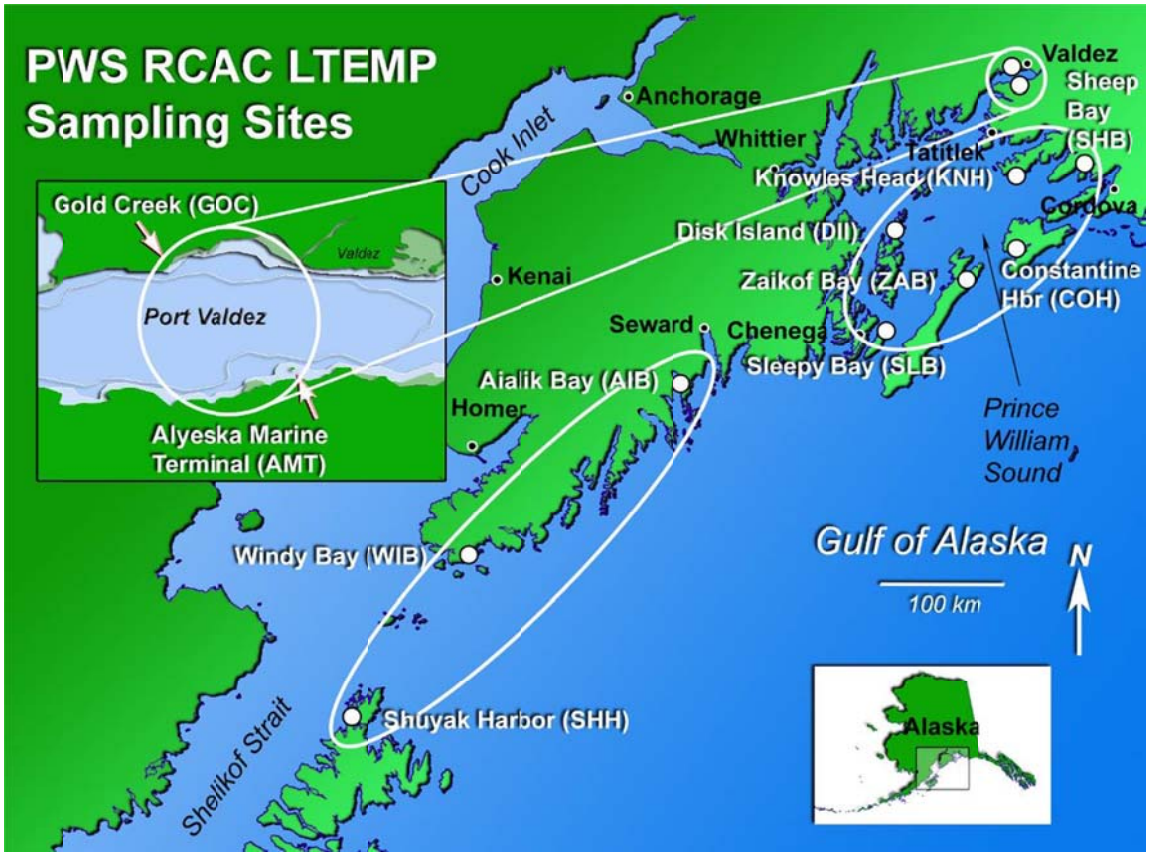

Figure 1 Map of the LTEMP sites. Circled regions represent sites with similar hydrocarbon signatures and events (discussed later).

New to this contract period is the inclusion of biomarkers for sediment samples along with the usual polycyclic aromatic hydrocarbons (PAH) and saturated hydrocarbon (SHC) data (Table 1). Petroleum biomarkers are unique for a given oil source and thus facilitate detection of AMT-derived, Alaska North Slope (ANS) crude-oil constituents in Port sediments. Since the inception of the program, low-level, combustion-derived PAH have been observed in the GOC sediments; oil-specific biomarkers would be much more useful at teasing out an ANS signal against the Port's glacial and pyrogenic inputs than the ubiquitous PAH. The biomarkers would not be as effective for the mussel tissues since unlike the accumulating sediments, mussels regularly purge and at most stations are currently only carrying trace-level, dissolved components.

Table 1 List of polycyclic aromatic hydrocarbon (PAH), saturated hydrocarbon (SHC), and biomarkers analytes in this study, along with analyte abbreviations used in figures throughout this report, and internal and surrogate standards.

ANALYTES	Abbreviation	Internal Standard	Surrogate Standard
PAH			
Naphthalene	N	A	1
C1-Naphthalene	N1	A	1
C2-Naphthalene	N2	A	2
C3-Naphthalene	N3	A	2
C4-Naphthalene	N4	A	2

ANALYTES	Abbreviation	Internal Standard	Surrogate Standard
Biphenyl	BI	A	2
Acenaphthylene	AC	A	2
Acenaphthene	AE	A	2
Fluorene	F	A	2
C1-Fluorenes	F1	A	2
C2-Fluorenes	F2	A	2
C3-Fluorenes	F3	A	2
Dibenzothiophene	D	A	3
C1-Dibenzothiophene	D1	A	3
C2-Dibenzothiophene	D2	A	3
C3-Dibenzothiophene	D3	A	3
C4-Dibenzothiophene	D4	A	3
Anthracene	A	A	3
Phenanthrene	P	A	3
C1-Phenanthrene/Anthracene	PA1	A	3
C2-Phenanthrene/Anthracene	PA2	A	3
C3-Phenanthrene/Anthracene	PA3	A	3
C4-Phenanthrene/Anthracene	PA4	A	3
Fluoranthene	FL	A	3
Pyrene	PYR	A	3
C1-Fluoranthene/Pyrene	FP1	A	3
C2-Fluoranthene/Pyrene	FP2	A	3
C3-Fluoranthene/Pyrene	FP3	A	3
C4-Fluoranthene/Pyrene	FP4	A	3
Benzo(a)Anthracene	BA	A	4
Chrysene	C	A	4
C1-Chrysenes	C1	A	4
C2-Chrysenes	C2	A	4
C3-Chrysenes	C3	A	4
C4-Chrysenes	C4	A	4
Benzo(b)fluoranthene	BB	A	5
Benzo(k)fluoranthene	BK	A	5
Benzo(e)pyrene	BEP	A	5
Benzo(a)pyrene	BAP	A	5
Perylene	PER	A	6
Indeno(1,2,3-cd)pyrene	IP	A	5
Dibenzo(a,h)anthracene	DA	A	5
Benzo(g,h,i)perylene	BP	A	5
Total PAH	**TPAH**		**5**

Saturated hydrocarbons (SHC or n-alkanes)

n-Decane	C10	B	7
n-Undecane	C11	B	7
n-Dodecane	C12	B	7
n-Tridecane	C13	B	7

ANALYTES	Abbreviation	Internal Standard	Surrogate Standard
n-Tetradecane	C14	B	8
n-Pentadecane	C15	B	8
n-Hexadecane	C16	B	8
n-Heptadecane	C17	B	8
Pristane	Pristane	B	8
n-Octadecane	C18	B	9
Phytane	Phytane	B	9
n-Nonadecane	C19	B	9
n-Eicosane	C20	B	9
n-Heneicosane	C21	B	9
n-Docosane	C22	B	10
n-Tricosane	C23	B	10
n-Tetracosane	C24	B	10
n-Pentacosane	C25	B	10
n-Hexacosane	C26	B	10
n-Heptacosane	C27	B	10
n-Octacosane	C28	B	10
n-Nonacosane	C29	B	11
n-Triacontane	C30	B	11
n-Hentriacontane	C31	B	11
n-Dotriacontane	C32	B	11
n-Tritriacontane	C33	B	11
n-Tetratriacontane	C34	B	11
Total n-Alkanes	TALK		

Calibrated analytes are identified by boldface. Internal standards:
A = hexamethylbenzene; B = dodecylcyclohexane.
Surrogate standards: 1 = naphthalene-d8, 2 = acenaphthene-d10,
3 = phenanthrene-d10, 4 = chrysene-d12, 5 = benzo[a]pyrene-d12,
6 = perylene-d12, 7 = dodecane-d26, 8 = hexadecane-d34, 9 = eicosane-d42,
10 = tetracosane-d50, and 11 = triacontane-d62.

47 **Petroleum Biomarkers**

Class	Biomarker	Abbrev
Terpanes	C23 tricyclic terpane	T4
	C24 tricycilic terpane	T5
	C25 tricyclic terpane (a)	T6
	C25 tricyclic terpane (b)	T6
	C24 tetracyclic terpane	T6a
	C26 tricyclic terpane (a)	T6c
	C26 tricyclic terpane (b)	T6b
	C28 tricyclic terpane (a)	T8
	C28 tricyclic terpane (b)	T7
	C29 tricyclic terpane (a)	T10
	C29 tricyclic terpane (b)	T9

Hopanes	18α(H),21β(H)-22,29,30-trisnorhopane	Ts
	17α(H),21β(H)-22,29,30-trisnorhopane	Tm
	17α(H),18α(H),21β(H)-28,30-bisnorhopane	14a
	17α(H),21β(H)-25-norhopane	14b
	17α(H),21β(H)-30-norhopane	T15
	18α(H),21β(H)-30-norneohopane	T16
	17β(H),21α(H)-30-norhopane (normoretane)	T17
	18α(H) and 18β(H)-oleanane	T18
	17α(H),21β(H)-hopane	T19
	17α(H)-30-nor-29-homohopane	
	17β(H),21α(H)-hopane (moretane)	T20
	22S-17α(H),21β(H)-30-homohopane	T21
	22R-17α(H),21β(H)-30-homohopane	T22
	Gammacerane	T22a
	22S-17α(H),21β(H)-30,31-bishomohopane	T26
	22R-17α(H),21β(H)-30,31-bishomohopane	T27
	22S-17α(H),21β(H)-30,31,32-trishomohopane	T30
	22R-17α(H),21β(H)-30,31,32-trishomohopane	T31
	22S-17α(H),21β(H)-30,31,32,33-tetrakishomohopane	T32
	22R-17α(H),21β(H)-30,31,32,33-tetrakishomohopane	T33
	22S-17α(H),21β(H)-30,31,32,33,34-pentakishomohopane	T34
	22R-17α(H),21β(H)-30,31,32,33,34-pentakishomohopane	T35
Steranes	C22 5α(H),14β(H),17â(H)-sterane	
	C27 20S-13β(H),17α(H)-diasterane (diacholestane)	S4
	C27 20R-13β(H),17α(H)-diasterane (diacholestane)	S5
	C27 20S-5α(H),14α(H),17α(H)-cholestane	S12
	C27 20R-5α(H),14β(H),17β(H)-cholestane	S14
	C27 20S-5α(H),14β(H),17β(H)-cholestane	S15
	C27 20R-5α(H),14α(H),17α(H)-cholestane	S17
	C28 20S-5α(H),14α(H),17α(H)-ergostane (methylcholestane)	S20
	C28 20R-5α(H),14β(H),17β(H)-ergostane (methylcholestane)	S22
	C28 20S-5α(H),14β(H),17β(H)-ergostane (methylcholestane)	S23
	C28 20R-5α(H),14α(H),17α(H)-ergostane (methylcholestane)	S24
	C29 20S-5α(H),14α(H),17α(H)-stigmastane (ethylcholestane)	S25
	C29 20R-5α(H),14β(H),17β(H)-stigmastane (ethylcholestane)	S26
	C29 20S-5α(H),14β(H),17β(H)-stigmastane (ethylcholestane)	S27
	C29 20R-5α(H),14α(H),17α(H)-stigmastane (ethylcholestane)	S28

48

RESULTS AND DISCUSSION

As in previous LTEMP reports, all analytes are reported on a ng/g dry weight (DW) basis, and corrected for surrogate recoveries. Surrogates are novel or deuterated compounds added in known amounts to each sample in order to assess the efficiency of extraction and analysis. In the Auke Bay Laboratory SOPs, surrogate recoveries are considered acceptable if they are between 30% and 120%. If more than 10 recoveries from an entire string (analytic batch) fall outside the recovery targets, the string fails QA criteria and is reprocessed. If the majority of the failed recoveries occur in an individual sample, only that sample is reprocessed. Surrogate recovery standards were met for 95.1% of all surrogate hydrocarbons analyzed during this reporting period. For the new biomarker analytes, median surrogate recovery was 114.4% for 36 analyses. For different QA reasons, the 2009 sediment batch was re-extracted and reanalyzed.

Laboratory method blanks for each analytic sample batch demonstrated no significant background interference from analytical procedures, thus assuring that the analytes in the field samples represented environmental constituents and not analytical artifacts. In addition, new method detection limits (MDLs), established in 2010, dramatically improved the confidence in accurately quantifying low-level PAH. Dropping an order of magnitude below previous MDLs, PAH limits are now down to a miniscule median 0.04 ng/g dry weight in sediments and 0.8 ng/g dry weight in tissues (Table 2). Likewise, MDLs for SHC dropped to a median 0.5 ng/g dry weight in sediments and 21 ng/g dry weight in tissues.

Table 2 Historic and current method detection limits (MDL) for quantifying hydrocarbon analytes at Auke Bay Laboratory. All values in ng/g dry weight (based on average 2008-2012 dry wt/wet wt measurements).

		Tissue				Sediment		
Analyte	**Abbrev**	**1993**	**1996**	**2010**		**1993**	**1996**	**2010**
naphthalene	N	24.4	19.1	1.9		0.98	2.48	0.06
2-methylnaphthalene		11.0	12.1	1.1		0.90	1.44	0.06
1-methylnaphthalene		14.6	31.4	1.0		1.98	1.08	0.06
2,6-dimethylnaphthalene		7.8	6.3	0.8		1.88	0.71	0.04
2,3,5-trimethylnaphthalene		4.7	7.6	0.7		0.90	0.37	0.02
biphenyl*	BI	8.3	26.6	20.7		4.13	0.90	0.19
acenaphthylene	AC	6.3	21.3	1.0		2.40	0.73	0.04
acenaphthene	AE	6.0	8.7	0.4		1.17	0.54	0.04
fluorene	F	5.6	19.7	1.3		1.75	1.31	0.04
dibenzothiophene	DBT	3.9	12.7	0.6		0.92	0.44	0.04
phenanthrene	P	9.2	12.3	0.8		1.29	0.71	0.02
1-methylphenanthrene		6.2	28.1	0.9		2.62	0.56	0.02
anthracene	A	7.2	9.9	0.9		3.19	0.50	0.02
fluoranthene	FL	13.1	23.1	0.8		0.88	0.44	0.02
pyrene	PYR	10.9	23.8	0.8		1.00	0.38	0.02
benzo(a)anthracene	BAA	4.8	8.2	0.3		0.33	0.31	0.04
chrysene	C	6.1	13.1	0.6		2.54	0.81	0.02
benzo(b)fluoranthene	BBF	6.7	37.6	0.6		1.17	0.46	0.08

benzo(k)fluoranthene	BKF	8.7	18.6	0.9		0.77	0.35	0.08
Benzo(e)pyrene	BEP	9.1	22.1	0.7		1.15	0.60	0.06
Benzo(a)pyrene	BAP	7.2	17.8	1.1		3.10	0.44	0.02
Perylene	PER	10.4	25.0	5.1		1.12	0.98	0.02
Indeno(1,2,3-cd)pyrene	IND	4.9	11.8	0.4		0.65	0.38	0.06
dibenzo(a,h)anthracene	DBA	4.2	14.7	0.3		0.48	0.35	0.06
benzo(ghi)perylene	BGHI	6.1	41.0	0.6		0.90	0.77	0.02
						0.00	0.00	0.00
min		3.9	6.3	0.3		0.33	0.31	0.02
max		24.4	41.0	20.7		4.13	2.48	0.19
median		7.2	18.6	0.8		1.15	0.56	0.04
extracted sample mass (g wet weight)		10	8	10		20	40	40
n-nonane	C9			20				0.97
n-decane	C10	186	643	31		5.9	6.7	0.52
n-undecane	C11	109	523	39		4.3	7.9	0.90
n-dodecane	C12	71	305	39		6.4	7.7	2.10
n-tridecane	C13	143	211	91		5.5	13.3	1.69
n-tetradecane	C14	272	284	38		4.3	15.5	1.58
n-pentadecane	C15	251	214	21		19.4	16.6	1.06
n-hexadecane	C16	394	168	14		8.5	18.7	0.58
n-heptadecane	C17	526	166	16		10.9	17.5	0.27
pristane	Prist	283	159	32		20.2	15.5	0.38
n-octadecane	C18	204	99	7		23.3	27.3	0.44
phytane	Phyt	204	98	8		23.3	19.2	0.50
n-nonadecane	C19	240	76	6		5.3	6.9	0.23
n-eicosane	C20	274	56	7		10.4	8.1	0.12
n-heneicosane	C21	201	38	7		9.1	8.1	0.19
n-docosasne	C22	75	60	13		6.0	8.3	0.21
n-tricosane	C23	149	52	9		21.3	8.1	0.62
n-tetracosine	C24	172	49	24		33.7	10.4	0.44
n-pentacosane	C25	101	25	15		7.3	8.6	0.27
n-hexacosane	C26	104	84	18		20.4	6.3	0.50
n-heptacosane	C27	196	78	32		16.4	5.1	0.31
n-octacosane	C28	179	137	30		13.5	16.9	0.44
n-nonacosane	C29	332	111	18		14.7	7.7	0.40
n-triacontane	C30	219	175	20		17.9	4.5	1.10
n-hentriacontane	C31	0	0	26		0.0	0.0	0.40

n-dotriacontane	C32	153	394	21		23.3	11.6	0.42
n-tritriacontane	C33	0	0	83		0.0	0.0	0.98
n-tetratriacontane	C34	89	407	99		13.9	57.3	2.92
n-pentatriacontane	C35	0	0	127		0.0	0.0	5.15
n-hexatriacontane	C36	0	0	134		0.0	0.0	7.00
min		71	25	6		4.3	4.5	0.12
max		526	643	134		33.7	57.3	7.00
median		196	137	21		13.5	8.6	0.50
extracted sample mass (g wet weight)		8	8	10		20	40	40

* Biphenyl is sometimes encountered as a laboratory artifact (as it was during the MDL study) thereby elevating the MDL for this constituent compared to the other analytes. It is not utilized to a great extent in the LTEMP data analysis.

PORT VALDEZ SEDIMENTS

In sediments from the Berth 4 site at the Alyeska Marine Terminal (AMT), average TPAH levels are very low, plateaued around 50-60 ng/g DW since March 2005 (Figure 2), but there has been a shift in the patterns. PAH patterns (examples in Figure 3; all samples in Appendix 1) suggest that the higher-molecular-weight PAH became more pyrogenic (i.e. from combustion sources, less petrogenic) starting in July 2009. A pyrogenic pattern is recognized by the dominant parent PAH relative to the alkylated homologues (e.g., in the bottom of Figure 3, the Ph, Fl and C are the non-alkylated parents); in petrogenic signatures, the analyte groups form a hump pattern in which the parent PAH no longer dominates. In the SHC plots, by the next year, July 2010, petrogenic alkanes begin to diminish relative to odd-carbon-numbered biogenic n-alkanes (C_{25}, C_{27}, C_{29}) derived from terrestrial plant waxes. By 2011, the intermediate-molecular-weight PAH (fluorenes and phenanthrenes/anthracenes) also became more pyrogenic in character with the SHC still dominated by biogenic constituents.

The Gold Creek reference site (GOC) sediments had lower TPAH concentrations than AMT throughout the duration of the program (Payne et al., 2008b) excepting two spill events (Figure 2), most recently with extremely low concentrations, 15-60 ng/g DW. GOC PAH profiles were dominated by pyrogenics (Payne et al., 2008a,b; 2010a) from April 2000 through this 2008-2012 reporting period (see Figure 4 and Appendix 1). In addition to the higher-molecular-weight pyrogenic PAH, Gold Creek sediments also contain a dominant and invariant suite of N_0-N_4 naphthalenes that are believed to derive from glacial and riverine sediment input to the Port (Payne et al. 2010a,b). SHC in the sediments are almost exclusively dominated by biogenic sources from marine phytoplankton and terrestrial plant waxes (i.e., n-C_{15}, n-C_{17}, pristane, and an odd-carbon-numbered suite of n-alkanes between n-C_{23} and n-$C_{33,}$ respectively).

In comparing the AMT and GOC sediment profiles, it is interesting that as the petrogenic profiles at AMT are disappearing, by July 2012 its signatures (Figure 3 bottom) begin to resemble the Gold Creek reference sediments (Figure 4). Only traces of the higher-molecular-weight petroleum waxes (> n-C_{32}) remain whereas they used to dominate the SHC profiles (Payne et al., 2008a,b).

In our 2010 LTEMP report (Payne et al., 2010a), we cautioned that at extremely low concentrations using our algorithmic PAH source-phase assignment model is problematic whereby a very minute change in a trace pattern could flip a phase assignment. For the 2008-2012 data where nearly all patterns at trace levels and near MDLs, we've abandoned that approach in favor of pattern descriptions and graphics. We also include the interpretations of Mark Carls (Appendix 3) in which he's applied a multivariate scoring procedure (Carls, 2006) to assign type and sources. His results generally corroborate what we're seeing in the histogram patterns.

We also noted that without biomarker data, attributing the very minor petrogenic signal observed in Gold Creek sediments to Alyeska Marine Terminal discharges would be confounded. From their 2005 EMP biomarker data, Shaw et al. (2005) concluded that EMP Stations 40 and 50 (near Gold Creek but at greater depths in the Port) contained petrogenic components derived from Alaska North Slope crude oil. To confirm this finding that our data only hinted at, a suite of biomarkers was added to the sediment analyte list with the 2009-2014 LTEMP contract.

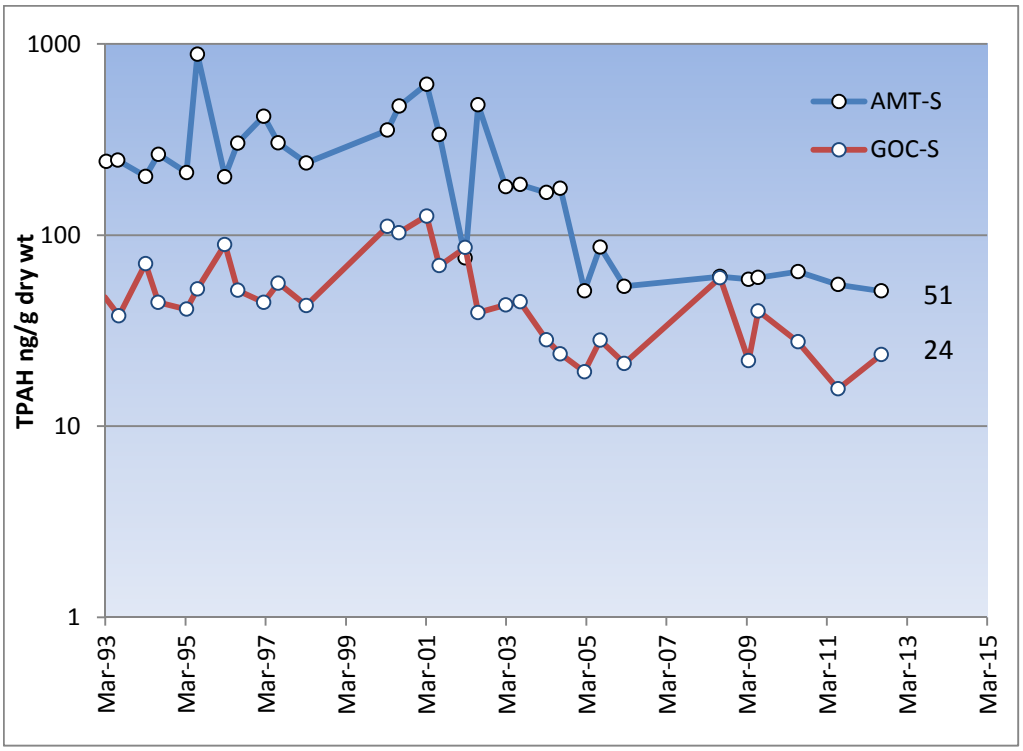

105

106 Figure 2 Time series of TPAH in sediments at Alyeska Terminal and Gold Creek.

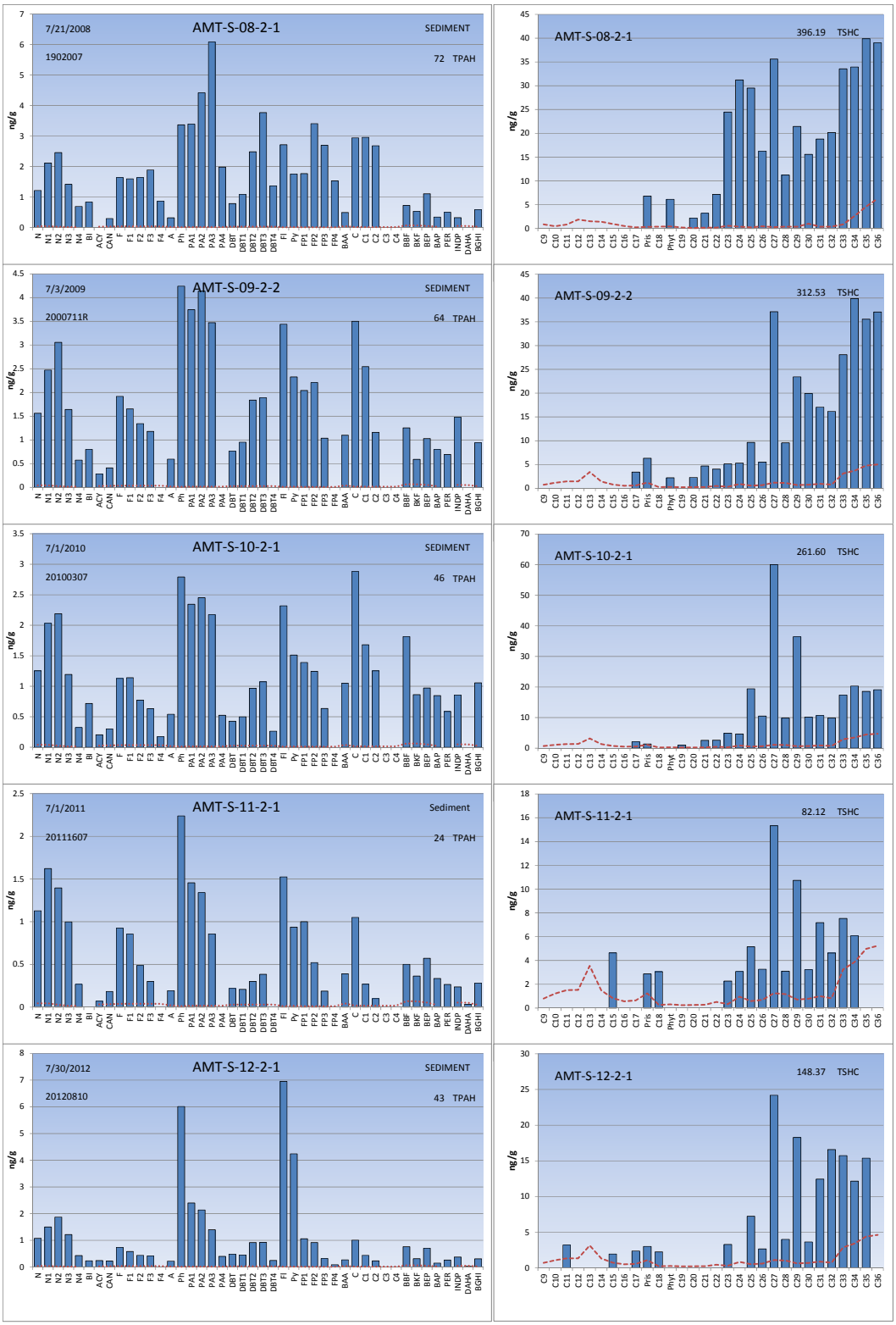

Figure 3 Example PAH and SHC signatures of sediments at Alyeska Terminal between July 2008 and July 2012 showing the progression from a primarily petrogenic to pyrogenic PAH signature with increasing terrestrial biogenic SHC and decreasing higher-molecular-weight n-alkane residuals. Red dashed line is sample-specific MDL. Sample ID code comprises station-matrix-year-season-rep.

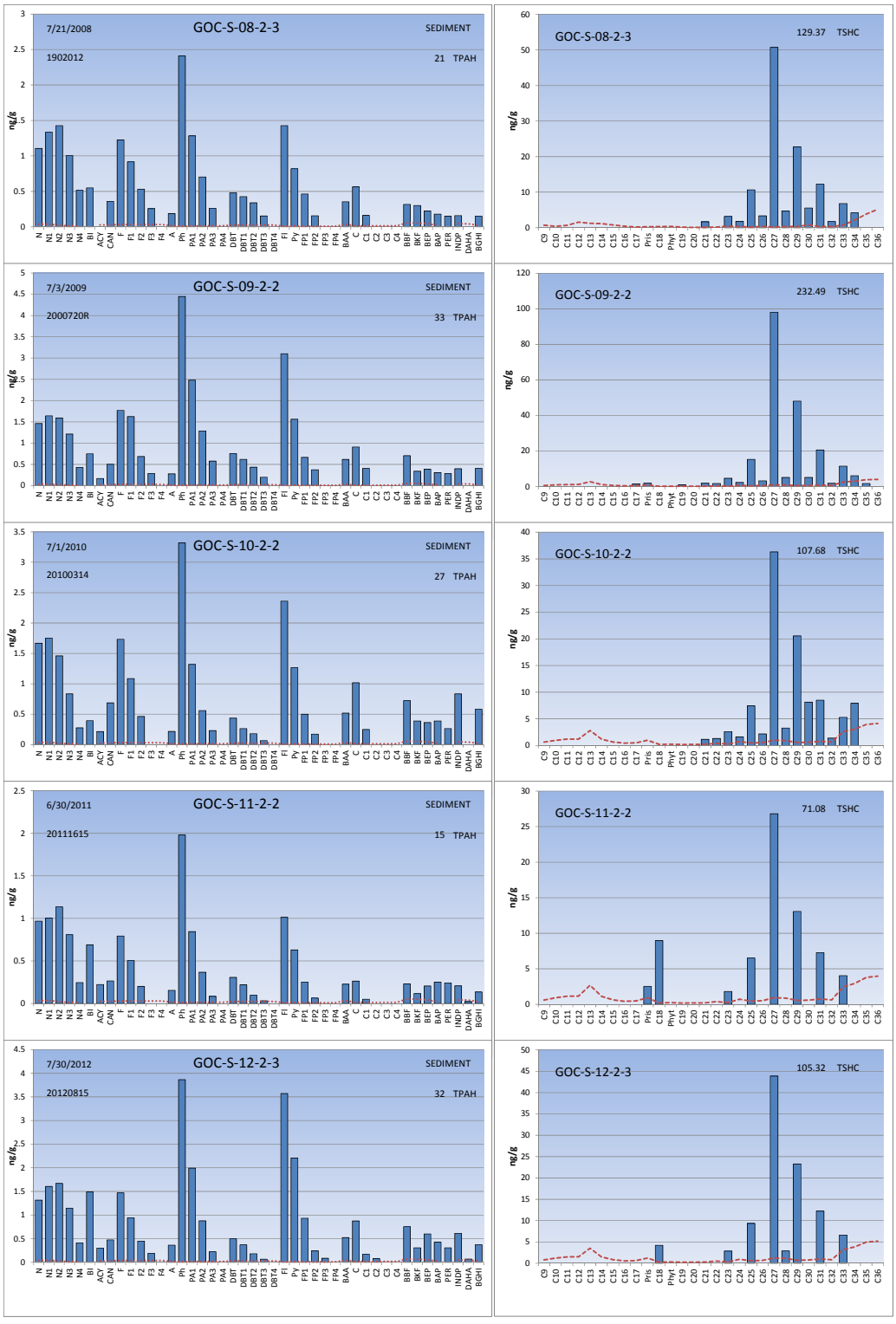

Figure 4 Example PAH and SHC signatures of sediments at Gold Creek between July 2008 and July 2012 showing the essentially invariant background naphthalene components and pyrogenic, parent-dominated, PAH. SHC patterns reflect constant terrestrial and marine biogenic input. Red dashed line is sample-specific MDL.

Sediment Biomarkers

At our request, in 2011, the Auke Bay Laboratory (ABL) modified their analytical procedures to report petroleum biomarkers. The method is an extension to the normal GC/MS 8270 method used to acquire PAH data; conceptually, three new ions are added to the mass spectrometer's list for selective ion monitoring (SIM). As a lab calibration standard, ABL runs the original *Exxon Valdez* oil (from the ship's hold, an ANS crude oil), in addition to a NIST standard reference material (SRM). But there are no certified standard values for biomarkers in these oils; we can only compare ABL results to other lab results for validation. We've done this for both ANS and Deepwater Horizon oils (also analyzed at ABL and now a NIST standard). The results are favorable; ABL's ANS reference oil results compare quite well with published ANS results (Figure 5); however, the lab has issues separating the triplet T6 terpane compounds, T6a, T6b and T6c (identified as peaks 8, 9 & 10 (Figure 5 center). This is unfortunate since the triplets are often used as diagnostic markers. In ABL-quantified plots of the field samples (Figure 6), there also seem to be deficits in the mid-terpane analytes (left third of the plot) but with this small number of samples from only two locations (and only two analytic strings), it is difficult to know, at this stage, if these results reflect actual environmental conditions or analytic artifacts. It is also possible that the biomarker patterns for ANS crude oil have changed slightly since 1989 as oil from several new North Slope fields are blended into the pipeline mixture. More samples of ANS oil are being requested from Alyeska to assess the PAH and biomarker composition of the current blend. Presumably, this will also reflect the biomarker composition in oil residues in the treated ballast water currently being discharged into the Port.

Multiple approaches have been suggested for interpreting biomarker data but some degree of expert-guided pattern matching must be employed. Most approaches involve various diagnostic ratios (Wang and Stout, 2007) with several ratios normalized on the highly conservative 17α(H),21β(H)-hopane (also labeled T19 or C30 hopane). But depending on the local environs and despite the purported persistence of biomarkers, all ratios are not equally effective and must be individually evaluated for a given spill/habitat. With LTEMP data, we initially screened results graphically with an overlaid ANS reference (Figure 6). We then used the frequently reliable, Ts/Tm and norhopane (T15)/hopane plus a suggested 22R homohopane (T22)/hopane ratios to confirm the visual similarities. Normally, the T6 triplets ratio also would be added to this list but not if the lab is having analytic issues. The final suite of diagnostic ratios can then be the basis for a rigorous methodology advocated by European agencies (NordTest plots) or adapted for other multivariate approaches (various authors in Wang & Stout, 2007). Mark Carls is currently exploring a novel scoring method.

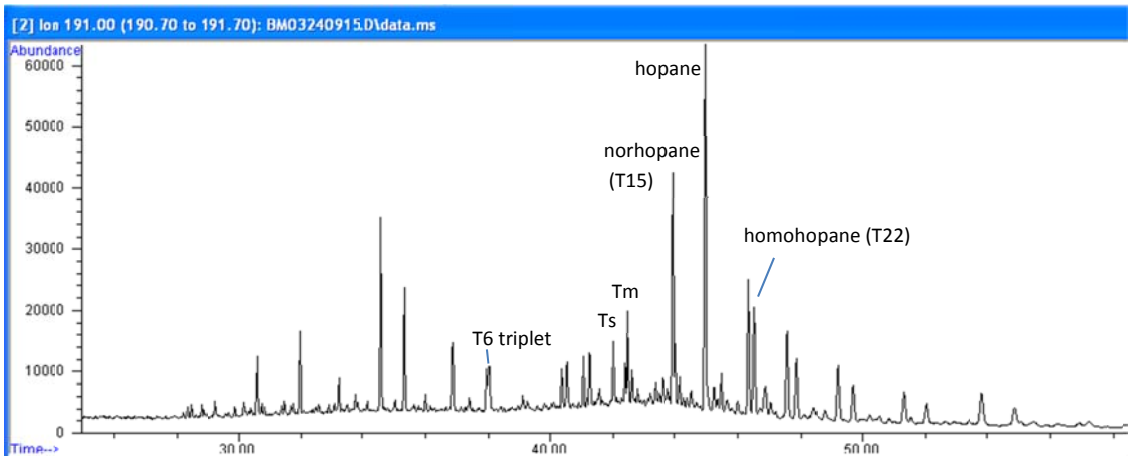

145

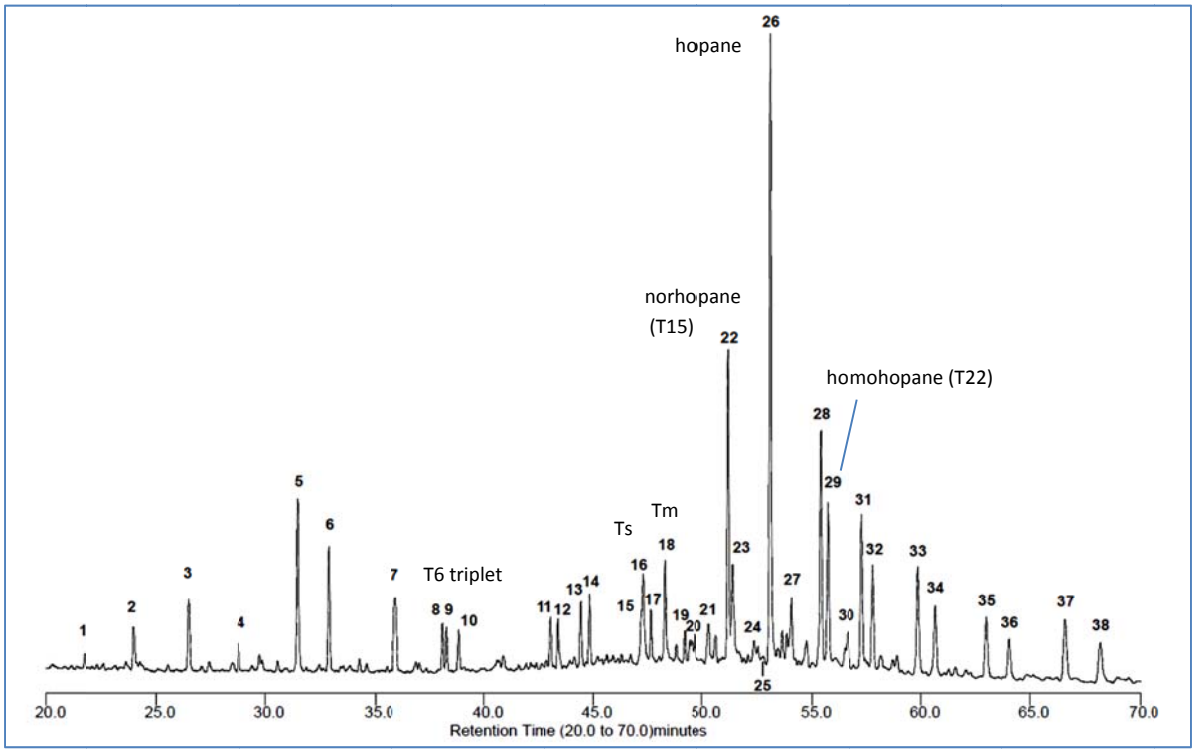

146

1	C19 Tricyclic terpane	14	C29 [22R] Tricyclic terpane	27	17b21a Moretane [C30]
2	C20 Tricyclic terpane	15	C30 [22S] Tricyclic terpane	28	22S Homohopane [C31]
3	C21 Tricyclic terpane	16	18a Trisnorneohopane [C27 Ts]	29	22R Homohopane [C31]
4	C22 Tricyclic terpane	17	C30 [22R] Tricyclic terpane	30	Gammacerane [C30]
5	C23 Tricyclic terpane	18	17a Trisnorneohopane [C27 Tm]	31	22S Bishomohopane [C32]
6	C24 Tricyclic terpane	19	C31 [22S] Tricyclic terpane	32	22R Bishomohopane [C32]
7	C25 Tricyclic terpane	20	C31 [22R] Tricyclic terpane	33	22S Trishomohopane [C33]
8	C26 [22S] Tricyclic terpane	21	Bisnorhopane [C28]	34	22R Trishomohopane [C33]
9	C26 [22R] Tricyclic terpane	22	Norhopane [C29]	35	22S Tetrakishomohopane [C34]
10	C24 Tetracyclic terpane	23	18a Neonorhopane [C29]	36	22R Tetrakishomohopane [C34]
11	C28 [22S] Tricyclic terpane	24	17b21a Normoretane [C29]	37	22S Pentakishomohopane [C35]
12	C28 [22R] Tricyclic terpane	25	Oleanane [C30]	38	22R Pentakishomohopane [C35]
13	C29 [22S] Tricyclic terpane	26	Hopane [C30]		

147

148 Figure 5 GC/MS m/z 191 ion traces for ANS reference oil from Auke Bay Laboratory (upper plot) and a similar North Slope oil
149 (lower plot) (Lilis et al., 1998) demonstrating comparability of detection.

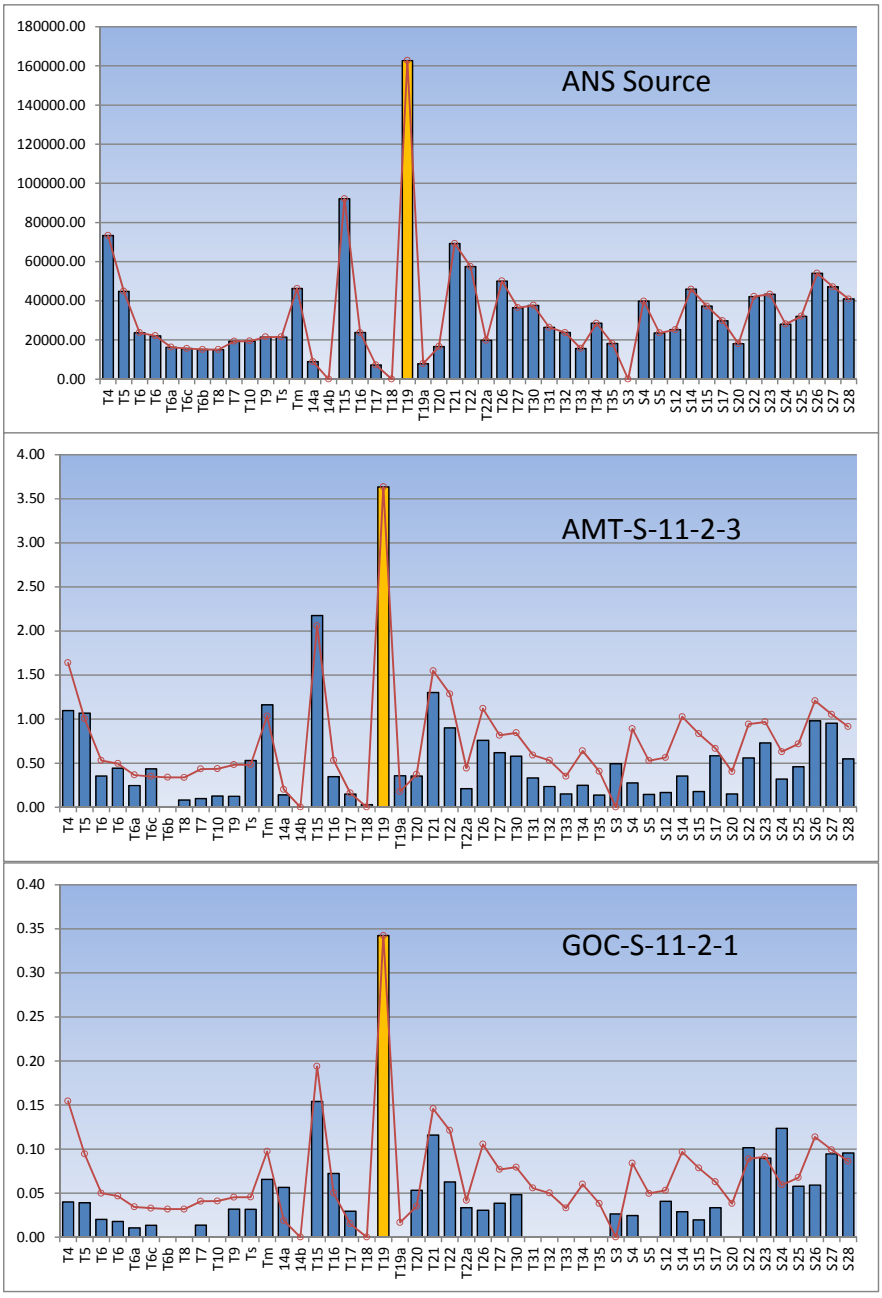

Figure 6 Representative ABL-quantified biomarker plots of EVOS (ANS) Crude Oil standard (top), AMT sediments from July 2011 (center), and GOC sediments from July 2011 (bottom). Red line denotes ANS reference normalized to the sample's hopane (highlighted in gold).

From the 2011 and 2012 LTEMP collections, eighteen samples were analyzed. Visual inspection of individual plots for sediment biomarkers and their associated diagnostic ratios (Appendix 2) show general agreement by stations and across sampling years. The AMT sites are consistently similar to the ANS reference profile in the mid-hopane suite of analytes (Ts through T22) (Figure 6). At GOC, the "fit" is similar but looser, and there are more non-detected analytes because the concentrations of biomarkers are lower (total biomarkers avg: 31.0 ng/g DW at AMT vs. 4.4 at GOC). Thus, there are some concerns with detection limits. However, even with a looser fit, the

selected GOC ratios are in agreement with the reference (Figure 7) for the three selected diagnostic ratios (T22, T15 and Ts/Tm), and when GOC's total biomarker concentrations peak (GOC-S-11-2-1D, 7.1 ng/g DW and GOC-S-12-2-1, 9.5 ng/g DW), the fit is excellent (Appendix 2).

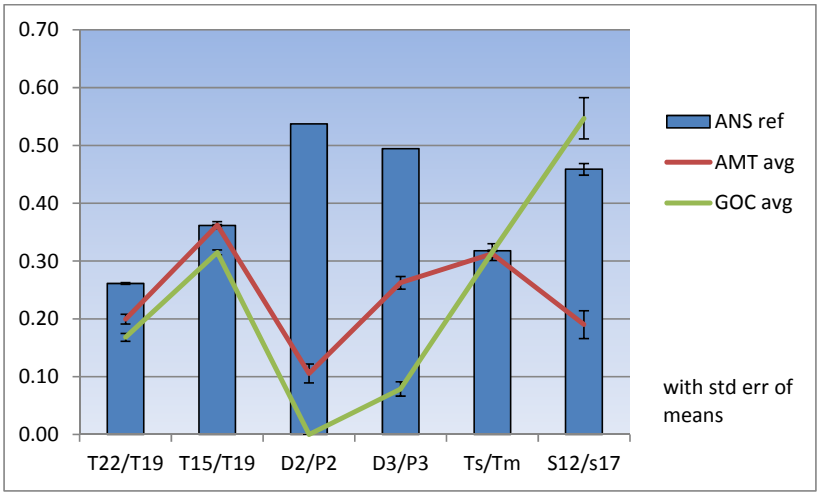

Figure 7 Comparison of average GOC and AMT diagnostic ratios with ANS reference. Only the three best ratios were used for final evaluations.

Plotting the diagnostic ratios in 3D space (Figure 8) shows samples clustering by station. Both stations differ from the EVOS-era ANS reference (in pink) with AMT (spheres) being more similar (closer) to the reference. Also note that GOC tends to remain tightly clustered across years (in these three parameters), more so than at AMT, which surprisingly suggests more a variable background influence in the AMT biomarker signature. Additional reference samples (described below) are also shown.

In these plots, the primary distinction between stations is driven by norhopane (T15) levels. But these are just the fine-scale differences; overall, these profiles are significantly different from two other petrogenic sources found in the Sound. As depicted by Bence et al. (1996) (Figure 9), the ANS-origin EVOS oil differs from Katalla and Yakataga regional sources east of PWS, primarily by the absence of the oleanane biomarker (seen just before the C30 hopane) plus various subtler differences (e.g., note Ts and Tm proportions in all non-EVOS plots). In the Gulf of Alaska, the Katalla/Yakataga materials become finely fragmented and get transported westward by Gulf currents eventually reaching all the way to Shelikof Straits and down the Alaska Peninsula but with some deposited in the PWS basin to become the much disputed (during-EVOS-era) PWS background. Also found in intertidal regions of the Sound are tarballs from Monterey formation oil (Kvenvolden et al., 1995), remnants from oil spilled during the 1964 earthquake. Imported in the pre-pipeline era from California, Monterey oil is also distinct from ANS oil by its inclusion of both oleanane and 28,30-bisnorhopane (just before norhopane Figure 9). Oleanane comes from the flowering angiosperms which only appeared in the later Triassic formations; apparently the North Slope deposits never saw the bloom. In one of the eighteen LTEMP sediment samples, a trace level of oleanane was detected, again confirming that like the dispersion seen in the 3D plots, the biomarker patterns represent mixtures with other background biomarker sources.

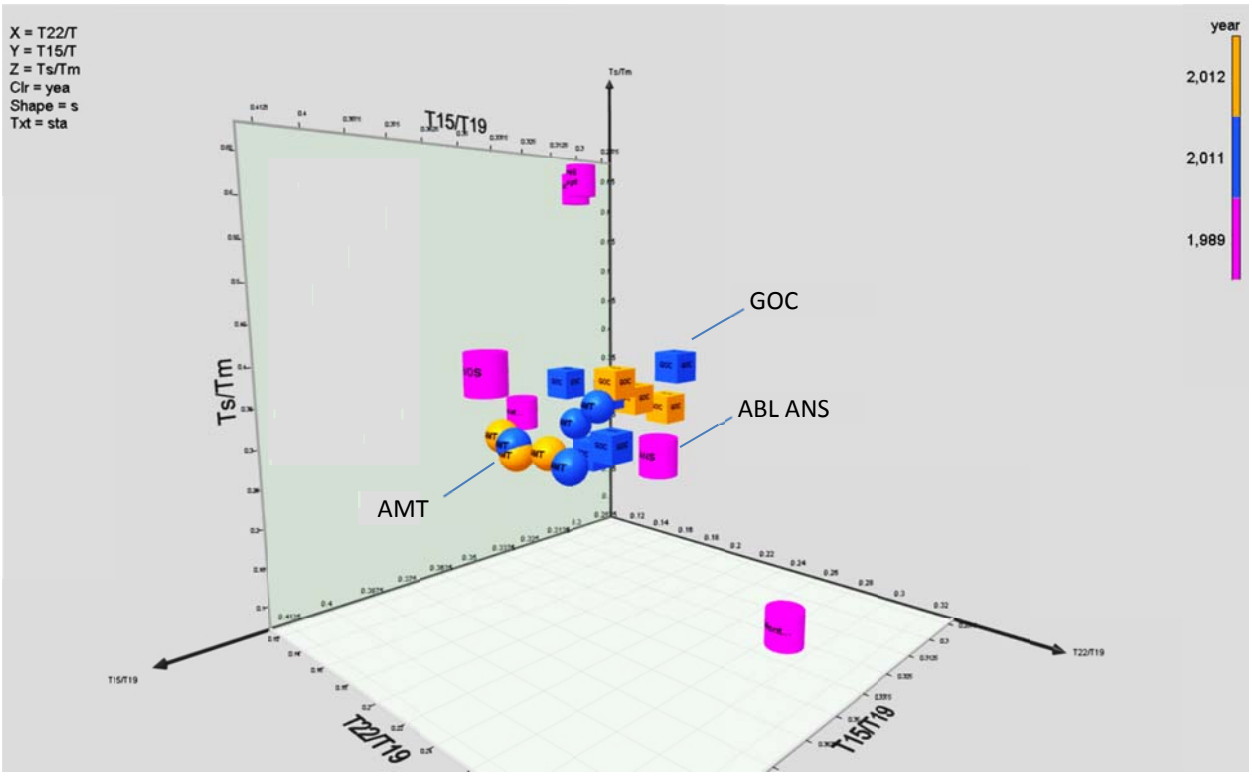
X = T22/T
Y = T15/T
Z = Ts/Tm
Clr = yea
Shape = s
Txt = sta
year
2,012
2,011
1,989
GOC
ABL ANS
AMT
Ts/Tm
T15/T19
T22/T19

186

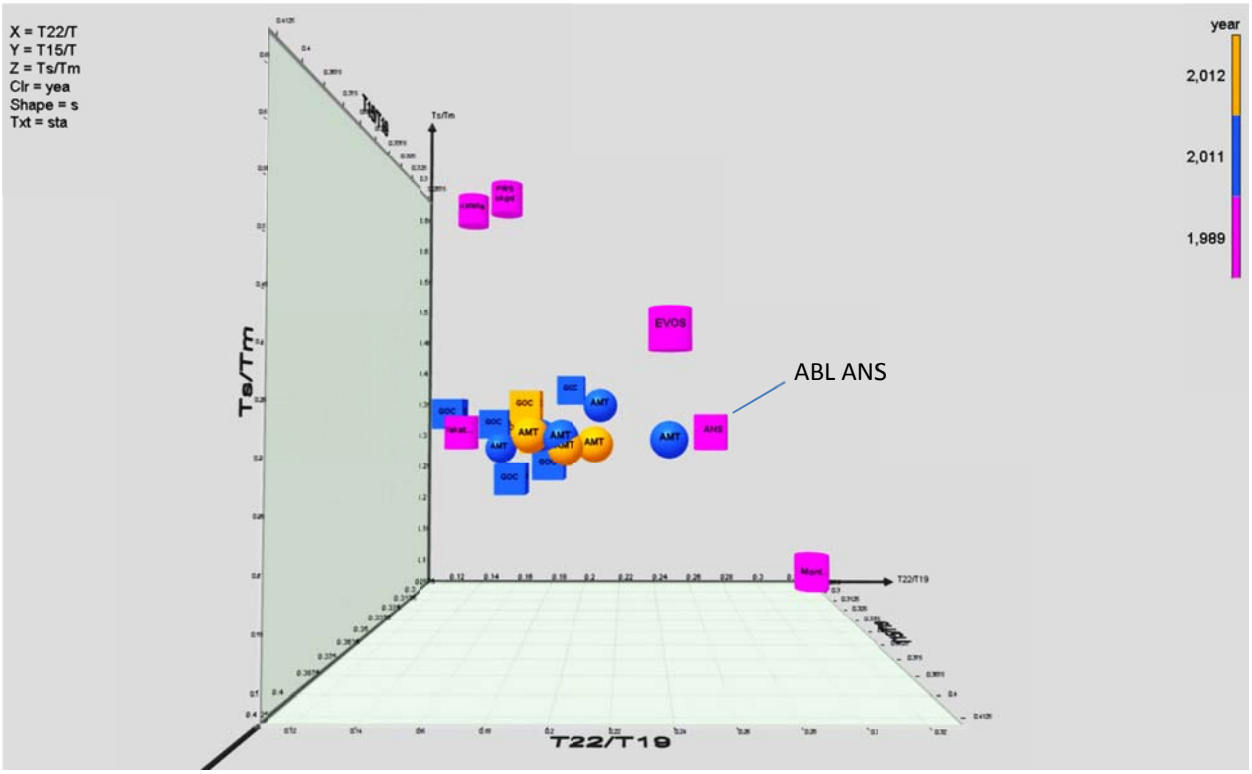
X = T22/T
Y = T15/T
Z = Ts/Tm
Clr = yea
Shape = s
Txt = sta
year
2,012
2,011
1,989
EVOS
ABL ANS
AMT
GOC
ANS
Ts/Tm
T22/T19

187

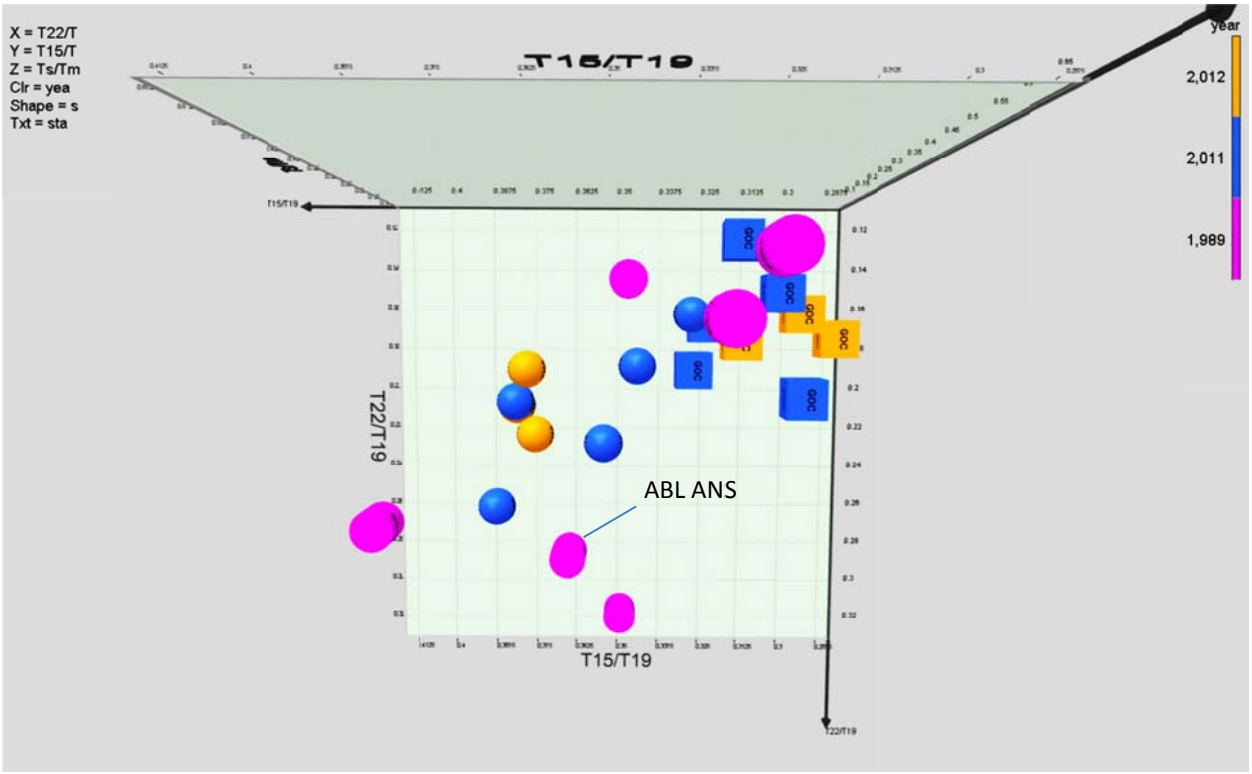

188

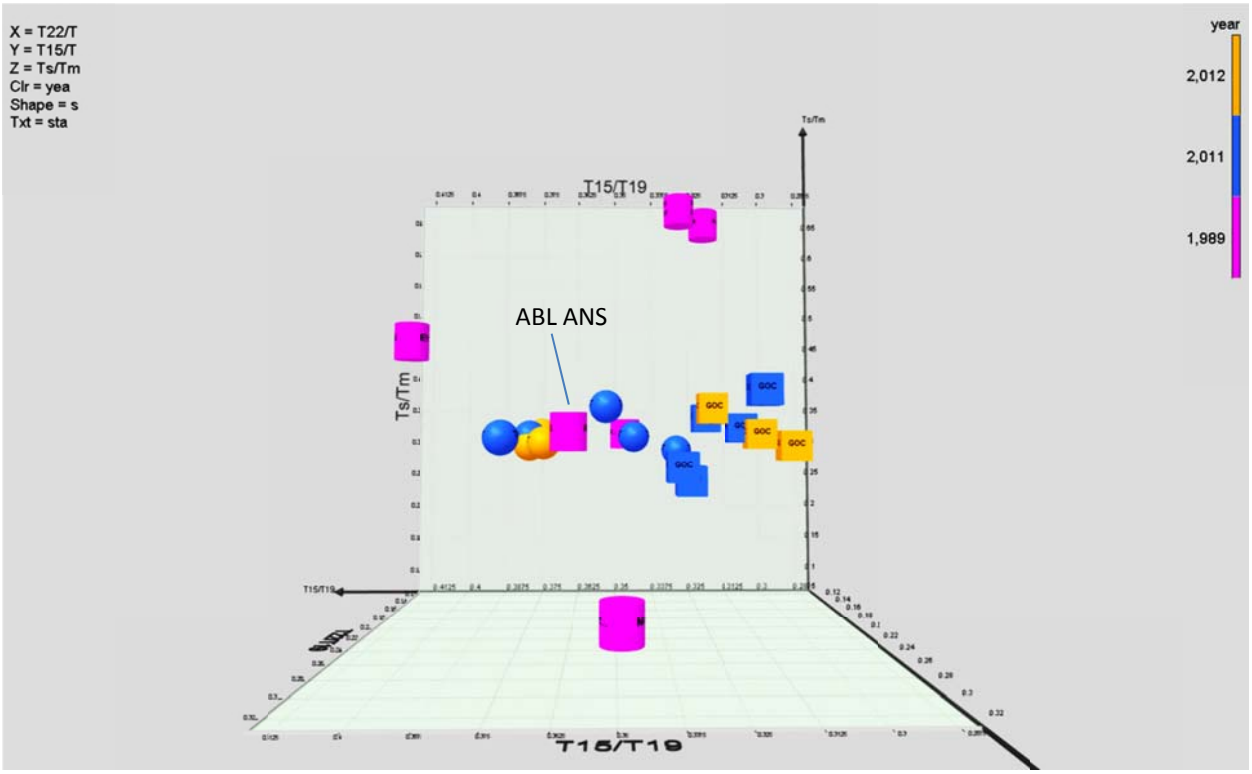

189

190 Figure 8 Diagnostic biomarker parameters showing discrete 3D clustering of AMT (spheres) and GOC (cubes) sediment
191 samples; oblique, front, top and right perspectives. Reference oils as pink cylinders; other colors indicate sampling years (1989,
192 2011 & 2012).

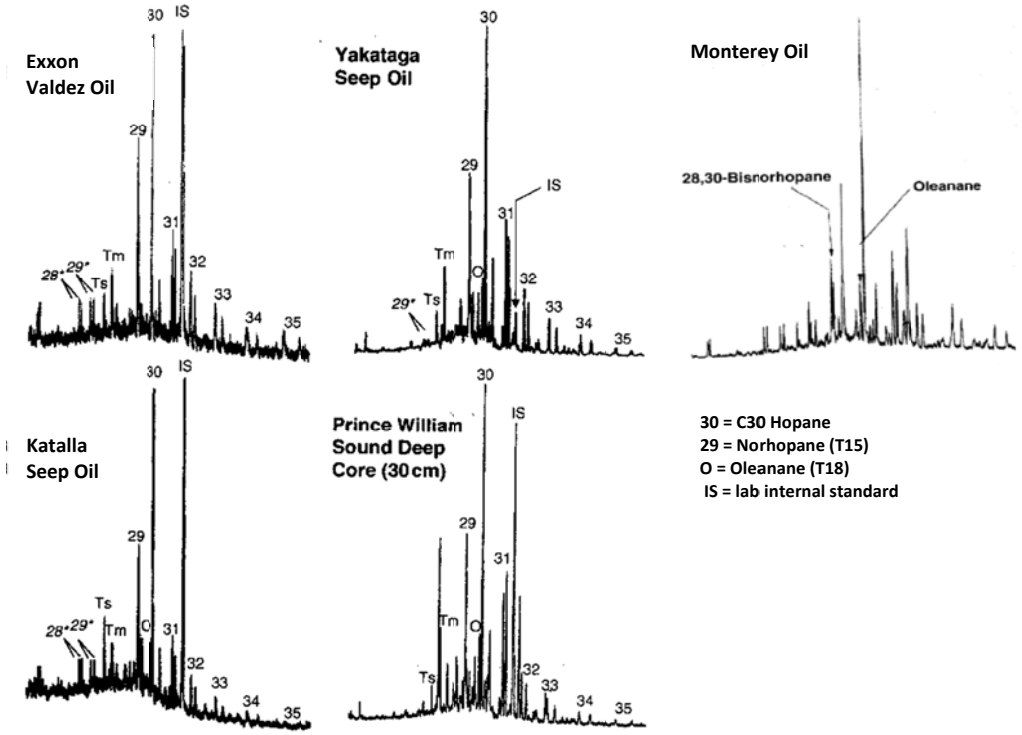

Figure 9 Ion traces of hydrocarbon sources found in PWS. Adapted from Wang and Stout, 2007.

Our preliminary assessments, pending accumulating a larger time series of samples, additional lab experience, and a more current ANS source sample, lead us to conclude that the mid-hopane-centric diagnostic ratios confirm the presence of ANS-derived biomarkers in both AMT and GOC sediments. Further, the form of variation in diagnostic biomarkers is site specific with both locations showing variants of the ANS source (i.e., weathering and/or mixtures with background biomarkers). These findings are corroborated by Shaw et al. (2005) in Alyeska's EMP, who, using C30 hopane and C29 norhopane, reported finding ANS biomarkers in deep Valdez basin sediments.

Sediment Grain Size

Sediment grain size samples were recently analyzed for all 2006-2013 collections, comprising both historic and "future" samplings. These data are presented in two formats: the standard cumulative (%) grain size curves and in 3D plots (Figure 10 & Figure 11). For this project, the grain size data only serve to demonstrate the constancy and comparability of the sampling site environs. Both sites are dominated by glacial flour inputs, showing approximately equal portions of clay and silt with minor sand components (Table 3) and both sites show minor trends and outliers. In the 3D plots, note there are annual shifts to higher sand content at both locations albeit still a minor component (<10%) and with a return to original conditions at GOC in 2013. More dramatically, at AMT, there has been a steady increase in clay content. The locations occupy a heterogeneous fjord floor dynamically swept by tidal currents (and prop wash at AMT) plus with sampling guided by GPS, the sites have been accruing grab-sampler pock marks and drag scars at the same locations for 20 years. Reassuringly, when we get off-site at GOC, we begin to see gravel in the grab. These shifts are noted with only modest confidence considering the non-rigorous collection methods, i.e., spooning up 250 ml of sample remnants after collecting the less consolidated surface floc for hydrocarbons.

215 Table 3 Average grain size components for GOC and AMT, 2006-2013

	% Clay	% Silt	% Sand
AMT	49.9	46.4	3.6
GOC	54.0	36.2	9.8

216

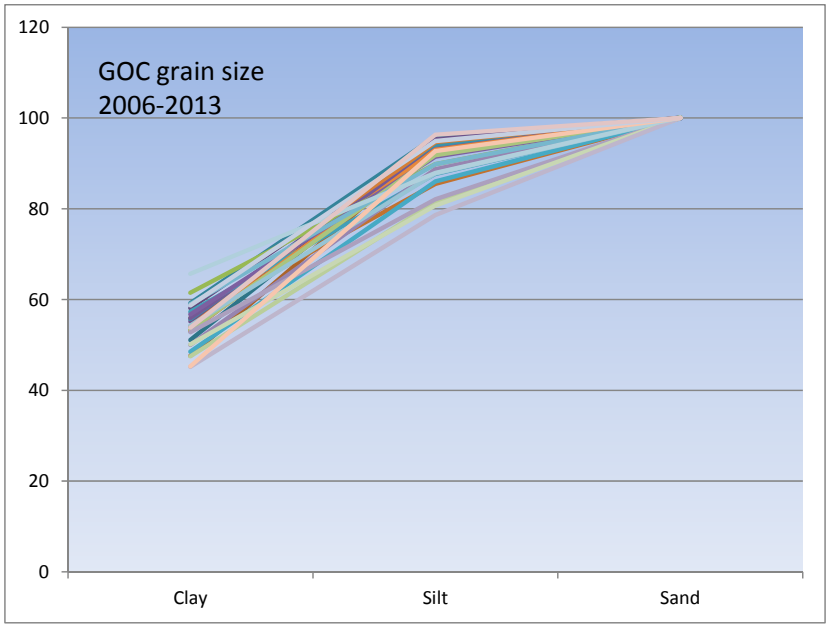

217

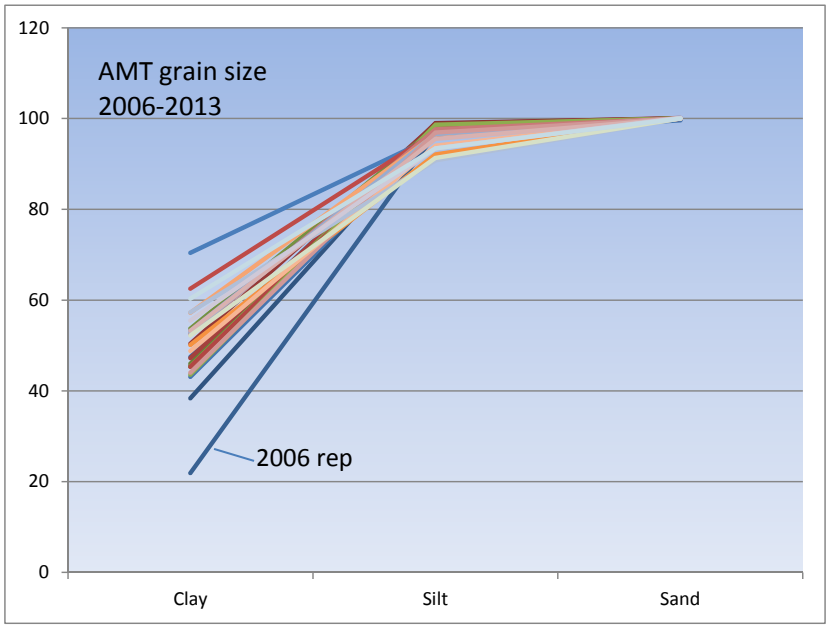

218

219 Figure 10 Cumulative grain size curves (%) for GOC and AMT, 2006-2013.

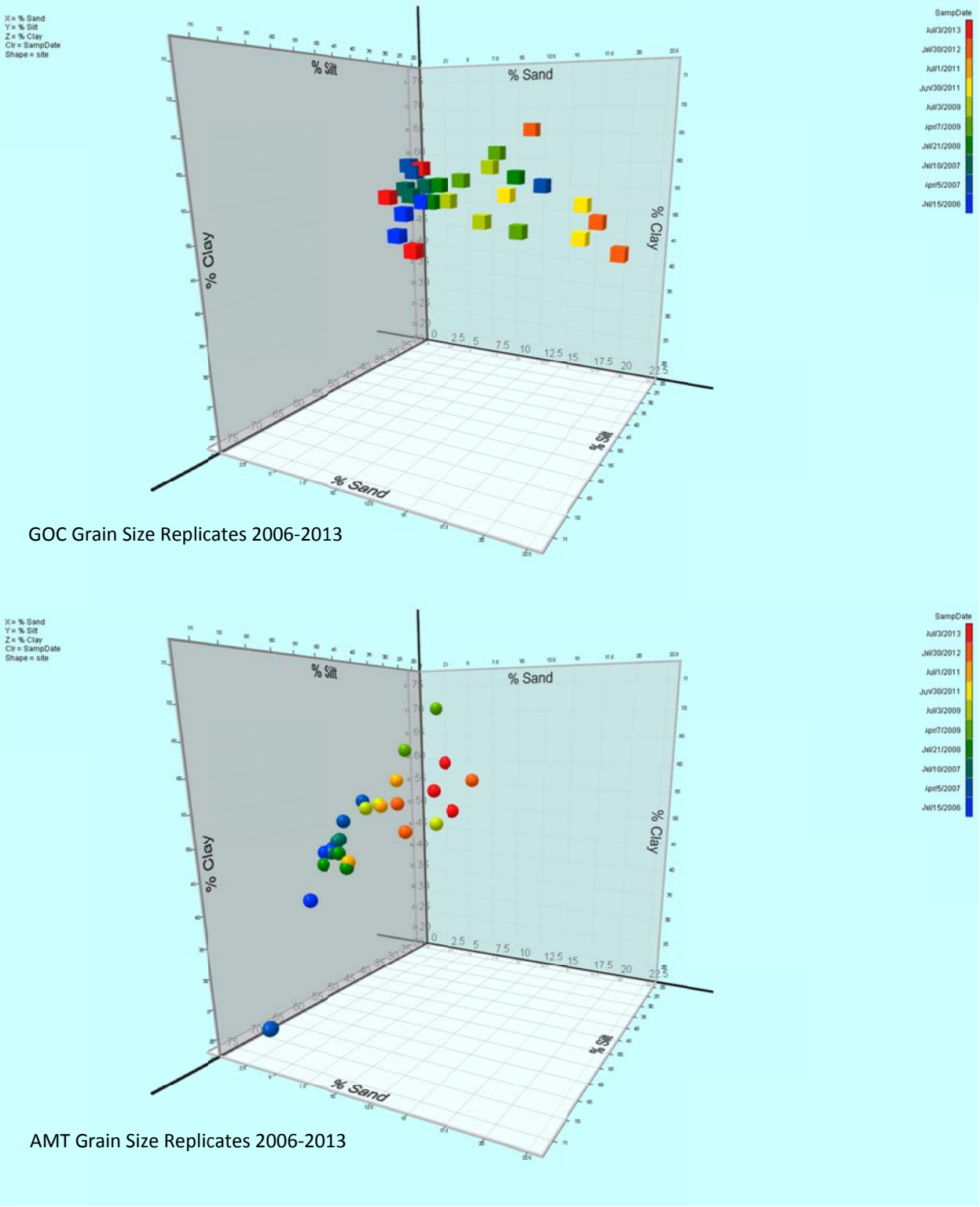

Figure 11 3D plots of grain size components from GOC and AMT 2006-2013. Sampling years color coded (blue 2006, red 2013). Note shifts to higher clay content at AMT plus higher sand content at both and then retro-shift in 2013 GOC samples back to original 2006 cluster.

TISSUES IN PORT VALDEZ AND KNOWLES HEAD

In July 2010, average TPAH levels in AMT tissue samples approached all-time lows, ~17 ng/g DW (Figure 12), and although they appear to have increased slightly (~46 ng/g DW) in July 2012, the majority of the PAH are pyrogenic not petrogenic in nature (see Figure 13 and other profiles in Appendix 1). Also note the appearance of perylene in July 2011 and 2012. This is a naturally occurring 4-ring unsubstituted PAH generated by biologic processes or in the early stages of diagenesis in marine sediments (Bence et al., 2007) and potentially being neither a non-petrogenic or pyrogenic PAH, is not included in TPAH calculations. Most of the saturated hydrocarbons (SHC) in AMT mussel tissues throughout this period are dominated by below-MDL biogenic constituents (e.g., n-C_{15}, n-C_{17}, pristane, and n-C_{27}). In July 2011, two of the three replicate tissue samples also showed traces of below-MDL, higher-molecular-weight SHC in the C_{23}-C_{30} range suggesting a possible petrogenic input, but this was not reflected in the PAH patterns.

Average TPAH levels in GOC mussel tissues have consistently been very low except for the Fall 2004 diesel spill (cleared by the following July – Figure 12). Beginning in the 1990's, mixed dissolved-phase, petrogenic, and pyrogenic signals were common at this site, roughly trending with similar patterns or discharge events at the Alyeska Marine Terminal (Payne et al., 2008a,b; 2010a). Between March 2003 and July 2008, with the exception of the aforementioned diesel spill, the signals became largely pyrogenic with occasional petrogenic components (DBTs) (Figure 14). From July 2005 to present, the TPAH levels have consistently been in the 28-75 ng/g DW range. SHC patterns at this site over the 2008-2012 period have been almost exclusively trace-level biogenic (e.g., n-C_{15}, n-C_{17}, pristane, and n-C_{27}). Exceptions included two of three replicates in April 2009, and one of three replicates in June/July 2011 when traces of petrogenic C_{24}-C_{30} SHC appeared (see Appendix 1). In none of these cases, however, were petrogenic sources suggested by the PAH profiles. Interestingly, traces of perylene noted in the AMT mussels in July 2011 and 2012 were also observed at GOC during the same collections.

Average TPAH levels in mussel samples from the tanker anchorage at KNH have been consistently low, ranging from 5-24 ng/g DW since March 2004 (Figure 12). With the exception of one sample in July 2004 that showed a petrogenic PAH profile (Payne et al., 2008a,b; 2010), the samples from this site have been dominated by trace level (at or just-above detection limit) naphthalenes and combustion-derived anthracenes/phenanthrenes since July 1999; this pattern has continued throughout the July 2008-July 2012 period (see Figure 15 and additional profiles in the Appendix 1). Also note the appearance of perylene that was also observed in the mussels at AMT and GOC in 2011 and 2012. Presumably this reflects some region-wide marine event. The near- or just below-MDL SHC patterns at KNH between July 2008 and July 2012 are almost exclusively biogenic (e.g., n-C_{15}, n-C_{17}, and pristane) except for one of three replicates in July 2011 when a slightly fuller, but below-MDL C_{24}-C_{30} pattern suggested the possibility of a petrogenic source. The PAH profile, however, did not support this observation (Figure 15).

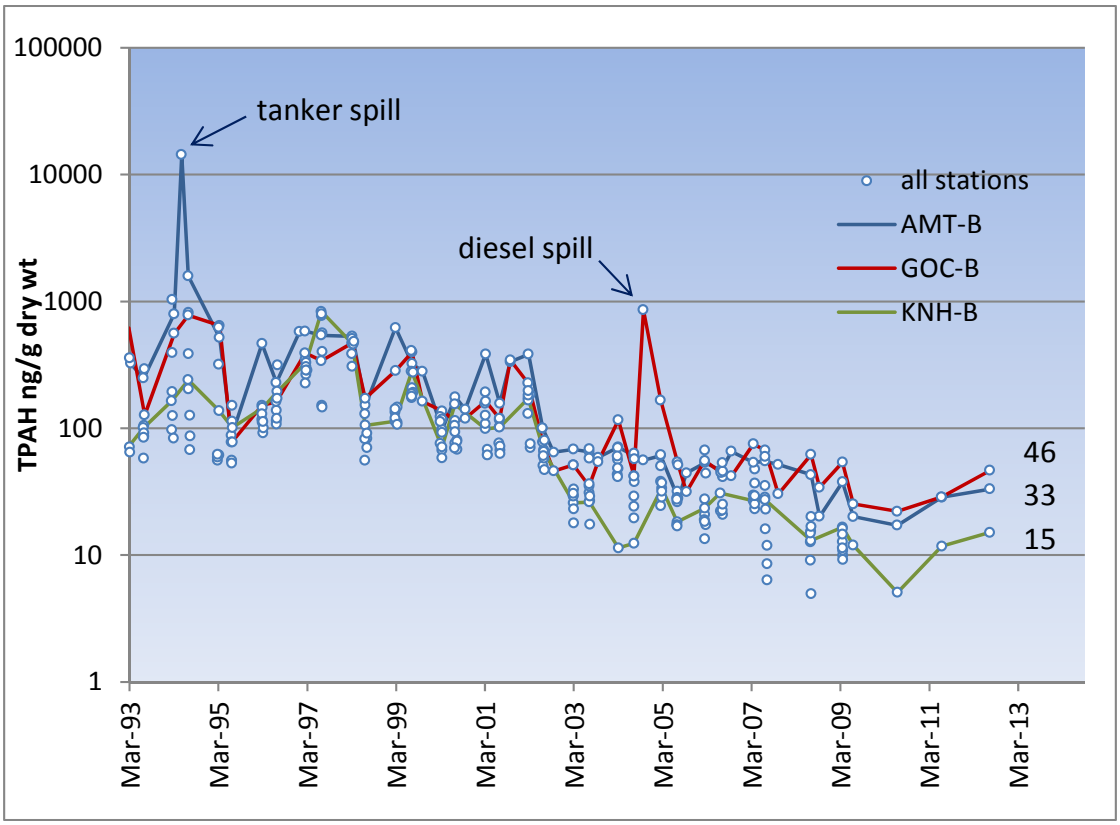

257

258 Figure 12 Time series of mussel tissues TPAH from Alyeska Terminal, Gold Creek and Knowles Head sites.

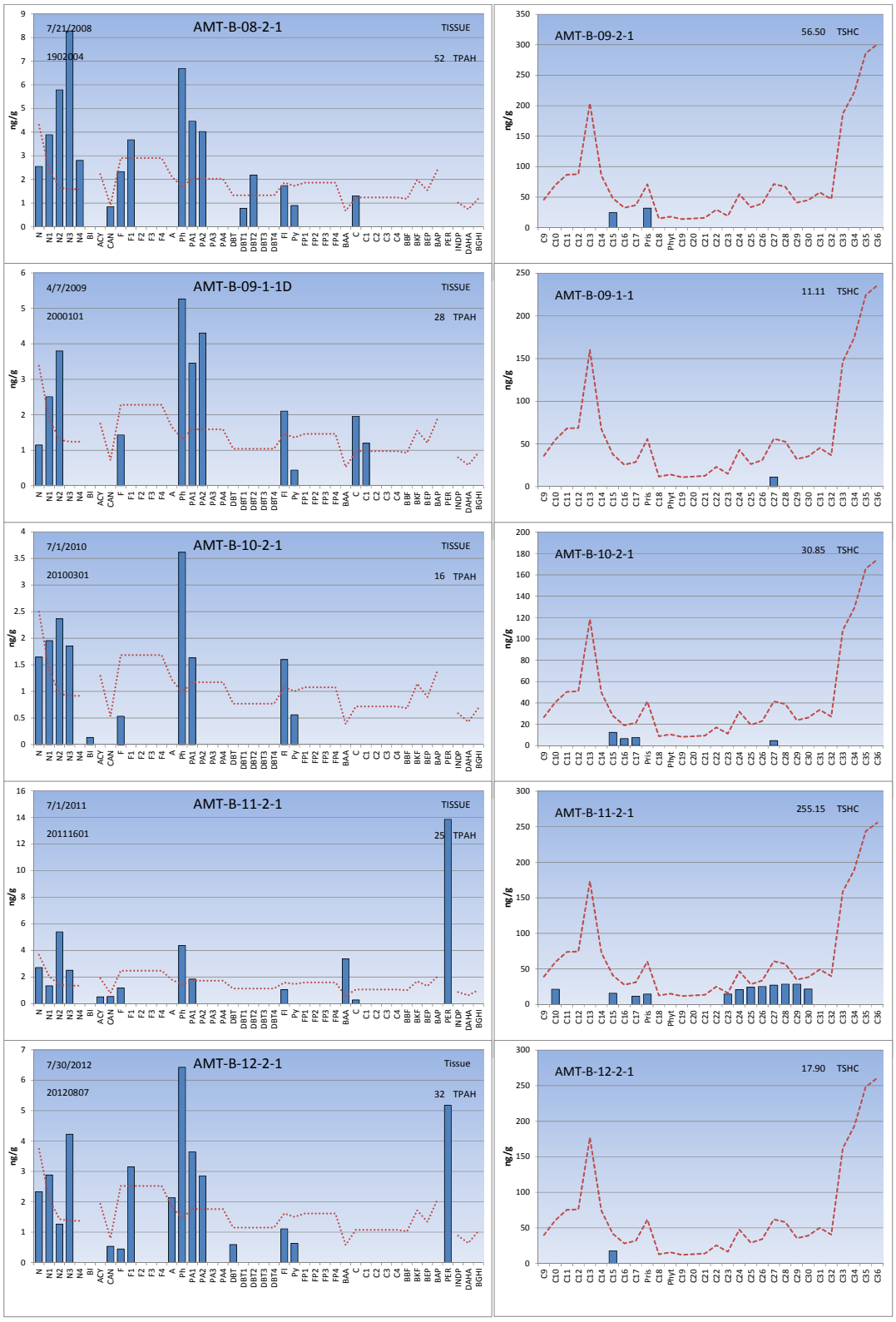

259

260 Figure 13 Representative PAH and SHC profiles from AMT mussel tissues between July 2008 and July2012 showing primarily
261 combustion products, perylene, and planktonic biogenic SHC and a trace of crude oil (in July 2011). Red dashed line is sample-
262 specific MDL.

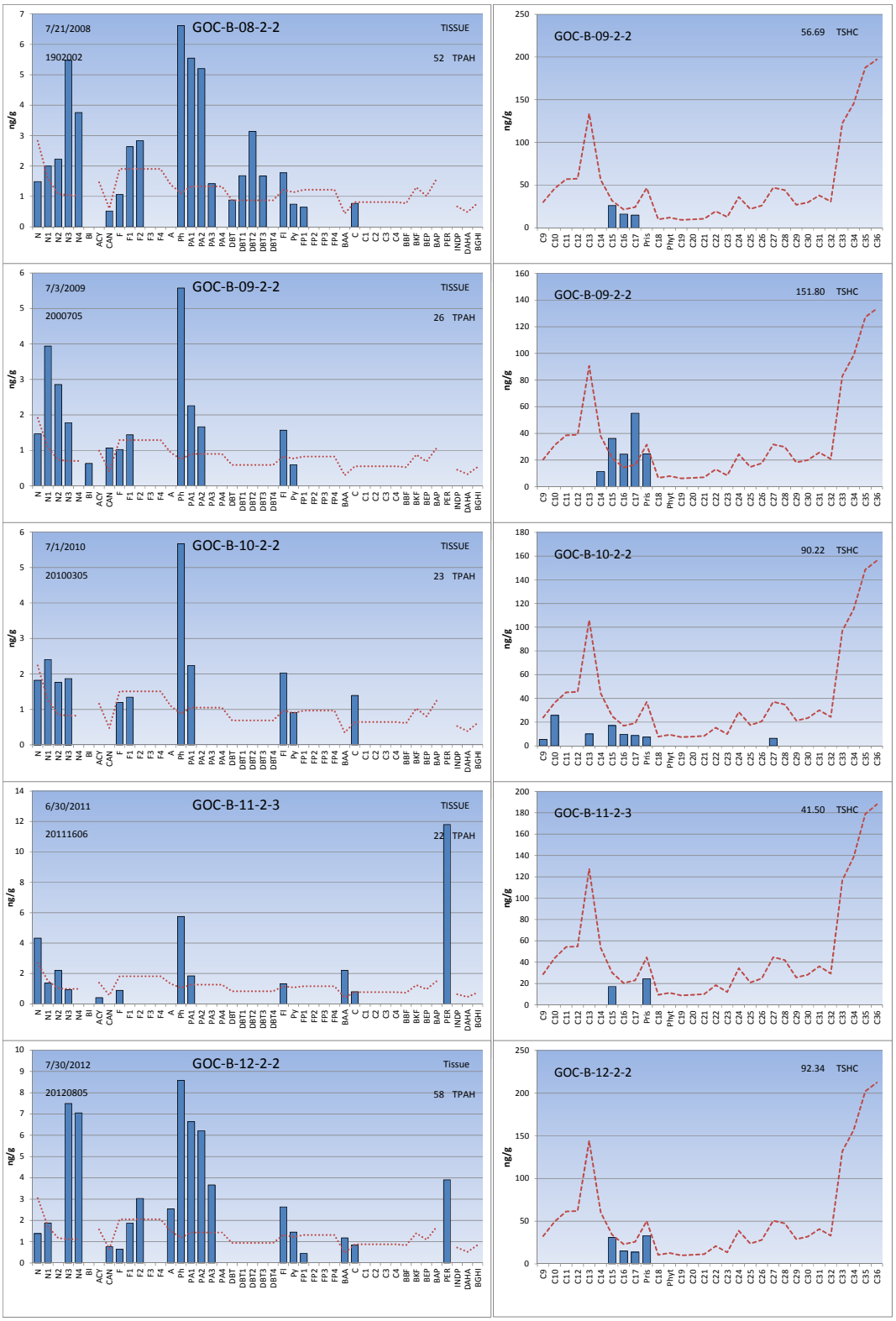

Figure 14 Representative PAH and SHC profiles from GOC mussel tissues between July 2008 and July2012 showing primarily combustion products, perylene, and planktonic/terrestrial biogenic SHC. Note the occurrence of perylene in 2011 and 2012 was also observed in the AMT mussels. Red dashed line is sample-specific MDL.

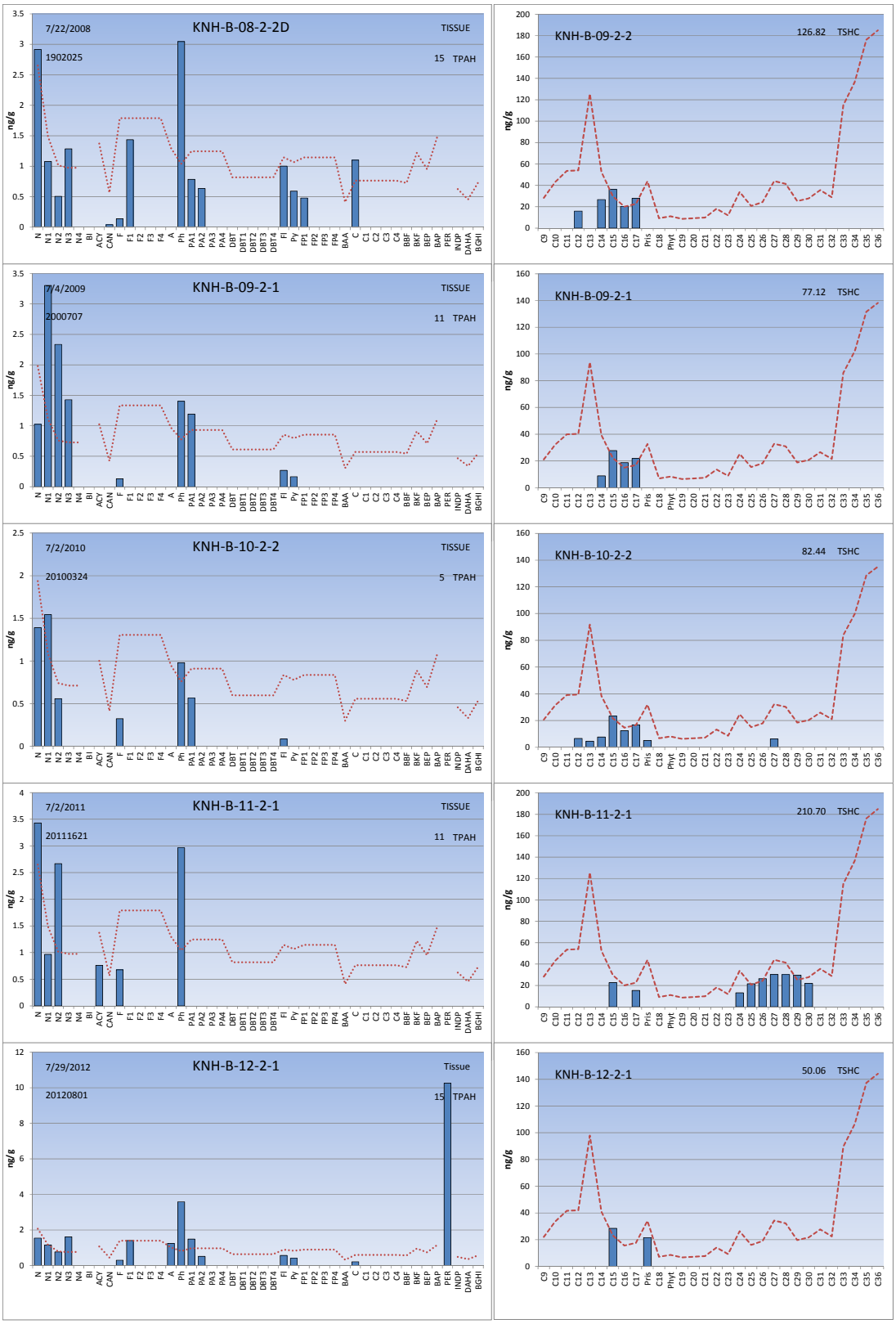

Figure 15 Representative PAH and SHC profiles from KNH mussel tissues between July 2008 and July2012 showing primarily trace-level combustion products, perylene (in 2012), and planktonic/terrestrial biogenic SHC.

PRINCE WILLIAM SOUND AND GOA MUSSEL TISSUES

Only one additional sampling (April 2009) has been added to the time series since the publication of our 2011 data report, and as of that sampling, overall TPAH levels at these central PWS and GOA sites continued to decline (Figure 16) although more recently, the annually-sampled Valdez sites have marginally rebounded.

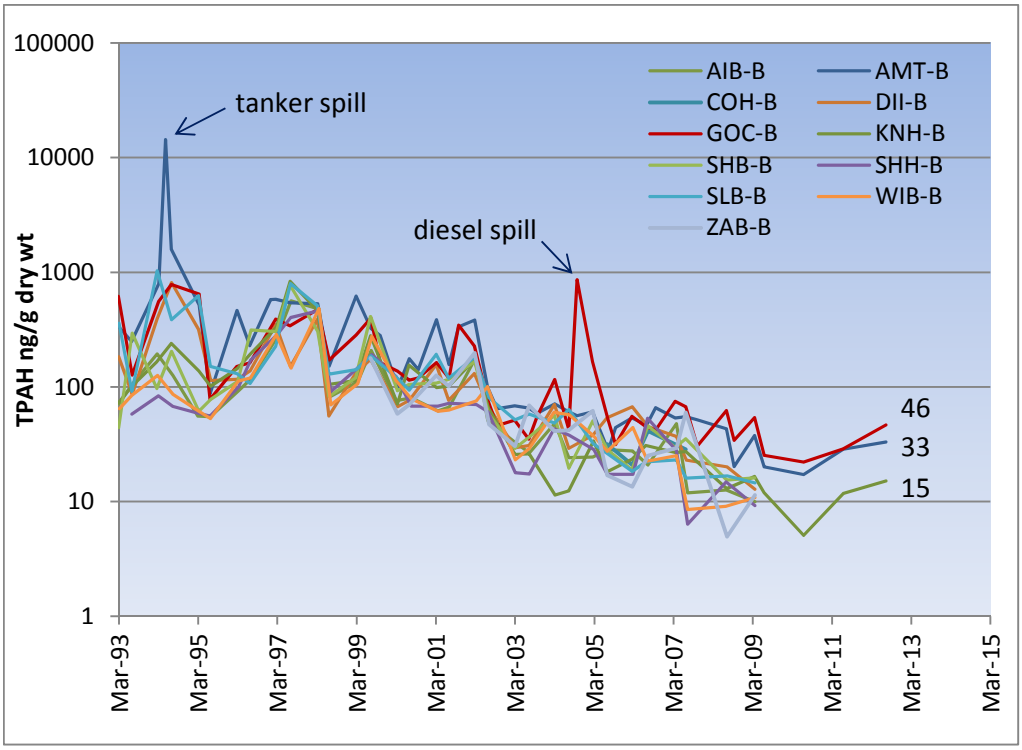

Figure 16 Mussel-tissue TPAH trends for all stations (1993-2012).

All of the PAH levels measured in the April 2009 samples are extremely low (mostly near or just below even the new MDLs), yet remarkable site fidelity exists within the PAH and SHC patterns for each stations' replicates (Figure 17 through Figure 20). And to a degree, regional patterns are still visible although weaker than in the previously reported 2006-08 data set (Payne et al., 2010a). We believe that despite the at-or-below MDL character of the data, the within-site and within-region consistency would not be achievable if data quality were uncontrolled at these trace-levels. The laboratory method blanks were also very clean (primarily only showing below-MDL traces of the problematic biphenyl), which again supports the notion that rather than laboratory noise, the observed patterns were truly due to low-level constituents in the mussel tissues at each site.

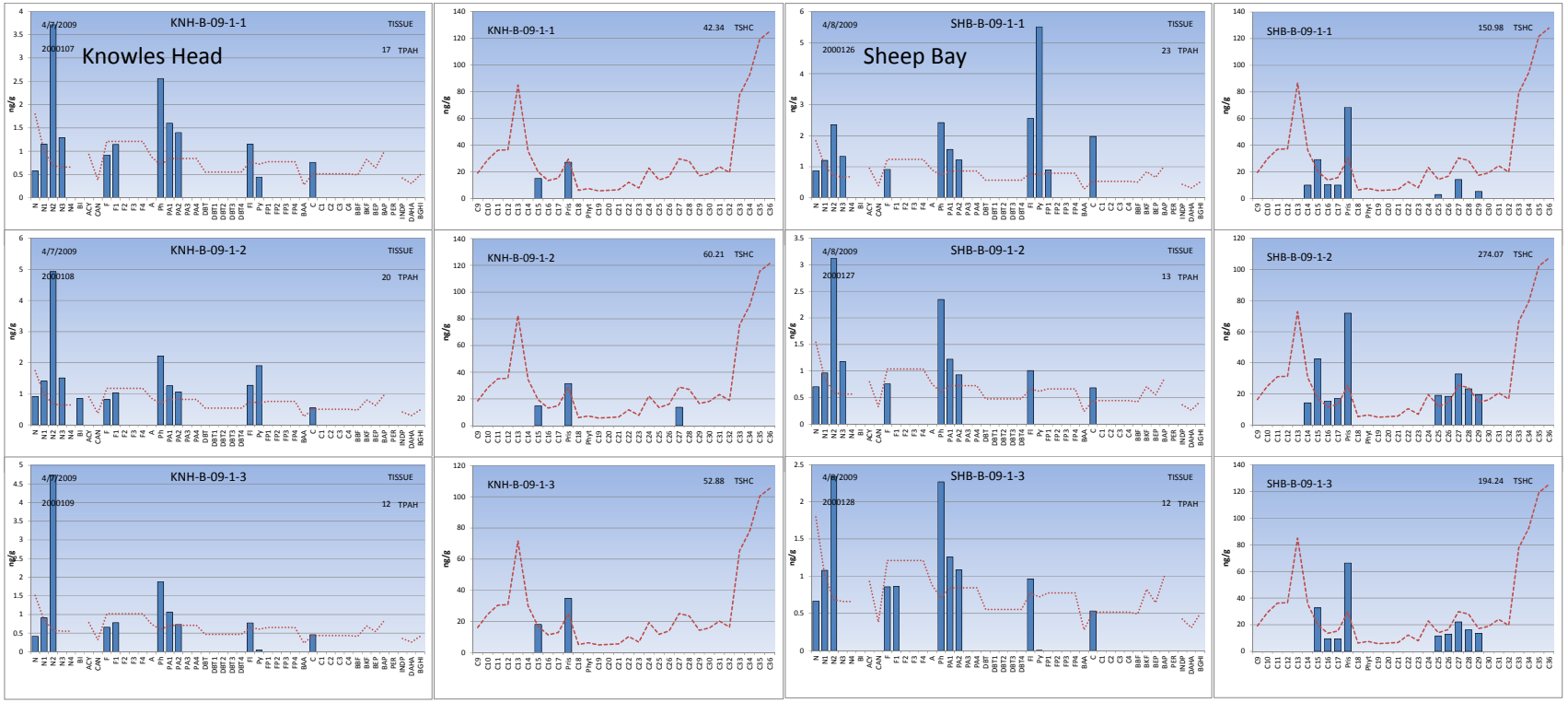

286

287 Figure 17 Mussel-tissue PAH histogram plots showing within-site fidelity among replicates and regional similarities between eastern PWS sites.

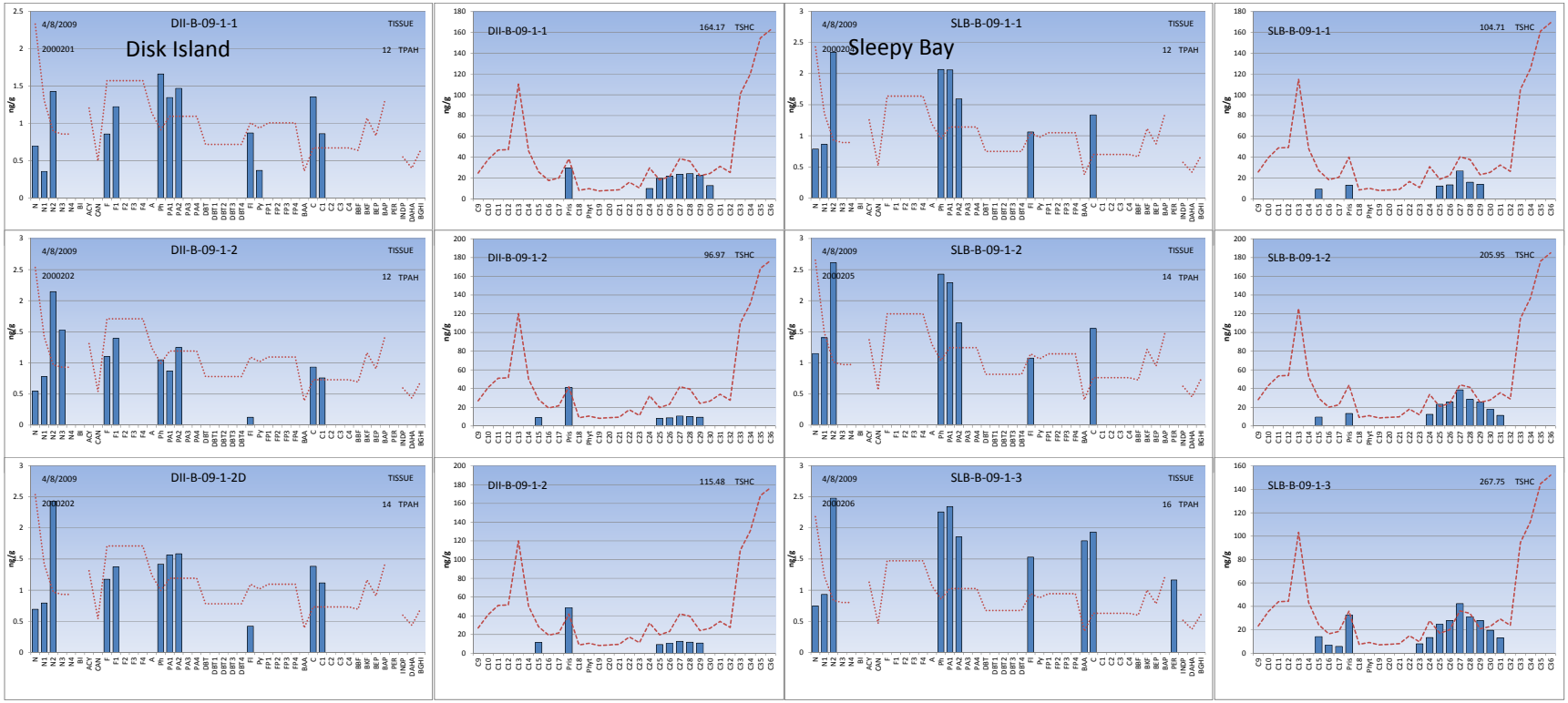

Figure 18 Mussel-tissue PAH histogram plots showing within-site fidelity among replicates and regional similarities between central and previously EVOS-oiled PWS sites.

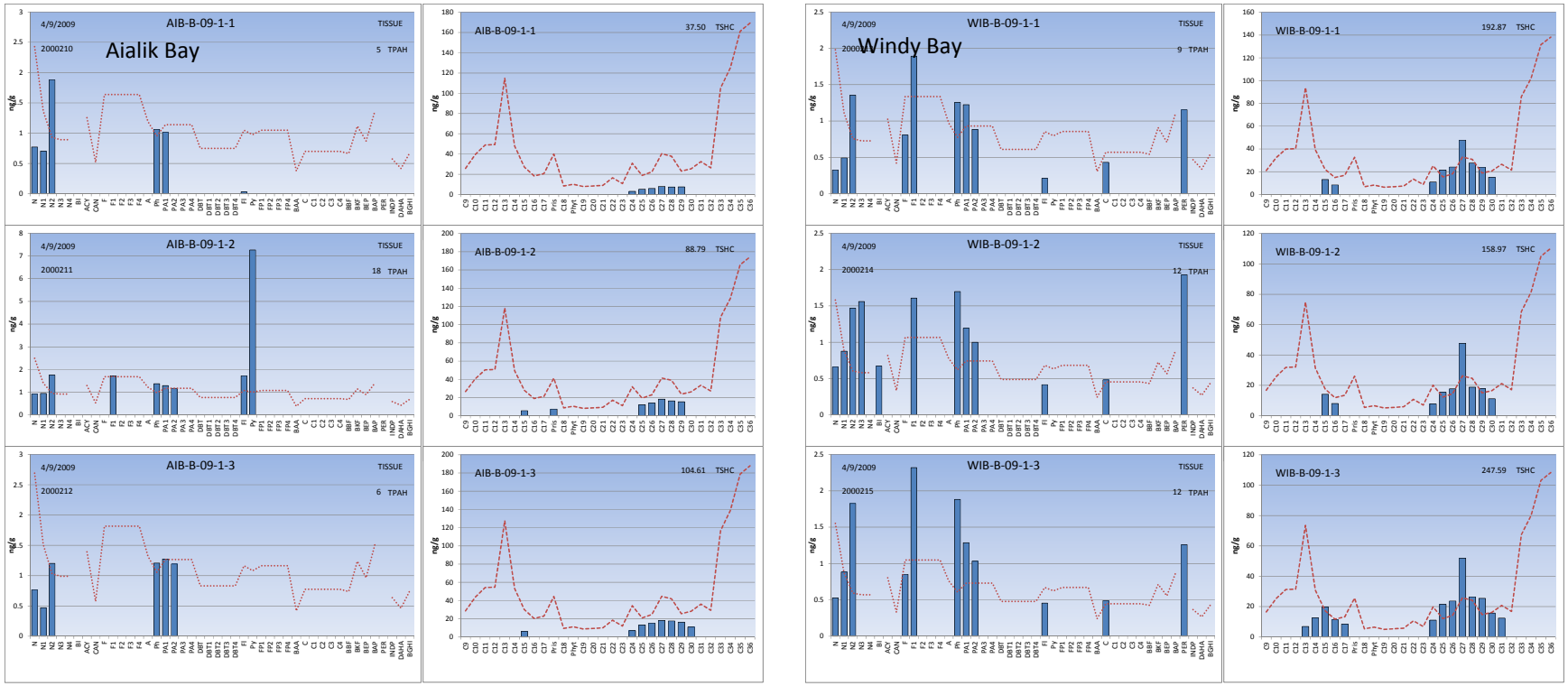

Figure 19 Mussel-tissue PAH histogram plots showing within-site fidelity among replicates and regional similarities between outer coast sites**.**

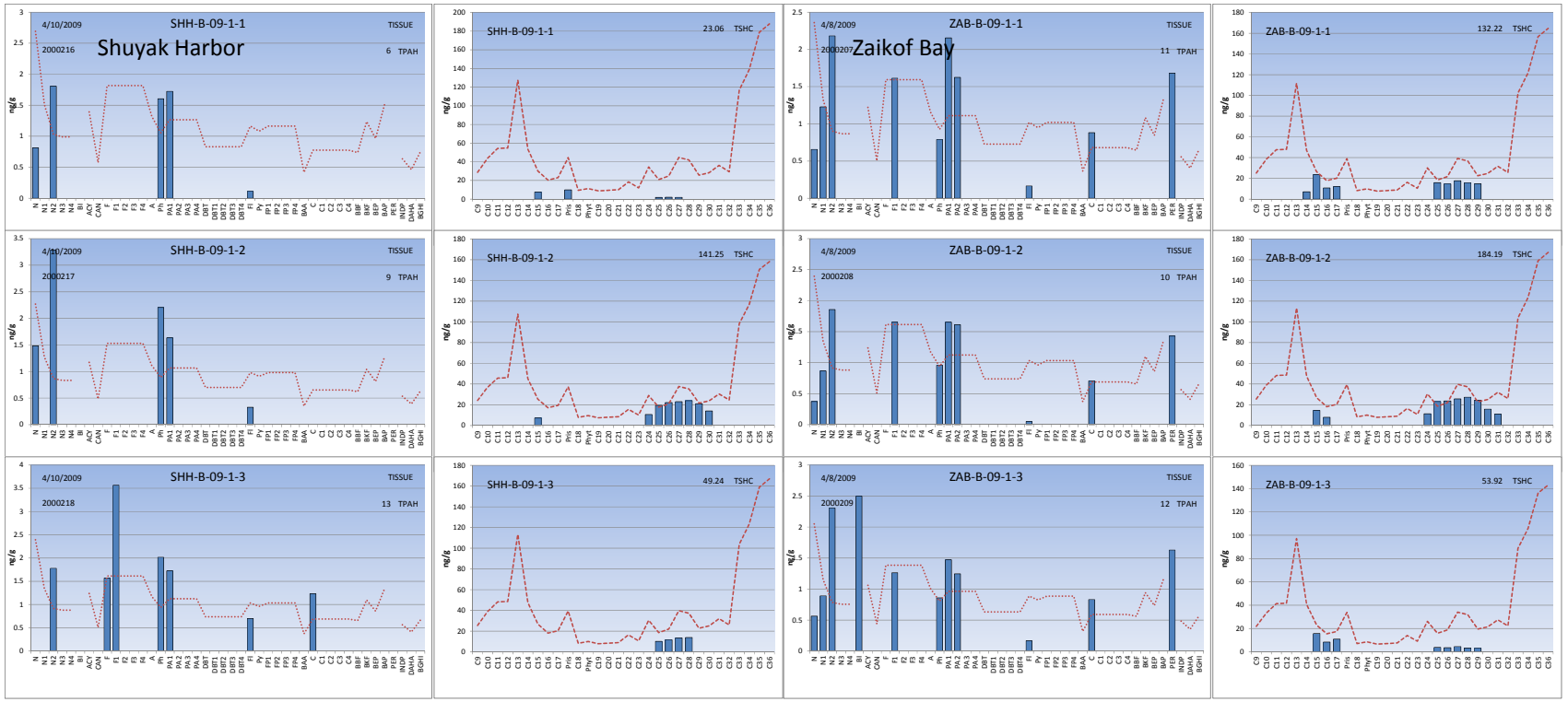

292

293 Figure 20 Mussel-tissue PAH histogram plots showing within-site fidelity among replicates.

All of the PWS and GOA stations (Figure 17 through Figure 20) show ubiquitous low-level naphthalene signals that we think are part of the overall background pattern (Payne et al., 2010a,b). Likewise, Knowles Head (KNH), Sheep Bay (SHB), and Windy Bay (WIB) show pyrogenic phenanthrenes/anthracenes along with lower concentrations of fluorenes and isolated peaks for parent fluoranthene, pyrene, and chrysene (all combustion products). The relative phenanthrene/anthracene homologue distribution patterns at Disk Island (DII) and Sleepy Bay (SLB) (both formerly EVOS-oiled sites) show a little more complexity and within-site variability suggesting the possibility of a more petrogenic influence, e.g., oil was still observed in disturbed intertidal substrates at DII in April 2009 (Payne et al., 2010a). Zaikof Bay (ZAB) also shows evidence of a minor petrogenic phenanthrene/anthracene pattern, and its fluoranthene/chrysene/perylene profile is unique among all the stations. Finally, Shuyak Harbor (SHH) and Aialik Bay (AIB) (with the exception of one replicate) show the least complex PAH patterns of all the stations examined. The SHC patterns at all of these sites are mostly below the sample-specific MDLs, but there appears to be sporadic indications of petrogenic SHC (n-C_{23}-n-C_{31}), again with remarkable site fidelity at several of the stations.

In the Sound, with the bulk of EVOS oil either dissipated or the remnants buried and sequestered, the regional sites that are physically remote from the chronic low input of BWTF discharge are currently looking very clean. As stated in our last report, TPAH levels in both the PWS and GOA regions are dropping at nearly identical rates. This parallelism suggests the decreases are influenced by similar (oceanographic-scale?) processes, but the occasional asynchrony of peak events also suggests regional variation in the dynamics. So what broad-scale sources might appear as an ambient background signal? Possibilities include atmospheric deposits from forest fires and volcanic activity, leaching of water-soluble constituents from the pervasive source-rock (oil shale or coal that constitutes much of the PAH-bearing material being transported through the region), some upwelling/climate-driven events, a combination of these or some novel mechanism relating to decadal oscillations and/or global warming. Based on a limited-scale partitioning experiment with clean seawater and intertidal sediment from Constantine Harbor (Payne et al. 2010b), we now believe that sedimentary material previously believed to only contain sequestered and non-bioavailable PAH, is a component of the ubiquitous dissolved-phase (naphthalene) signals observed throughout Prince William Sound.

Another question is how low will this generally declining trend in TPAH values go? Obviously, at some point, the trend must level out. Follow-up sampling in 2004 for oil residues from the 1997 *M/V Kuroshima* grounding in Summer Bay, Unalaska, found TPAH levels between 25 and 85 ng/g DW, with an average of 57 ng/g DW (Table 4, Helton et al., 2004). This compares favorably and is actually higher than LTEMP's April 2009 range of 4-23 ng/g DW inside the Sound and 6-18 ng/g DW at Gulf of Alaska sites (overall average 12 ng/g DW). These data also suggest a natural dissolved-phase background TPAH somewhere below 20-30 ng/g DW--a range in which analytical sensitivity can be highly susceptible to procedural artifacts. It could easily be the case that the LTEMP data are currently tracking subtle variations in the background PAH, and that we are near or at the minimum.

For relative comparisons, data from the 2004-2005 National Status and Trends, Mussel Watch Program (Table 4, Figure 21) and 2008-2010 Alaskan sites (Figure 22) (now summing 38 parent and alkylated PAH homologues versus 44 LTEMP PAH analytes) show that PAH concentration in mussels for other West Coast sites is nearly 66 times higher at 825 ng/g DW. The highest level reported on the West Coast was 6,962 ng/g DW in Seattle, Washington. The lowest, 63 ng/g DW, was from mussels collected on Santa Catalina Island, 26 miles offshore of Orange County in Southern California. In 2004-5, the average TPAH concentration in mussels from the five Alaskan Mussel Watch sites (Ketchikan, Nahku Bay, Port Valdez, Unakwik Inlet, and Cook Inlet) was 267 ng/g DW with levels ranging from 105-441 ng/g DW (Kimbrough et al., 2008). Considering these and even more recent 2008-2010 values from the MW data portal (Table 4), the LTEMP results for the PWS and GOA sites demonstrate that these remote locations are exceptionally clean.

338 Table 4 Current TPAH concentrations in regional mussel tissues (ppb, ng/g DW) relative to 2004-2010 NOAA Mussel Watch
339 monitoring data and a recovered Alaskan oil-spill event.

LTEMP	2012	Port Valdez		15-73
	2009	PWS		4-23
	2009	GOA		6-18
West Coast Mussel Watch		average (Kimbrough et al., 2008)		825
		So. Calif.	Santa Catalina Island	63
		Seattle	Elliot Bay, WA	6,962
Alaska Mussel Watch	2008	Cook Inlet	Bear Cove	119
		Cook Inlet	Homer Spit	208
		Port Valdez	Alyeska Marine Terminal	52
		Port Valdez	Gold Creek	31
	2009	Ketchikan	Mountain Point	231
		Nahku Bay	East Side	229
		Port Valdez	Mineral Creek Flats	332
		Resurrection Bay	Nash Road	602
		Resurrection Bay	Nash Road	765
		Resurrection Bay	Nash Road	929
		Resurrection Bay	Nash Road	713
		Unakwit Inlet	Siwash Bay	257
	2010	Resurrection Bay	Nash Road	1,570
		Nanwalek	Nanwalek	194
		Port Graham	Port Graham	376
		Port Graham	Murphy's Slough	428
		Seldovia Bay	Powder Island	652
M/V Kuroshima (1997)		Unalaska	2004 followup	25-85

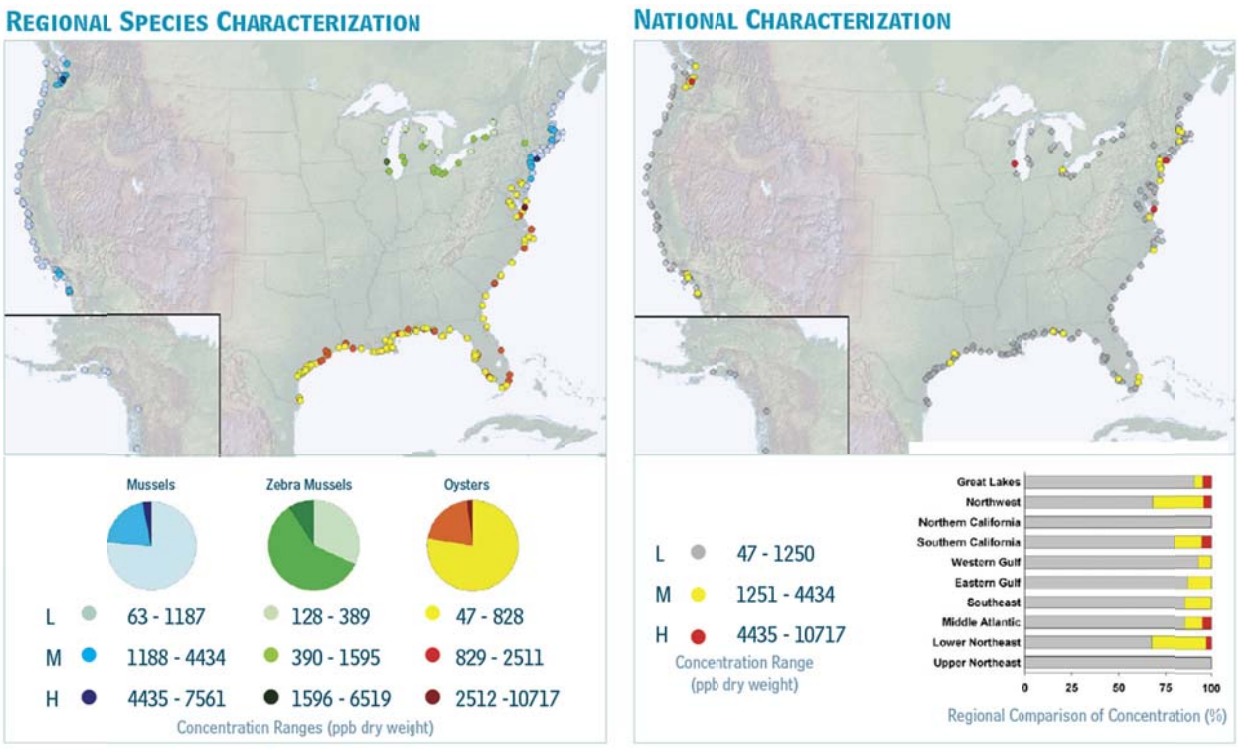

340

341 Figure 21 Status and trends result from national Mussel Watch data (Kimbrough et al., 2008). All Alaskan sites characterized as
342 low concentrations.

APPENDIX 2: RESULTS BY STATE

ALASKA (AK)

Regional (r)
Mussels (M)
- Medium
- High

Zebra Mussels (ZM)
- Medium
- High

Oysters (O)
- Medium
- High

Status (s)
National Status
- Medium
- High

Trend (t)
National Trend
- Decreasing
- Increasing

Concentrations derived from 2004-2005 data.

Markers represent the Regional Species Characterization (r), National Characterization (s) and National Trends maps (t).

Site	Latitude	Longitude	General Location	Location
KTMP	55.2938	-131.5480	Ketchikan	Mountain Point
NBES	59.4533	-135.3365	Nahku Bay	East Side
PVMC	61.1328	-146.4610	Port Valdez	Mineral Creek Flats
UISB	60.9608	-147.6460	Unakwit Inlet	Siwash Bay
CIHS	59.6145	-151.4442	Cook Inlet	Homer Spit

METALS (ppm)

Site	Spec	AS	r	s	t	CD	r	s	t	CU	r	s	t	HG	r	s	t	NI	r	s	t	PB	r	s	t	SN	r	s	t	ZN	r	s	t
KTMP	M	11		●		7.1	●	●		7				0.06				1.2				0.59				0				97			
NBES	M	9.2				5.4	●	●	▲	6				0.1				2				2.1		●		0				72			
PVMC	M	12	●	●		3.5		●		27	●			0.09				8.9	●	●		3	●	●		0.18				89			▼
UISB	M	12	●	●		2.6				33	●			0.11				7.4	●			2				1.4	●	●		108			
CIHS	M	12	●	●		1.7				10				0.12				3.4				1.3				0				105			

ORGANICS (ppb)

Sites	Spec	Butyltins	r	s	t	Chlordanes	r	s	t	DDTs	r	s	t	Dieldrins	r	s	t	PAHs	r	s	t	PCBs	r	s	t
KTMP	M	2.1				0.47				1.4				0.58				152				3.5			
NBES	M	3.7				2.7				2.2				0.98				316				7.7			
PVMC	M	7.3				2.6				1.7				0.31				441				6.4			
UISB	M	1.7				0.87				0.38				0.56				176				3.7			
CIHS	M	4.4				1.1				0.3				0.42				250				11			

Figure 22 Summary page of Alaska regional Mussel Watch results and trends based on 2004-05 data from Kimbrough et al., 2008.

Finally, a 2005 EVOS Trustees Program, Long-term Monitoring of Anthropogenic Hydrocarbons in the *Exxon Valdez* Oil Spill Region, examined ten intertidal sites within the Naked-Knight-Southwest Island complex to measure the extent of buried oil still present 16 years after the spill. At previously heavily-oiled EVOS sites, 10 to 50 random pits (depending on the beach width) were excavated to a depth of ~0.5 m to look for residual oil. If oil was detected, available nearby mussels were also collected. The results have been published elsewhere (Short et al., 2007) but, as co-authors, PAH and SHC sample profiles were included in Appendix E of our 2005/2006 Report (Payne et al., 2008a). Briefly, TPAH levels in the oiled pits ranged from a low of 42 ng/g (on Knight Island) to a high of 567,000 ng/g (on Latouche Island) with the oil showing states of weathering varying from very fresh to

extensively degraded. On the other hand, nearby mussel samples only showed low dissolved-phase TPAH (11-42 ng/g DW, derived primarily from naphthalenes and phenanthrenes/anthracenes) that were in the same concentration range but compositionally different from the signals observed at LTEMP PWS and GOA sites sampled in April 2009. From these studies, it was concluded that although in 2005, there were still persistent buried EVOS residues at a number of beaches, they were highly sequestered and did not appear to be bioavailable unless disturbed. Rates of disappearance had diminished to an estimated 4% yr^{-1}. If left undisturbed, Short et al. (2007) predicted they would be there for decades. To address these residual deposits, for the last three years EVOS Trustees have sponsored beach remediation projects.

CONCLUSIONS

Based on the sediment and mussel data, petrogenic hydrocarbon inputs from the Alyeska Marine Terminal and tanker operations continue to decline. Within Port Valdez, and as concluded in our last LTEMP report (Payne et al., 2010a), the decrease likely reflects a combination of reduced BTWF discharge volumes from decreased North Slope oil production, the transition to double-hulled tankers with segregated ballast tanks, and improved BWTF efficiency at removing particulate/oil-phase PAH. In the 2012 tissue collections at the Terminal, the mussels showed a predominant pyrogenic, not petrogenic, profile, and even the sediments at this site are beginning to look more like Gold Creek's background-reference, pyrogenic profiles. Biomarker data show evidence of low-level ANS oil in the Port sediments. At GOC, concentrations are seven times lower than those at AMT and the profiles indicate mixing with background sources.

With the April 2009 mussel collections at the central PWS and GOA sites, the overall TPAH levels at these stations continued to decline. All of the PAH levels measured in the April 2009 samples are extremely low (mostly near or just below even the new MDLs), yet remarkable site fidelity exists within the PAH and SHC patterns for each stations' replicates. The SHC patterns at all of these sites are mostly below the sample-specific MDLs, but there appears to be sporadic indications of petrogenic SHC (n-C_{23}-n-C_{31}), again with remarkable site fidelity at several of the stations. However, in corresponding PAH fractions when trace-level petrogenic SHC signals were observed, there was little or no evidence of oil contamination. Compared to 2004-05 West Coast Mussel Watch data and the more recent Alaskan Mussel Watch sites, the LTEMP results for the PWS and GOA sites demonstrate that the region is exceptionally clean.

ACKNOWLEDGEMENTS

This success of this project reflects the efforts of many more individuals than currently appear in the author's list. From our stalwart vessel operator, tireless supporter and colleague, Dave Janka (and Annette Janka), our primary pilots, Terry Kennedy and Jose DeCreft, our former and current colleagues at Auke Bay Lab (including the project newbie, Dr. L. Schaufler), project managers, Lisa Ka'aihue and Joe Banta, our many prior and current SAC advisors, and the every-ready folks on RCAC staff…and our families…for the years of Alaskan adventures and productive science--BIG THANKS!

REFERENCES

Bence, A.E., K.A. Kvenvolden, M.C. Kennicutt II 1996. Organic geochemistry applied to environmental assessments of Prince William Sound, Alaska, after the Exxon Valdez oil spill—a review. Organic Geochemistry, Volume 24, Issue 1, January 1996, Pages 7-42

Bence, A.E., D.S. Page, and P.D. Boehm (2007). Advances in forensic techniques for petroleum hydrocarbons: the Exxon Valdez Experience. Pp 449-487 *In* Wang, Z. and S.A. Stout (eds). Oil Spill Environmental Forensics: Fingerprinting and Source Identification. Academic Press, Burlington, MA, USA. 554 pp.

Carls, M. G. 2006. Nonparametric identification of petrogenic and pyrogenic hydrocarbons in aquatic ecosystems. Environ. Sci. Technol. 40:4233-4239.

Driskell, W.B. and J.R. Payne. 2011. Preliminary Data Report for LTEMP 2008-2010. 4pp

Helton, D., A. Moles, J. Short, J. Rice 2004. Results of the *M/V Kuroshima* Oil Spill Shellfish Tissue Analysis 1999, 2000 and 2004. Report to the *M/V Kuroshima* Trustee Council. Prepared by NOAA Office of Response and Restoration, Seattle, Washington and NOAA Auke Bay Laboratory, Juneau, Alaska. December 2004, 7 pp.

Kimbrough, K. L., W. E. Johnson, G. G. Lauenstein, J. D. Christensen and D. A. Apeti 2008. An Assessment of Two Decades of Contaminant Monitoring in the Nation's Coastal Zone. Silver Spring, MD. NOAA Technical Memorandum NOS NCCOS 74. 105 pp.

Kvenvolden K. A., Hostettler F. D., Carlson P. R., Rapp J. B., Threlkeld C., and Warden A. 1995. Ubiquitous tar balls with a California source signature on the shorelines of Prince William Sound, Alaska. Environ. Sci. Technol. 29(10), 2684–2694.

Lillis, Paul G., Michael D. Lewan, Augusta Warden, S. Mark Monk, and J. David King 1999. Identification And Characterization Of Oil Types And Their Source Rocks in *The Oil and Gas Resource Potential of the 1002 Area, Arctic National Wildlife Refuge, Alaska*, by ANWR Assessment Team, U.S. Geological Survey Open-File Report 98-34. *http://pubs.usgs.gov/of/1998/ofr-98-0034/OA.pdf*

Payne, James R., William B. Driskell, Jeffrey W. Short, Marie L. Larsen. 2008a. Final 2005-2006 LTEMP Oil Monitoring Report, Exxon Valdez Oil Spill Restoration Project Final Report (Restoration Project 050763), Prince William Sound Regional Citizen's Advisory Council, Anchorage, Alaska. 137 pp.

Payne, J.R., W.B. Driskell, J.W. Short and M.L. Larsen. 2008b. Long-term monitoring for oil in the *Exxon Valdez* spill region. *Marine Pollution Bulletin* 56: 2067-2081.

Payne, J.R., W.B. Driskell, J.W. Short, and M. Larsen. 2010a Long-Term Environmental Monitoring Program: Final 2006-2008 LTEMP Monitoring Report. Prince William Sound Regional Citizen's Advisory Council, Anchorage, Alaska. 198 pp

Payne, J.R., W.B. Driskell, and D. Janka 2010b. A possible source for dissolved-phase PAH signals observed in *Mytilus* samples throughout Prince William Sound, Alaska. 2010 AMOP Conference. Halifax, Nova Scotia, CA.

Shaw, D., A.L. Blanchard, and D.L. Hawkins. 2005. Chapter 2 – Hydrocarbon Studies in Environmental Studies in Port Valdez, Alaska: 2004. Final Report to Alyeska Pipeline Service Co., Inst. of Marine Science, Univ. Alaska Fairbanks, 221 pp.

Short, J.W., G.V. Irvine, D.H. Mann, J.M. Maselko, J.J. Pella, M.R. Lindeberg, J.R. Payne, W.B. Driskell, and S.D. Rice. 2007. Slightly weathered *Exxon Valdez* oil persists in Gulf of Alaska beach sediments after 16 years. *Environmental Science & Technology*. 41(4): 1245-1250.

429 Wang, Zhendi and Scott A. Stout (ed.). 2007. Oil Spill Environmental Forensics: Fingerprinting and Source
430 Identification. Academic Press, New York.

APPENDICES

Appendix 1 – PAH and SHC Plots

Appendix 2 – Biomarker Plots

Appendix 3 – LTEMP PAH interpretation using multivariate scoring methods

APPENDIX 1 – PAH AND SHC PLOTS

This appendix contains plots for all 2008-2012 LTEMP samples. Sample ID code comprises station-matrix-year-season-rep, e.g., AMT-S-12-2-1 means Alyeska Marine Terminal, Sediment, 2012, summer (July), rep 1.

SEDIMENT

ALYESKA MARINE TERMINAL-- AMT

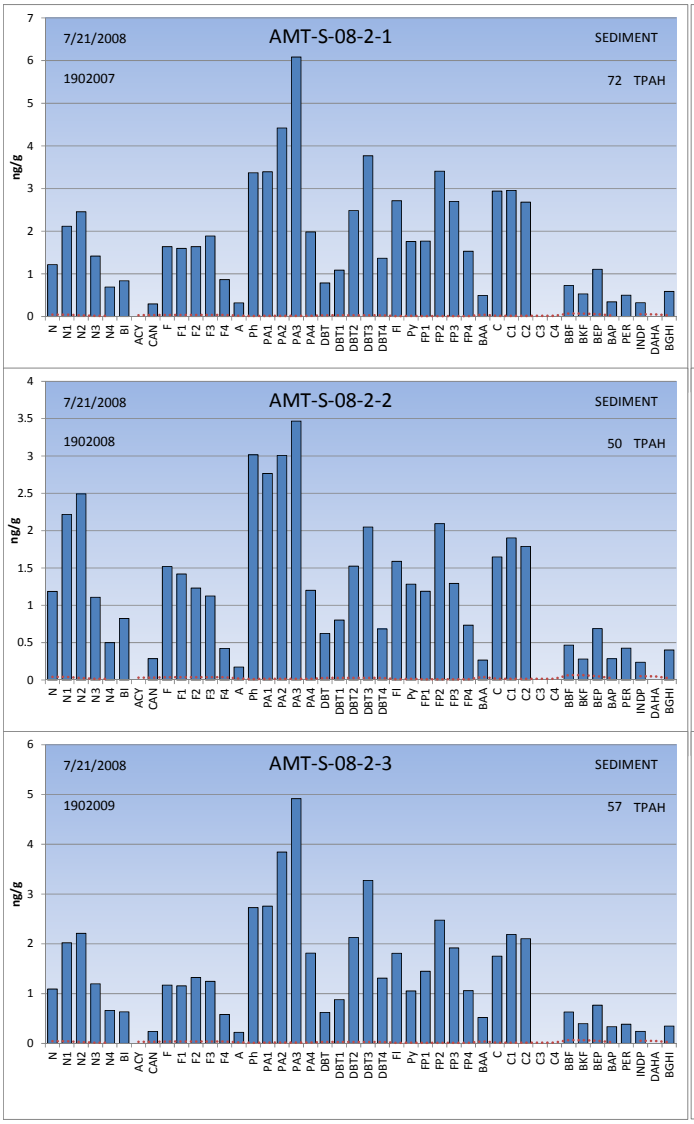

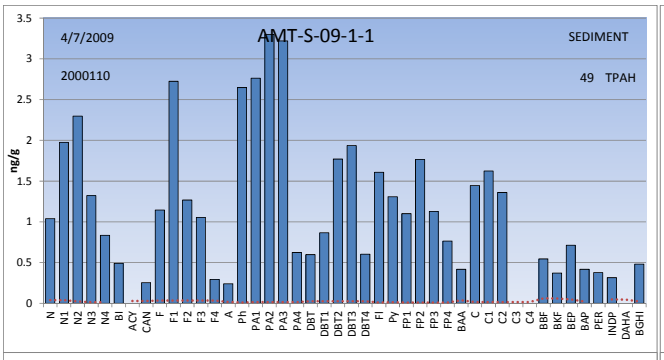
4/7/2009
AMT-S-09-1-1
SEDIMENT
2000110
49 TPAH
ng/g

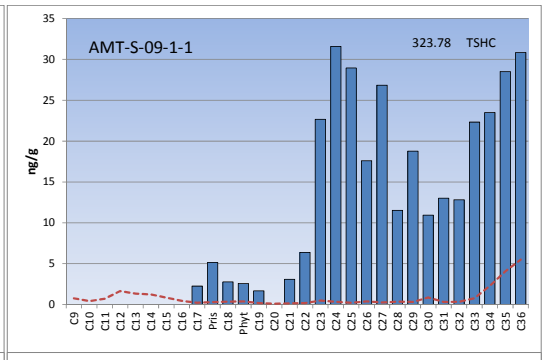
AMT-S-09-1-1
323.78 TSHC
ng/g

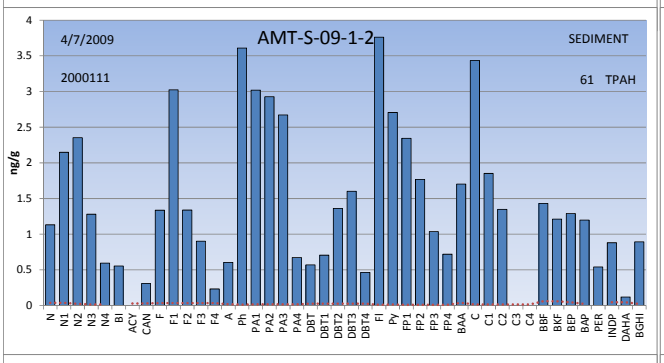
4/7/2009
AMT-S-09-1-2
SEDIMENT
2000111
61 TPAH
ng/g

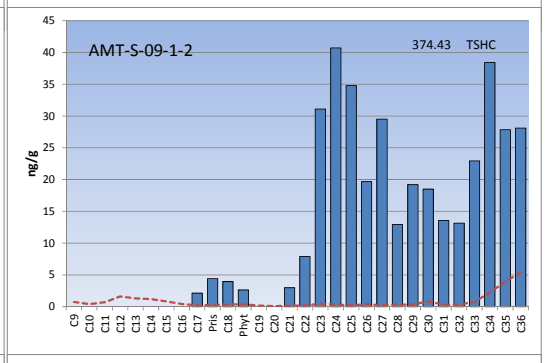
AMT-S-09-1-2
374.43 TSHC
ng/g

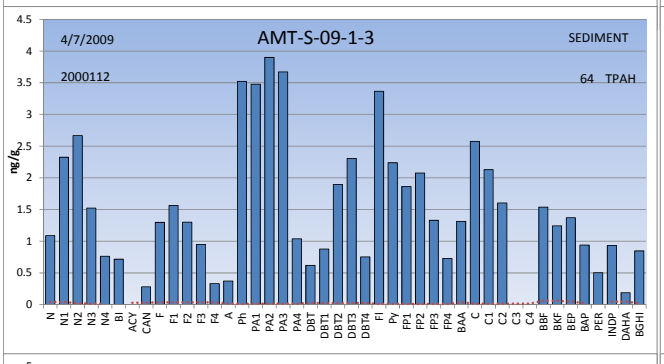
4/7/2009
AMT-S-09-1-3
SEDIMENT
2000112
64 TPAH
ng/g

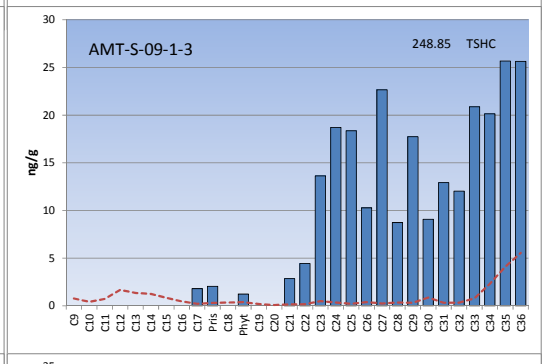
AMT-S-09-1-3
248.85 TSHC
ng/g

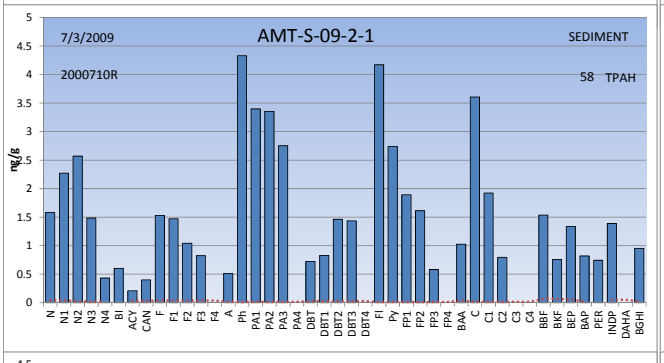
7/3/2009
AMT-S-09-2-1
SEDIMENT
2000710R
58 TPAH
ng/g

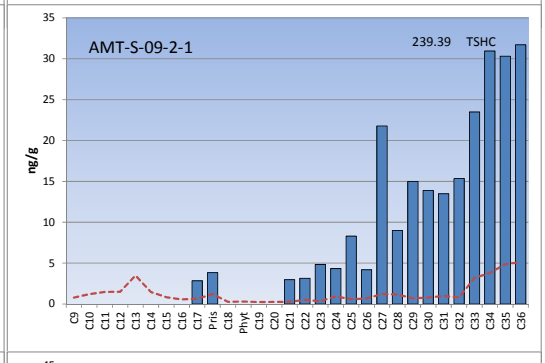
AMT-S-09-2-1
239.39 TSHC
ng/g

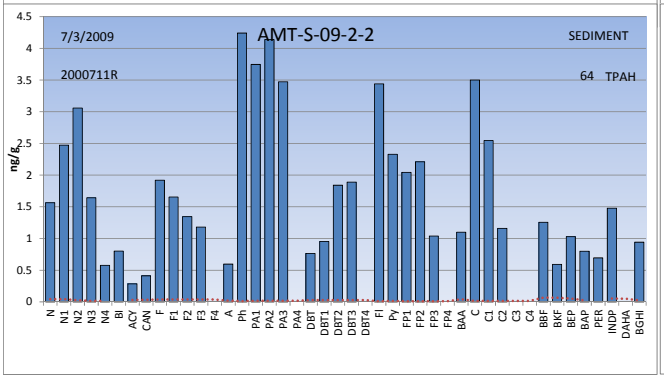
7/3/2009
AMT-S-09-2-2
SEDIMENT
2000711R
64 TPAH
ng/g

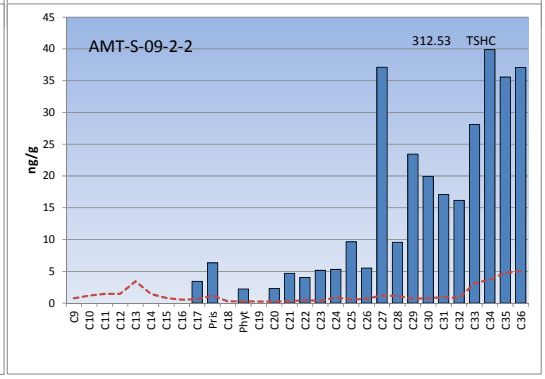
AMT-S-09-2-2
312.53 TSHC
ng/g

441

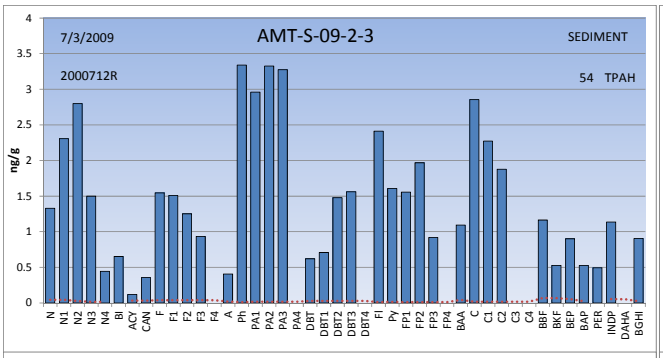
7/3/2009
AMT-S-09-2-3
SEDIMENT
2000712R
54 TPAH
ng/g

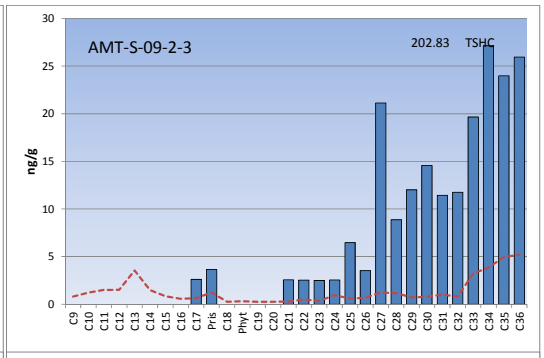
AMT-S-09-2-3
202.83 TSHC
ng/g

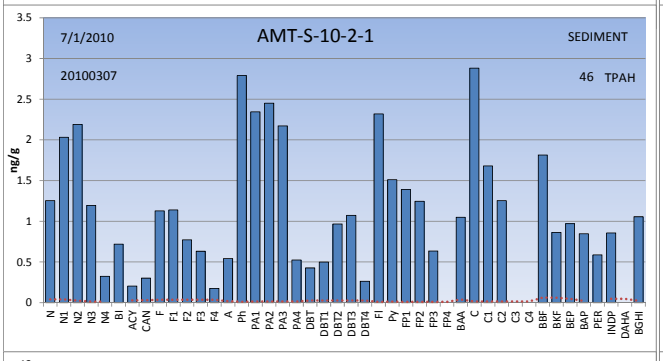
7/1/2010
AMT-S-10-2-1
SEDIMENT
20100307
46 TPAH
ng/g

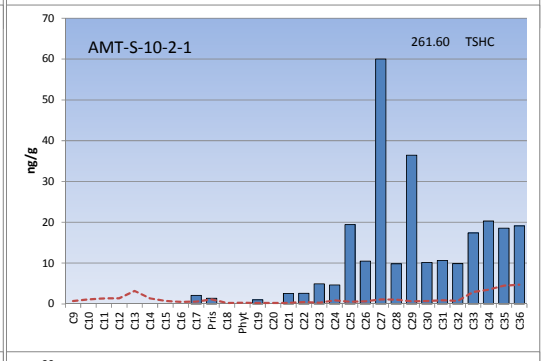
AMT-S-10-2-1
261.60 TSHC
ng/g

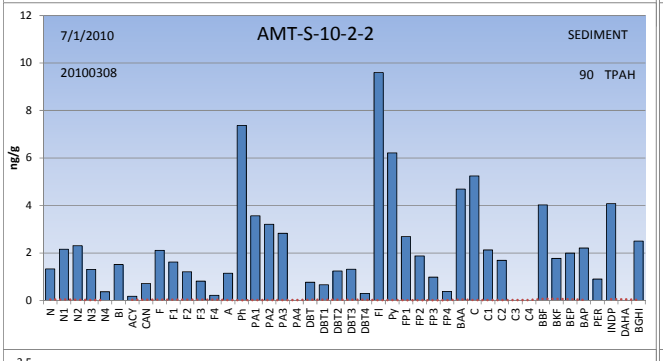
7/1/2010
AMT-S-10-2-2
SEDIMENT
20100308
90 TPAH
ng/g

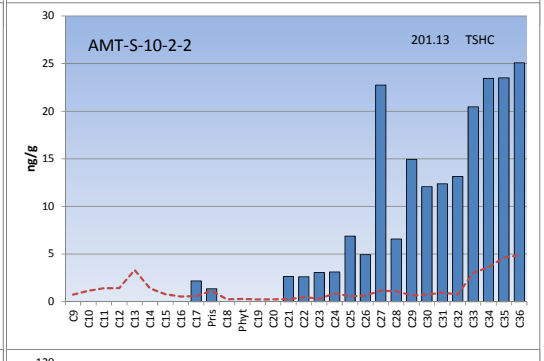
AMT-S-10-2-2
201.13 TSHC
ng/g

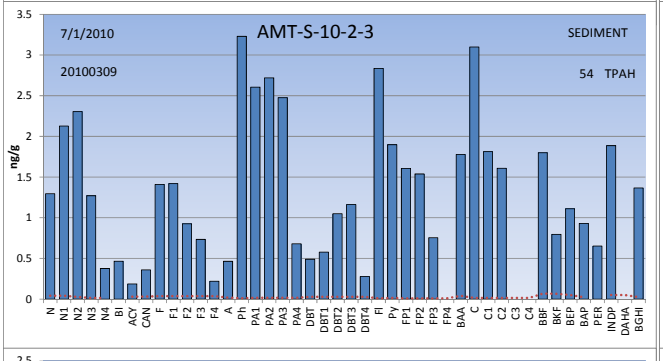
7/1/2010
AMT-S-10-2-3
SEDIMENT
20100309
54 TPAH
ng/g

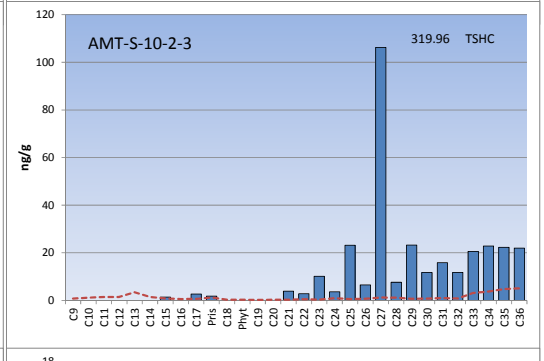
AMT-S-10-2-3
319.96 TSHC
ng/g

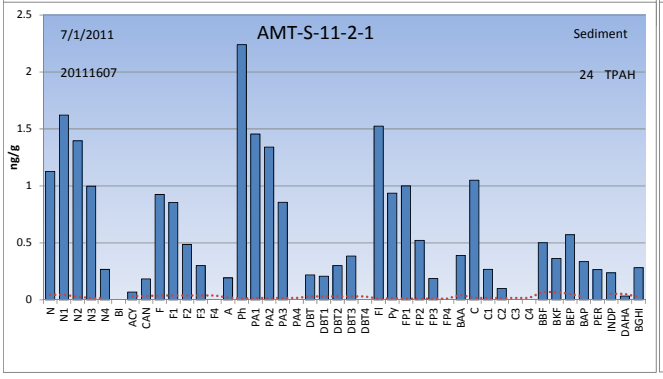
7/1/2011
AMT-S-11-2-1
Sediment
20111607
24 TPAH
ng/g

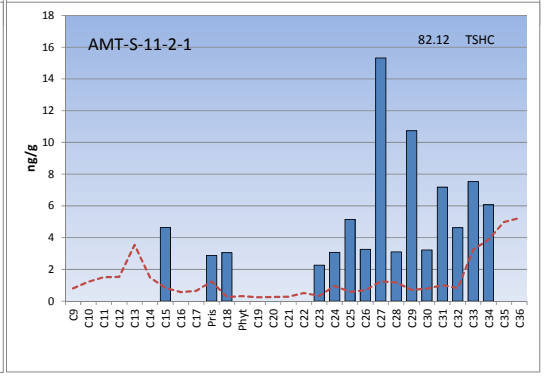
AMT-S-11-2-1
82.12 TSHC
ng/g

442

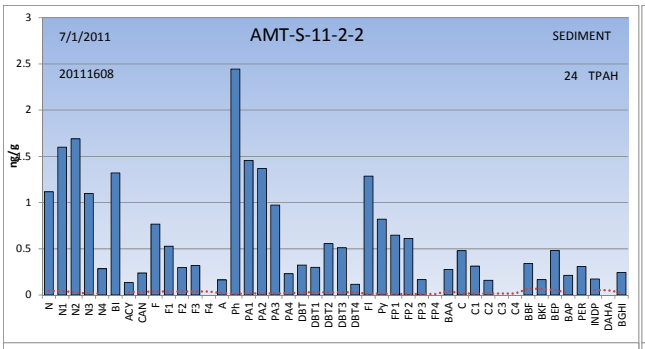
7/1/2011
AMT-S-11-2-2
SEDIMENT
20111608
24 TPAH
ng/g

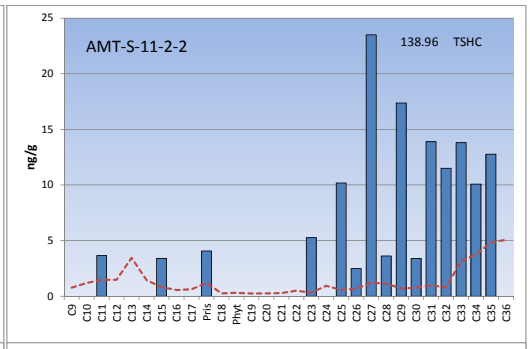
AMT-S-11-2-2
138.96 TSHC
ng/g

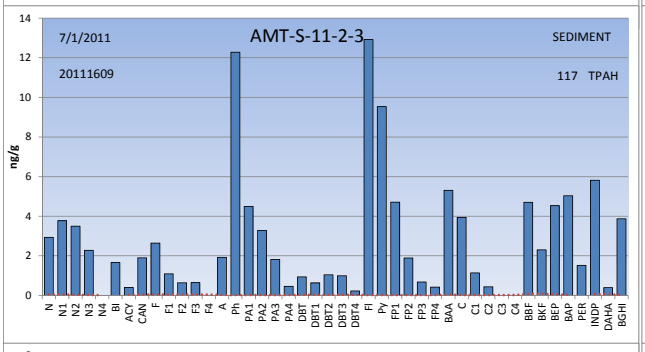
7/1/2011
AMT-S-11-2-3
SEDIMENT
20111609
117 TPAH
ng/g

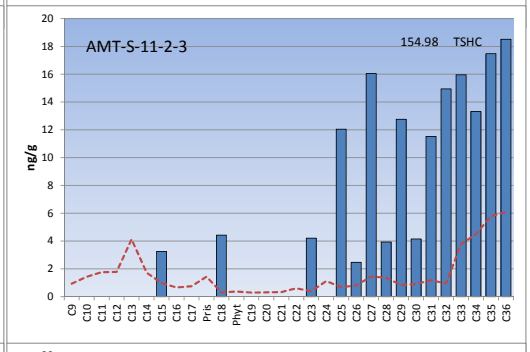
AMT-S-11-2-3
154.98 TSHC
ng/g

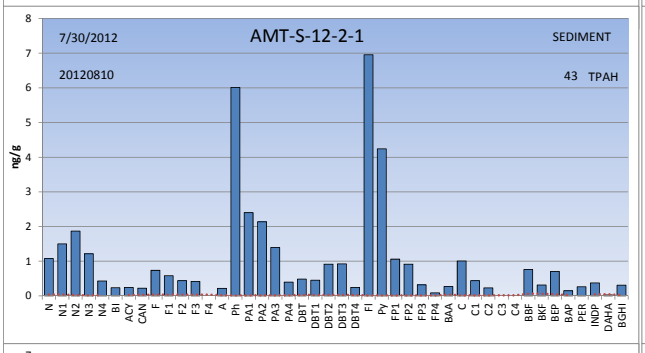
7/30/2012
AMT-S-12-2-1
SEDIMENT
20120810
43 TPAH
ng/g

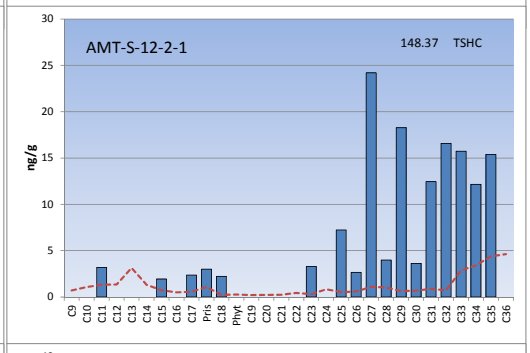
AMT-S-12-2-1
148.37 TSHC
ng/g

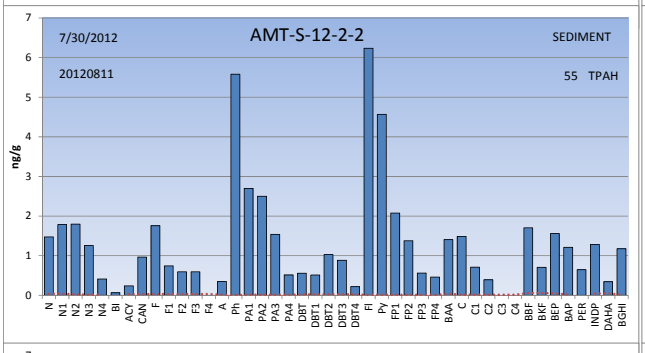
7/30/2012
AMT-S-12-2-2
SEDIMENT
20120811
55 TPAH
ng/g

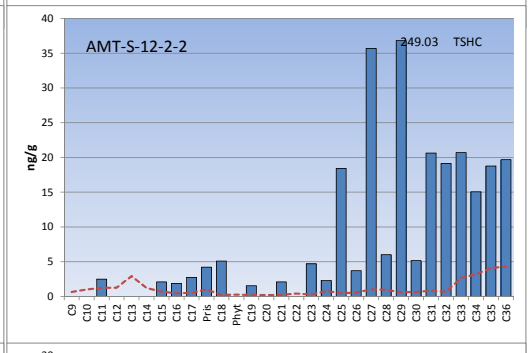
AMT-S-12-2-2
249.03 TSHC
ng/g

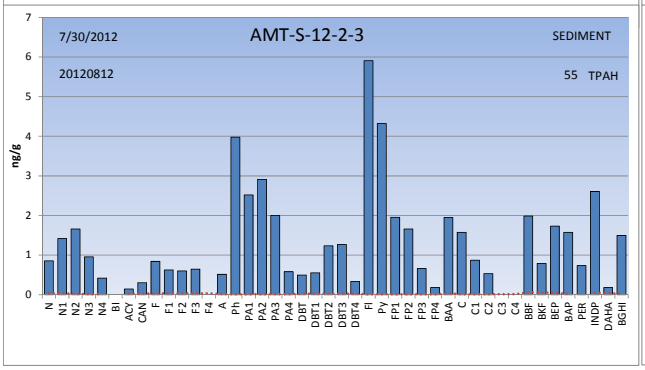
7/30/2012
AMT-S-12-2-3
SEDIMENT
20120812
55 TPAH
ng/g

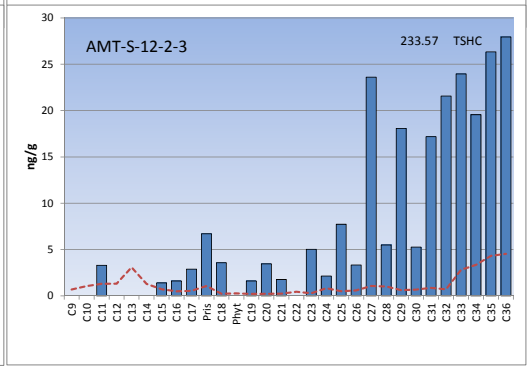
AMT-S-12-2-3
233.57 TSHC
ng/g

443

GOLD CREEK -- GOC

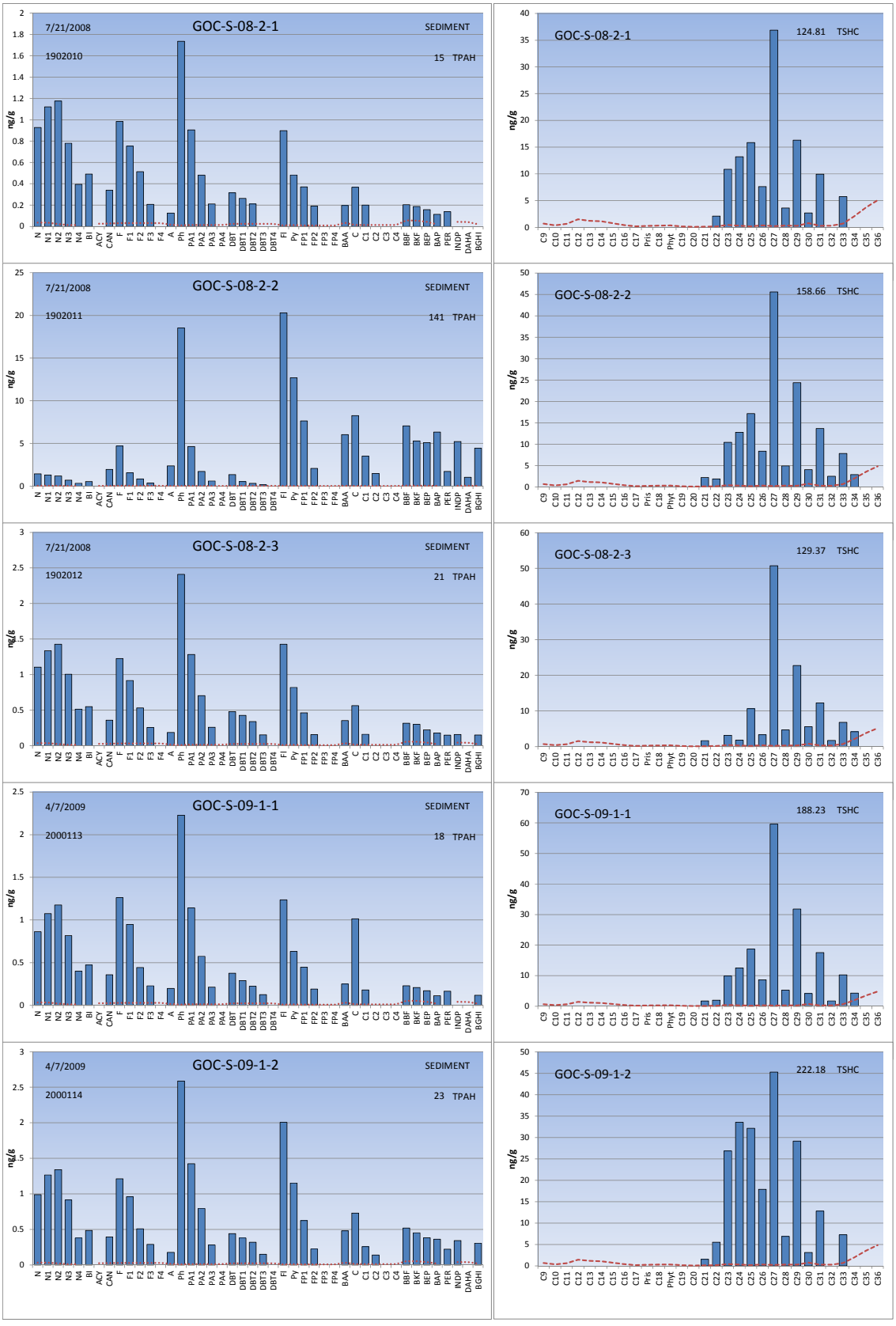

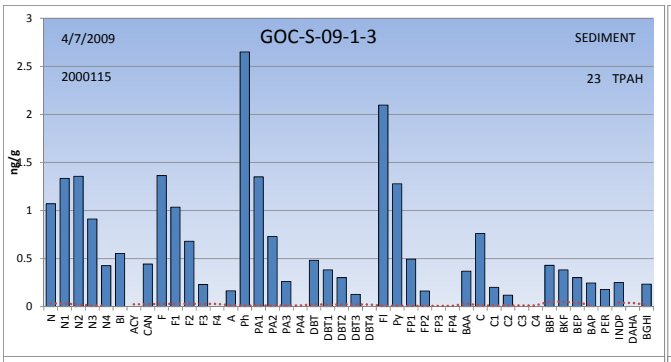
4/7/2009
2000115
GOC-S-09-1-3
SEDIMENT
23 TPAH
ng/g

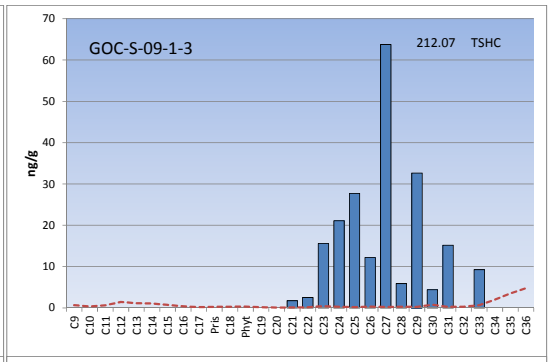
GOC-S-09-1-3
212.07 TSHC
ng/g

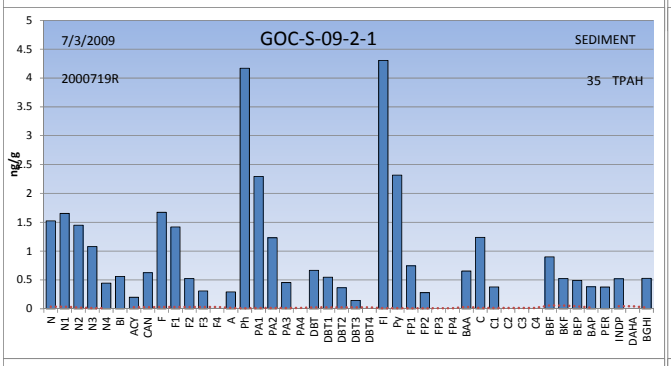
7/3/2009
2000719R
GOC-S-09-2-1
SEDIMENT
35 TPAH
ng/g

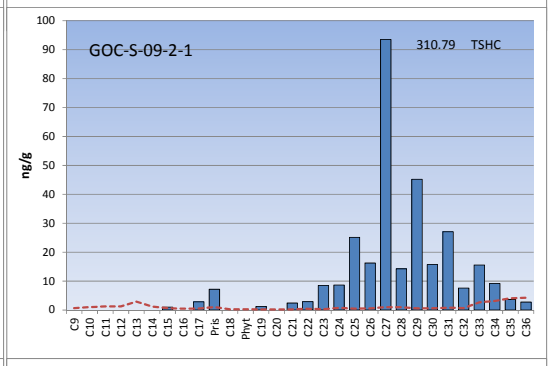
GOC-S-09-2-1
310.79 TSHC
ng/g

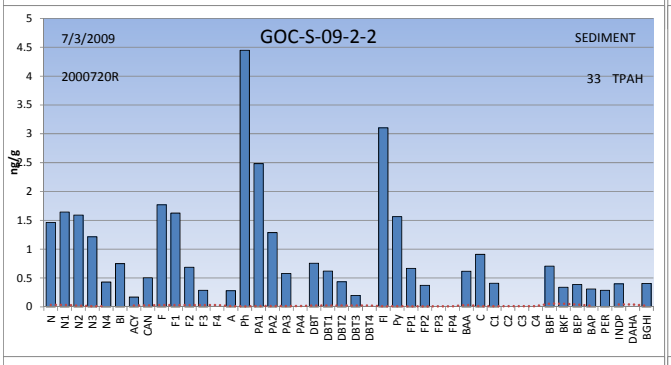
7/3/2009
2000720R
GOC-S-09-2-2
SEDIMENT
33 TPAH
ng/g

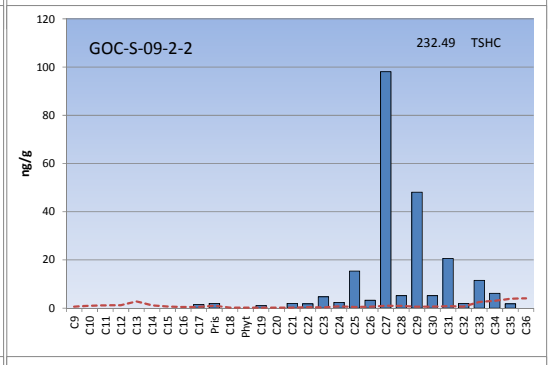
GOC-S-09-2-2
232.49 TSHC
ng/g

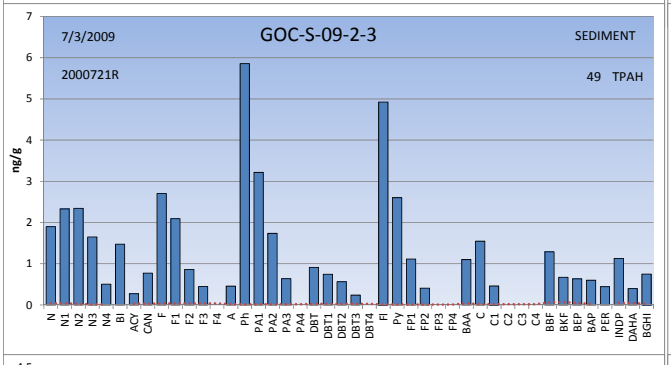
7/3/2009
2000721R
GOC-S-09-2-3
SEDIMENT
49 TPAH
ng/g

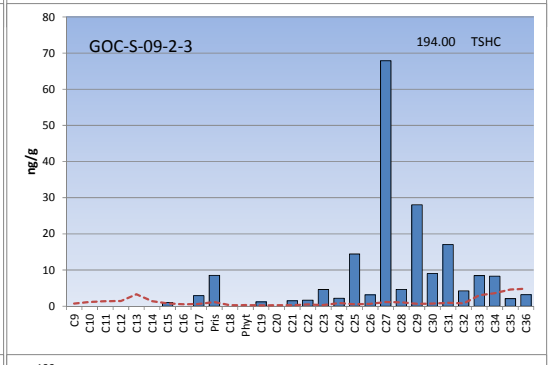
GOC-S-09-2-3
194.00 TSHC
ng/g

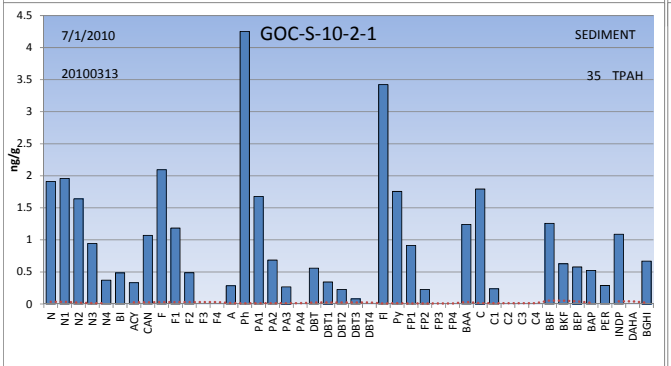
7/1/2010
20100313
GOC-S-10-2-1
SEDIMENT
35 TPAH
ng/g

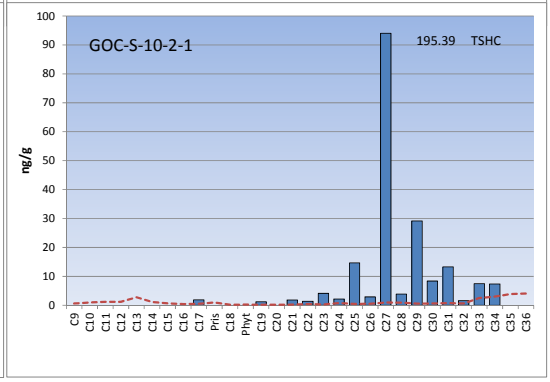
GOC-S-10-2-1
195.39 TSHC
ng/g

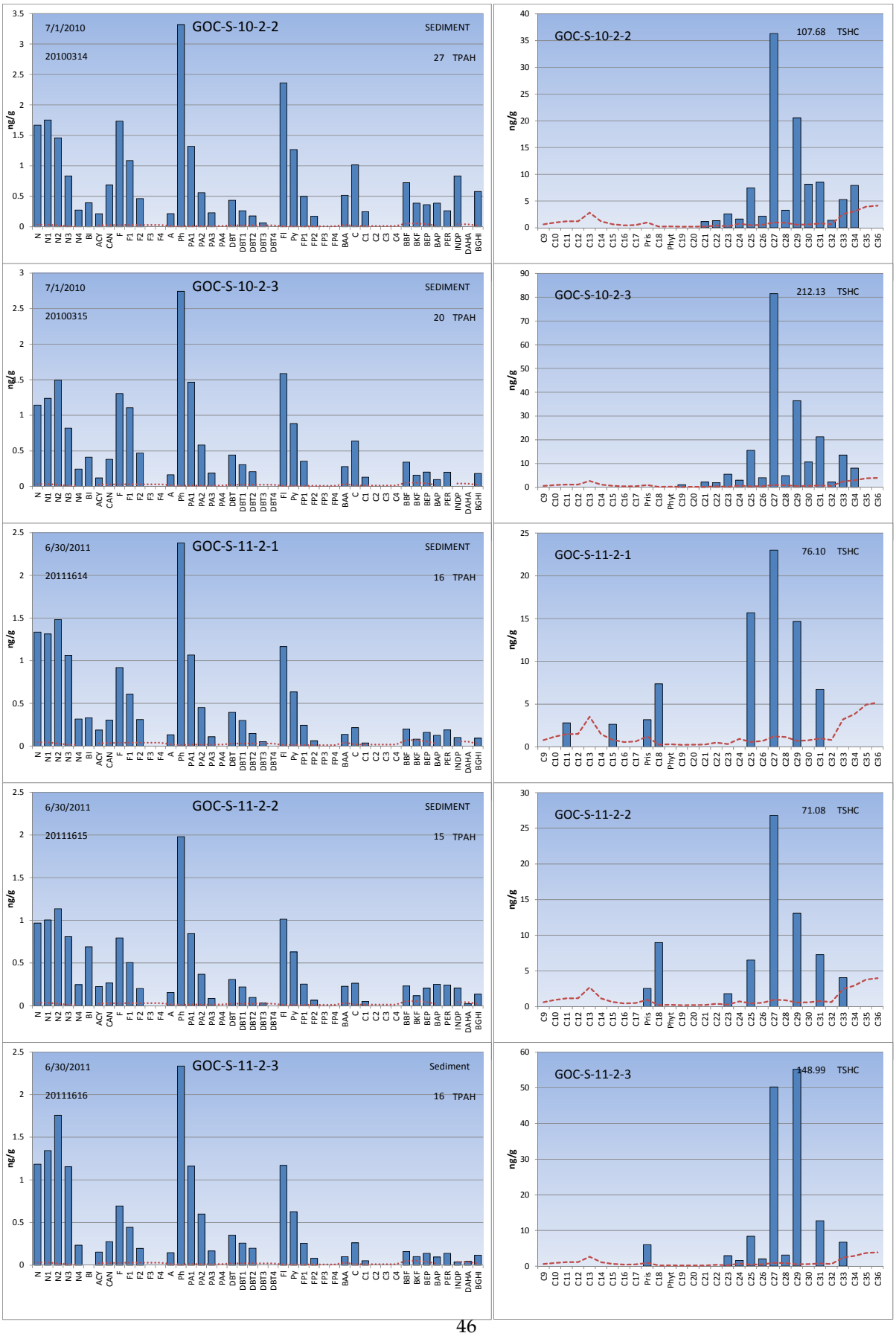
7/1/2010
GOC-S-10-2-2
SEDIMENT
20100314
27 TPAH
GOC-S-10-2-2
107.68 TSHC
7/1/2010
GOC-S-10-2-3
SEDIMENT
20100315
20 TPAH
GOC-S-10-2-3
212.13 TSHC
6/30/2011
GOC-S-11-2-1
SEDIMENT
20111614
16 TPAH
GOC-S-11-2-1
76.10 TSHC
6/30/2011
GOC-S-11-2-2
SEDIMENT
20111615
15 TPAH
GOC-S-11-2-2
71.08 TSHC
6/30/2011
GOC-S-11-2-3
Sediment
20111616
16 TPAH
GOC-S-11-2-3
148.99 TSHC
ng/g

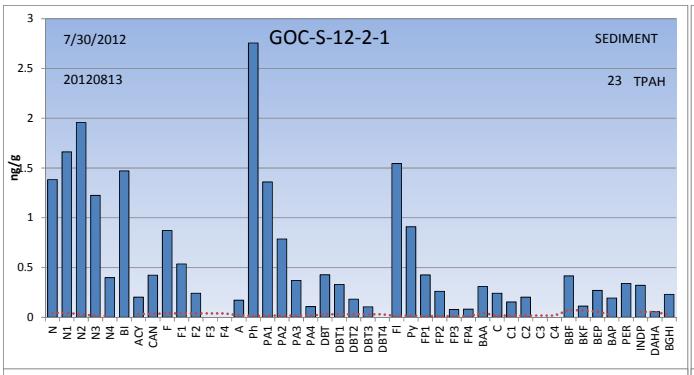
7/30/2012
GOC-S-12-2-1
SEDIMENT
20120813
23 TPAH
ng/g
N N1 N2 N3 N4 BI ACY CAN F F1 F2 F3 F4 A Ph PA1 PA2 PA3 PA4 DBT DBT1 DBT2 DBT3 DBT4 FI Py FP1 FP2 FP3 FP4 BAA C C1 C2 C3 C4 BBF BKF BEP BAP PER INDP DAHA BGHI

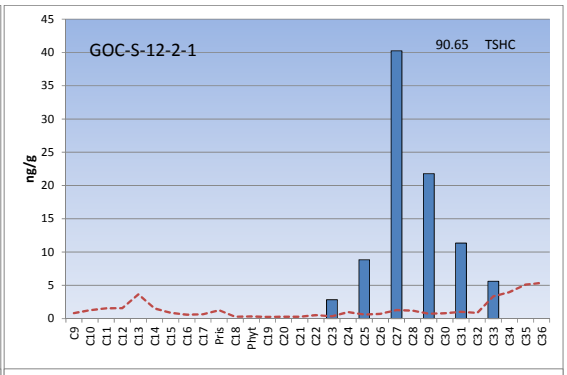
GOC-S-12-2-1
90.65 TSHC
ng/g
C9 C10 C11 C12 C13 C14 C15 C16 C17 Pr5 C18 Phyt C19 C20 C21 C22 C23 C24 C25 C26 C27 C28 C29 C30 C31 C32 C33 C34 C35 C36

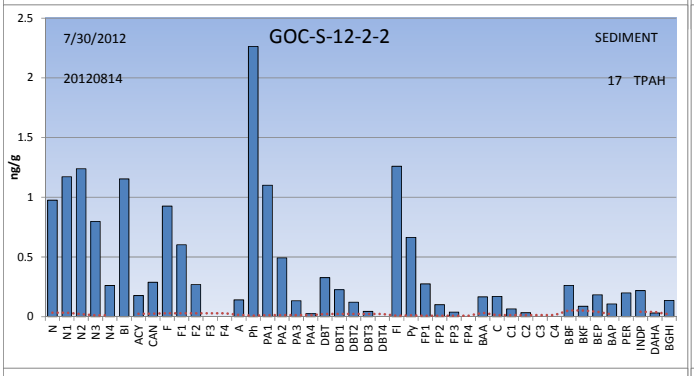
7/30/2012
GOC-S-12-2-2
SEDIMENT
20120814
17 TPAH
ng/g
N N1 N2 N3 N4 BI ACY CAN F F1 F2 F3 F4 A Ph PA1 PA2 PA3 PA4 DBT DBT1 DBT2 DBT3 DBT4 FI Py FP1 FP2 FP3 FP4 BAA C C1 C2 C3 C4 BBF BKF BEP BAP PER INDP DAHA BGHI

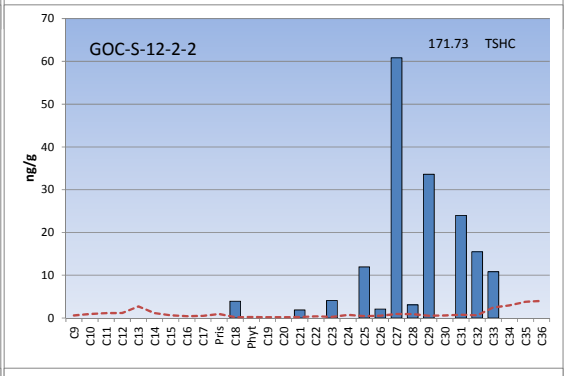
GOC-S-12-2-2
171.73 TSHC
ng/g
C9 C10 C11 C12 C13 C14 C15 C16 C17 Pr5 C18 Phyt C19 C20 C21 C22 C23 C24 C25 C26 C27 C28 C29 C30 C31 C32 C33 C34 C35 C36

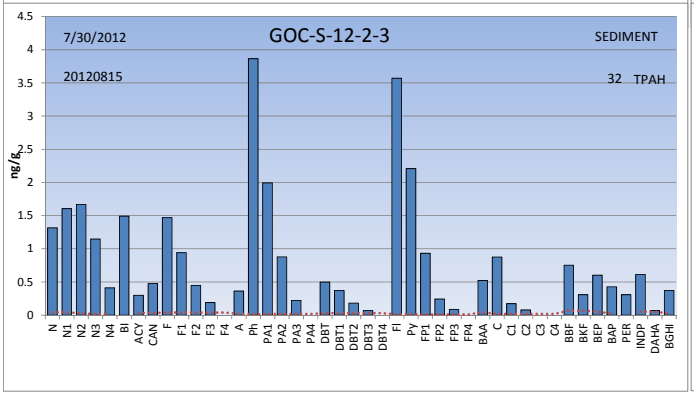
7/30/2012
GOC-S-12-2-3
SEDIMENT
20120815
32 TPAH
ng/g
N N1 N2 N3 N4 BI ACY CAN F F1 F2 F3 F4 A Ph PA1 PA2 PA3 PA4 DBT DBT1 DBT2 DBT3 DBT4 FI Py FP1 FP2 FP3 FP4 BAA C C1 C2 C3 C4 BBF BKF BEP BAP PER INDP DAHA BGHI

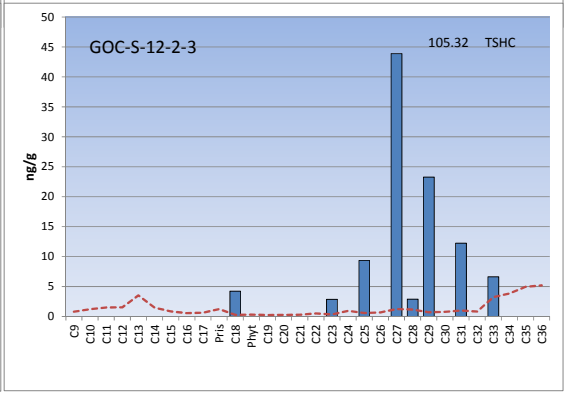
GOC-S-12-2-3
105.32 TSHC
ng/g
C9 C10 C11 C12 C13 C14 C15 C16 C17 Pr5 C18 Phyt C19 C20 C21 C22 C23 C24 C25 C26 C27 C28 C29 C30 C31 C32 C33 C34 C35 C36

448

449 TISSUES

450 ALYESKA MARINE TERMINAL--AMT

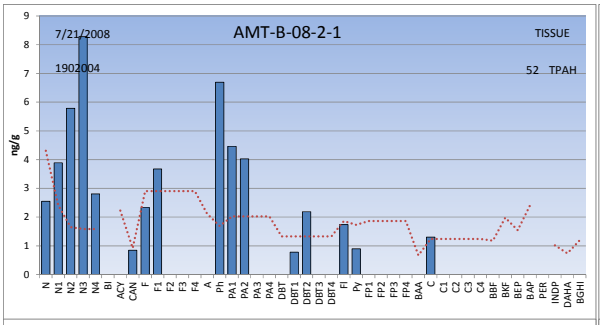

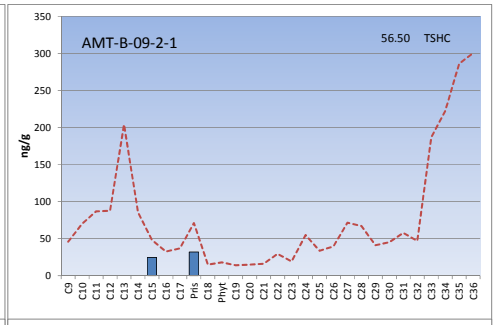

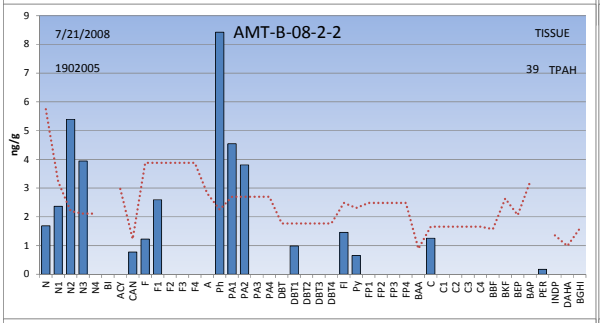

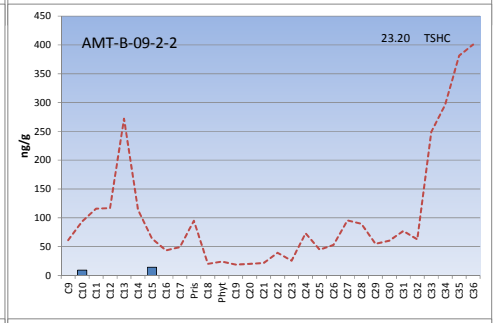

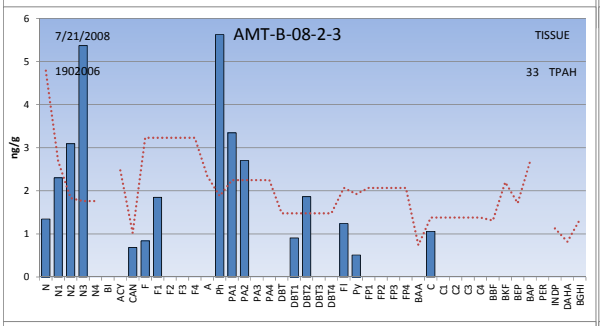

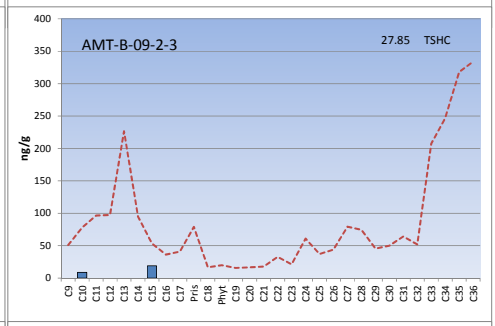

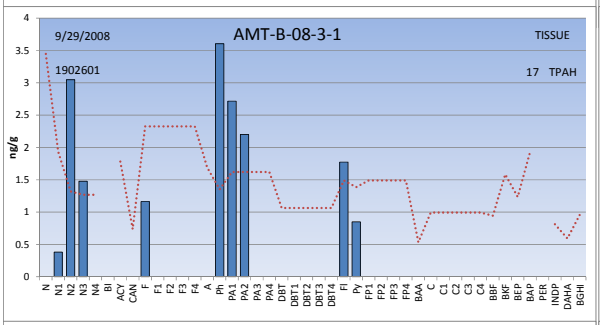

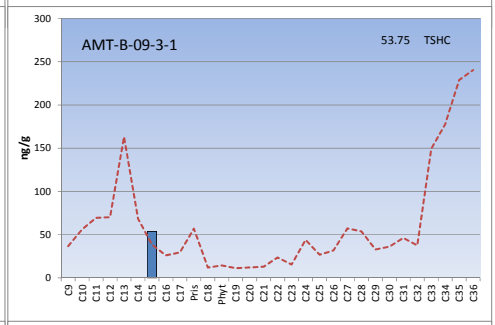

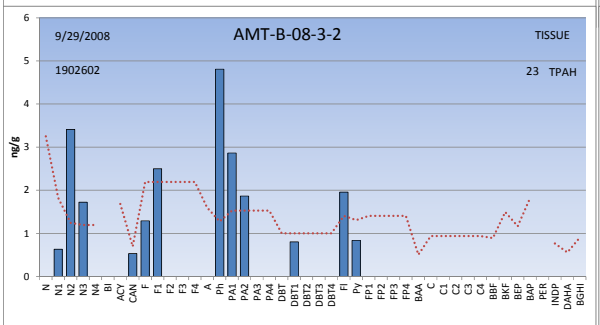

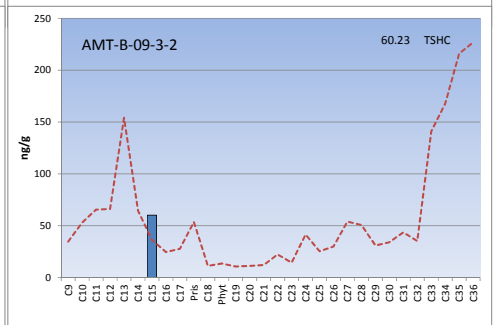

451

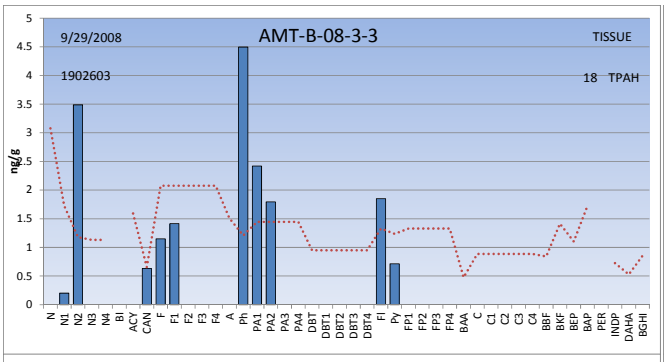
9/29/2008
AMT-B-08-3-3
TISSUE
1902603
18 TPAH
ng/g

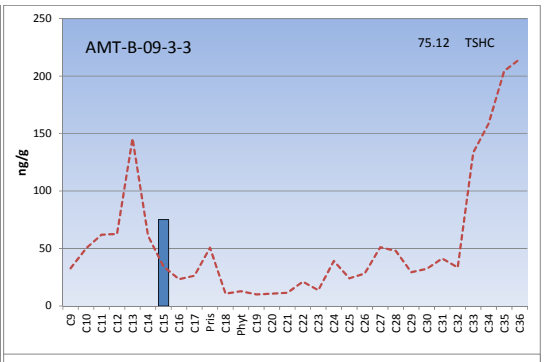
AMT-B-09-3-3
75.12 TSHC
ng/g

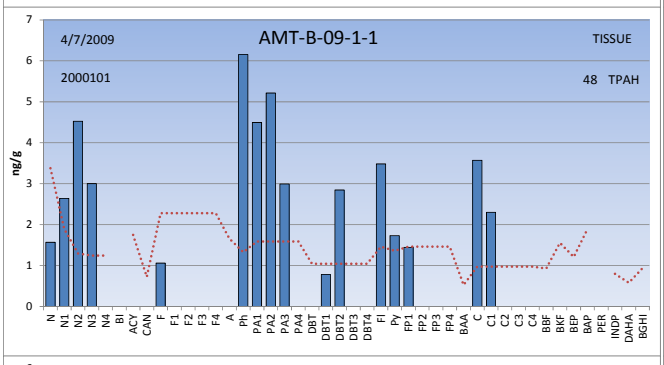
4/7/2009
AMT-B-09-1-1
TISSUE
2000101
48 TPAH
ng/g

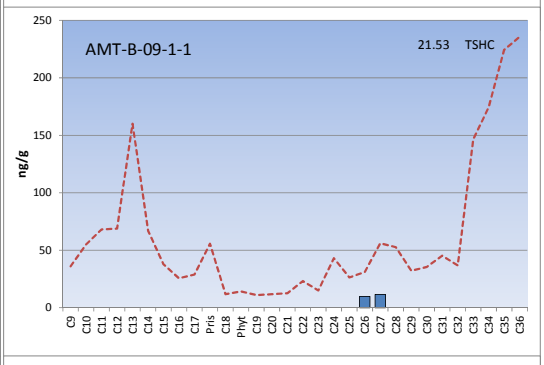
AMT-B-09-1-1
21.53 TSHC
ng/g

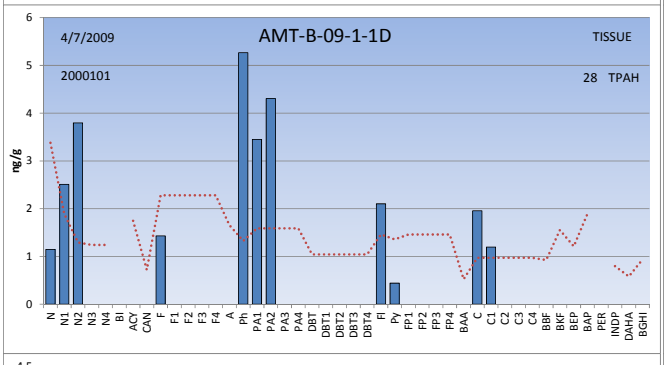
4/7/2009
AMT-B-09-1-1D
TISSUE
2000101
28 TPAH
ng/g

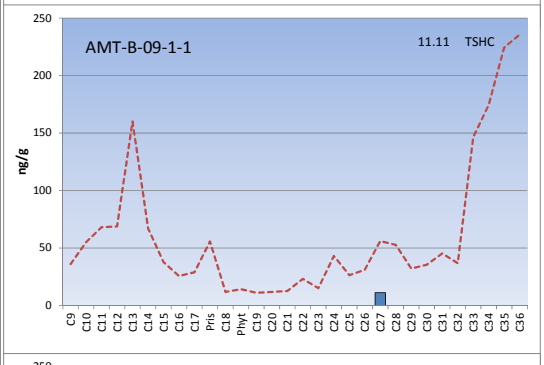
AMT-B-09-1-1
11.11 TSHC
ng/g

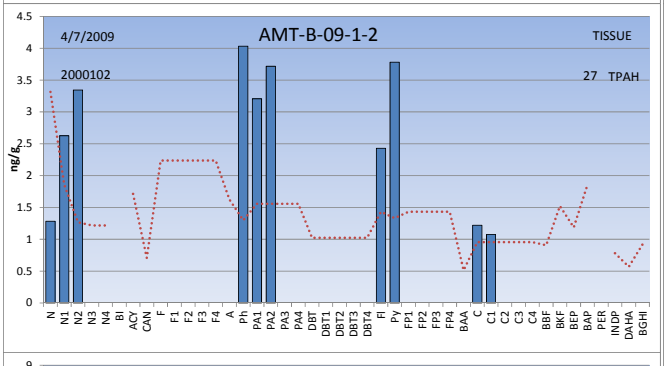
4/7/2009
AMT-B-09-1-2
TISSUE
2000102
27 TPAH
ng/g

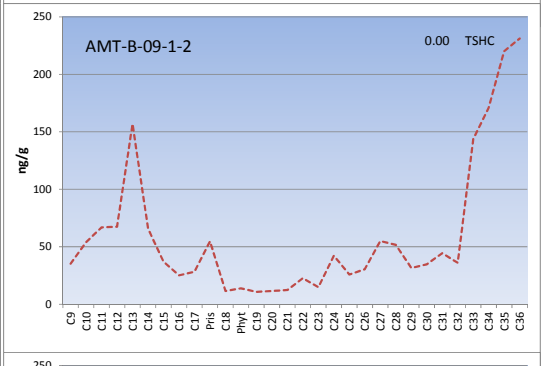
AMT-B-09-1-2
0.00 TSHC
ng/g

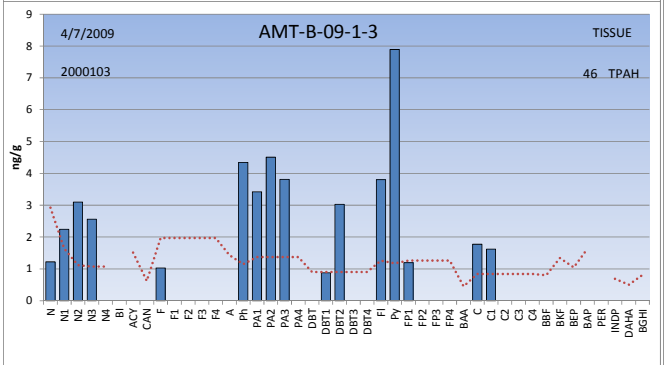
4/7/2009
AMT-B-09-1-3
TISSUE
2000103
46 TPAH
ng/g

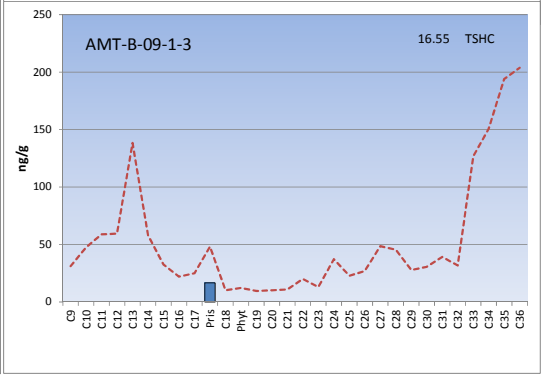
AMT-B-09-1-3
16.55 TSHC
ng/g

452

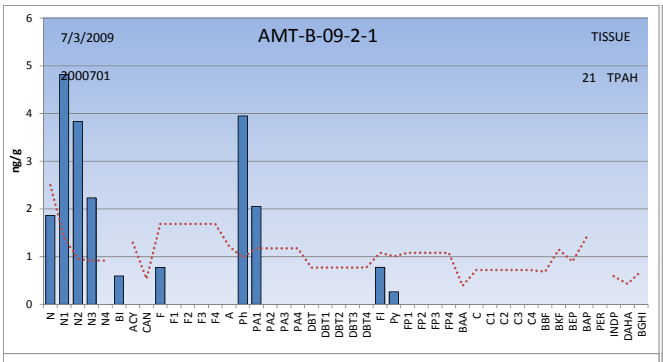
7/3/2009
AMT-B-09-2-1
TISSUE
2000701
21 TPAH
ng/g

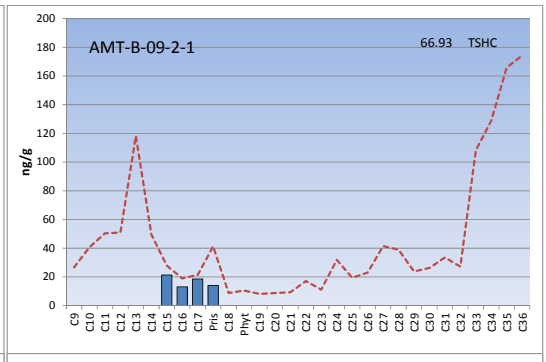
AMT-B-09-2-1
66.93 TSHC
ng/g

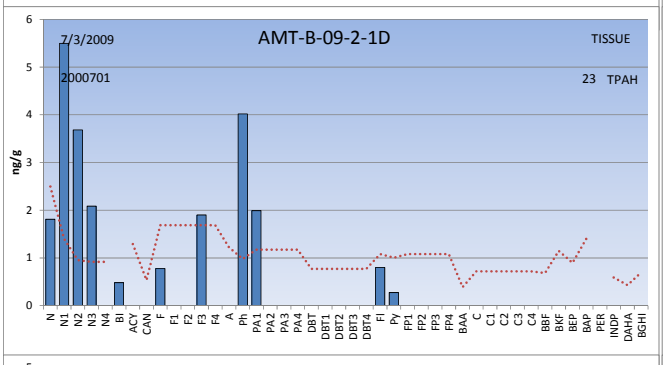
7/3/2009
AMT-B-09-2-1D
TISSUE
2000701
23 TPAH
ng/g

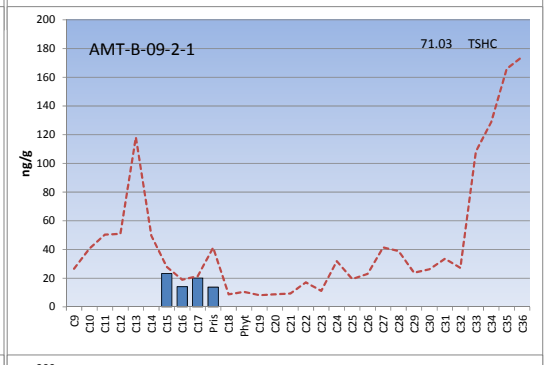
AMT-B-09-2-1
71.03 TSHC
ng/g

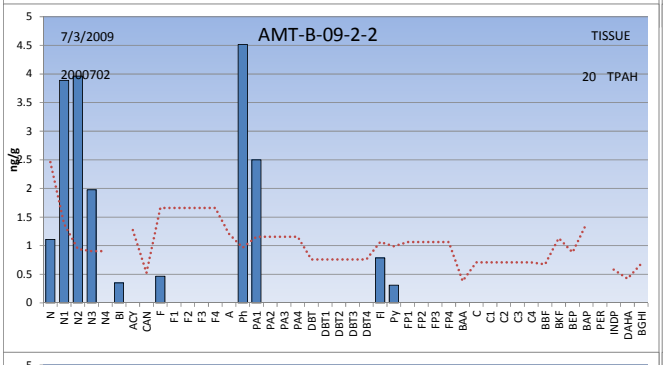
7/3/2009
AMT-B-09-2-2
TISSUE
2000702
20 TPAH
ng/g

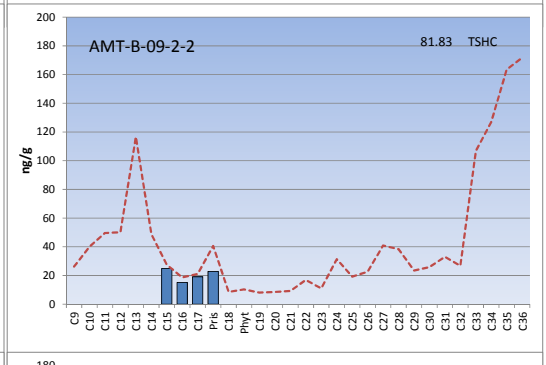
AMT-B-09-2-2
81.83 TSHC
ng/g

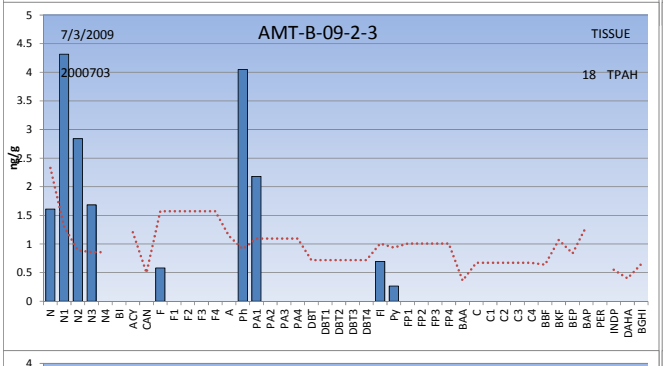
7/3/2009
AMT-B-09-2-3
TISSUE
2000703
18 TPAH
ng/g

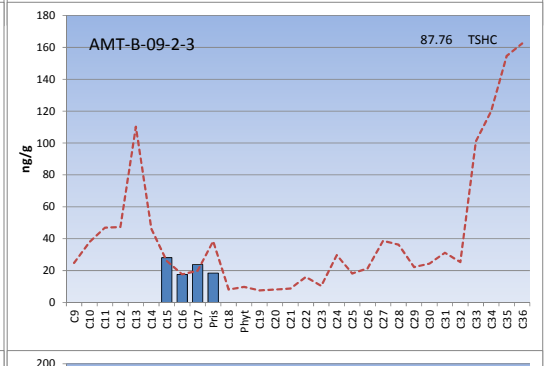
AMT-B-09-2-3
87.76 TSHC
ng/g

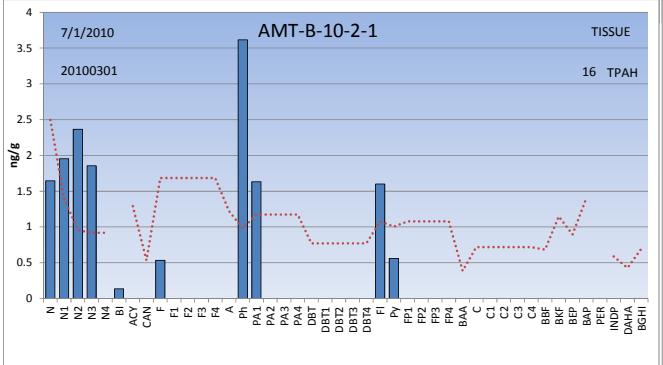
7/1/2010
AMT-B-10-2-1
TISSUE
20100301
16 TPAH
ng/g

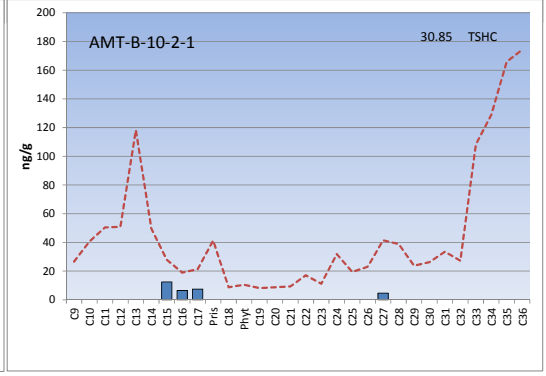
AMT-B-10-2-1
30.85 TSHC
ng/g

453

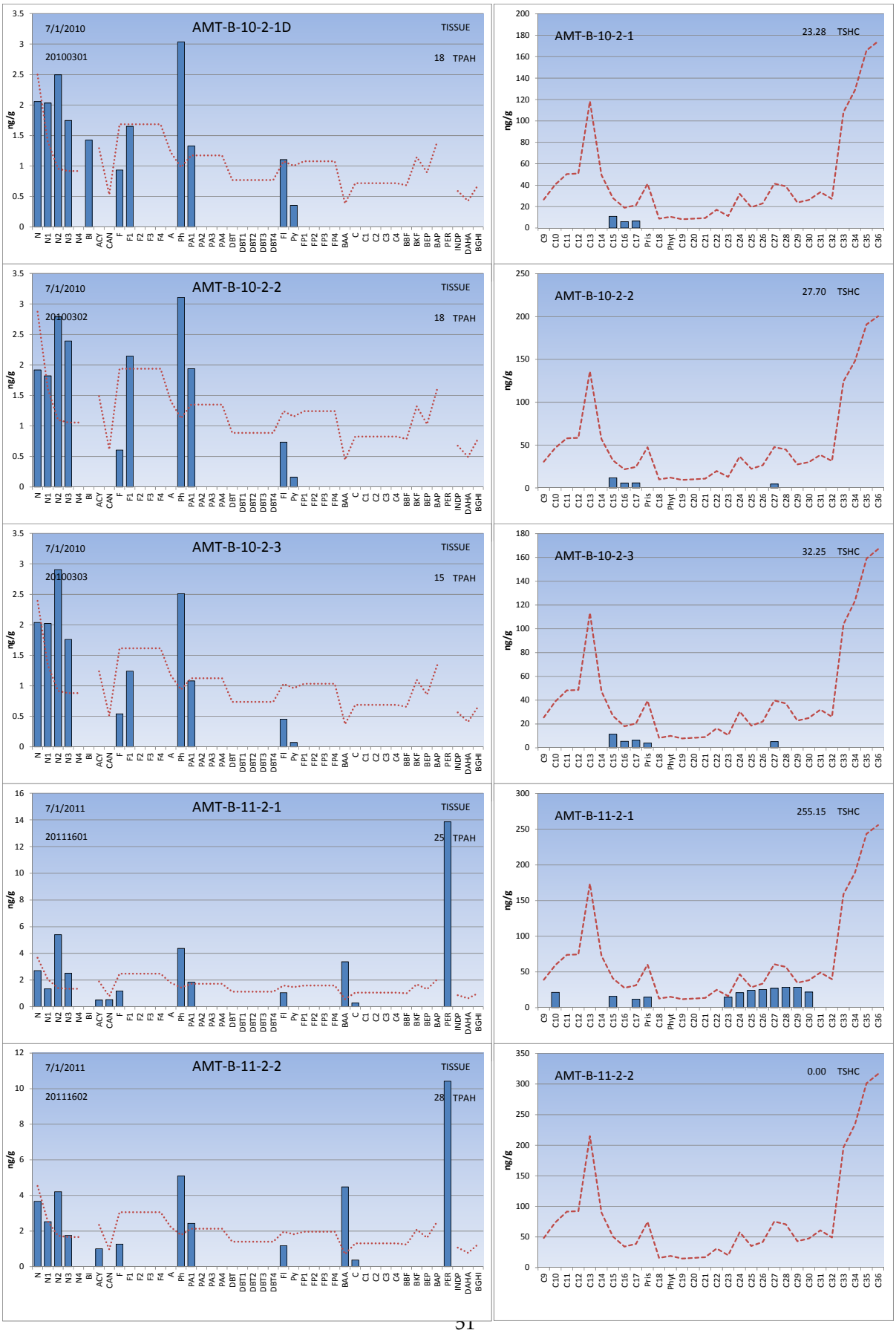
7/1/2010
AMT-B-10-2-1D
TISSUE
20100301
18 TPAH
ng/g
AMT-B-10-2-1
23.28 TSHC
7/1/2010
AMT-B-10-2-2
TISSUE
20100302
18 TPAH
AMT-B-10-2-2
27.70 TSHC
7/1/2010
AMT-B-10-2-3
TISSUE
20100303
15 TPAH
AMT-B-10-2-3
32.25 TSHC
7/1/2011
AMT-B-11-2-1
TISSUE
20111601
25 TPAH
AMT-B-11-2-1
255.15 TSHC
7/1/2011
AMT-B-11-2-2
TISSUE
20111602
28 TPAH
AMT-B-11-2-2
0.00 TSHC

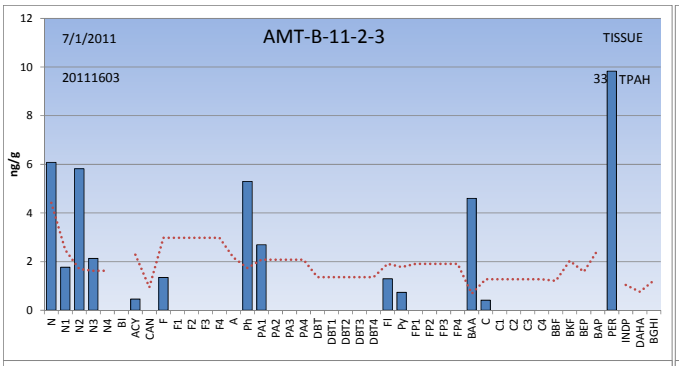
7/1/2011
AMT-B-11-2-3
TISSUE
20111603
33 TPAH
ng/g

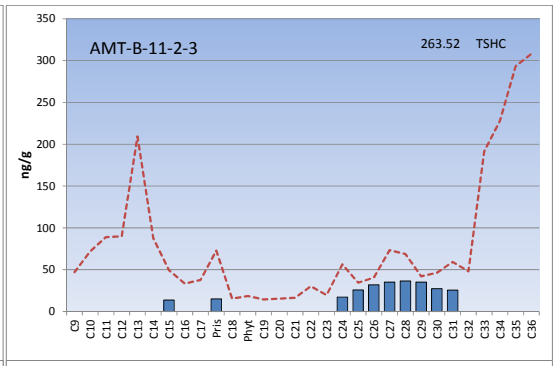
AMT-B-11-2-3
263.52 TSHC
ng/g

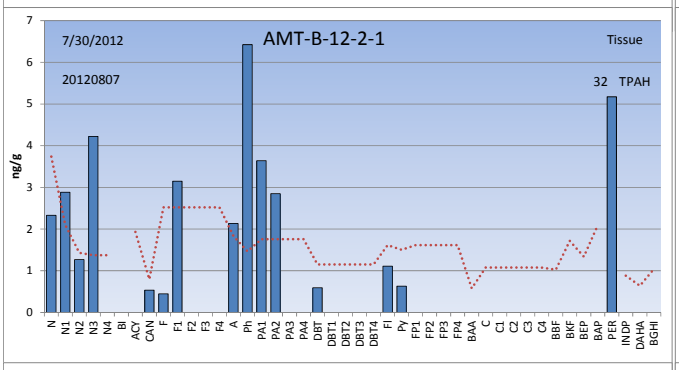
7/30/2012
AMT-B-12-2-1
Tissue
20120807
32 TPAH
ng/g

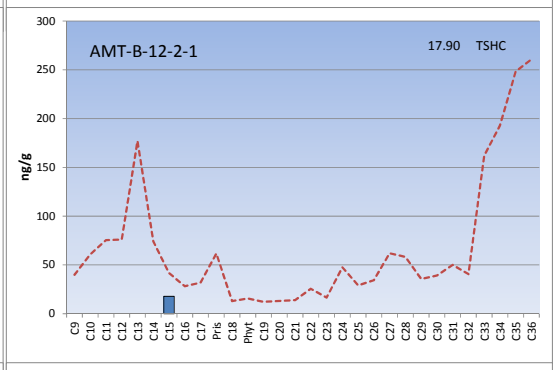
AMT-B-12-2-1
17.90 TSHC
ng/g

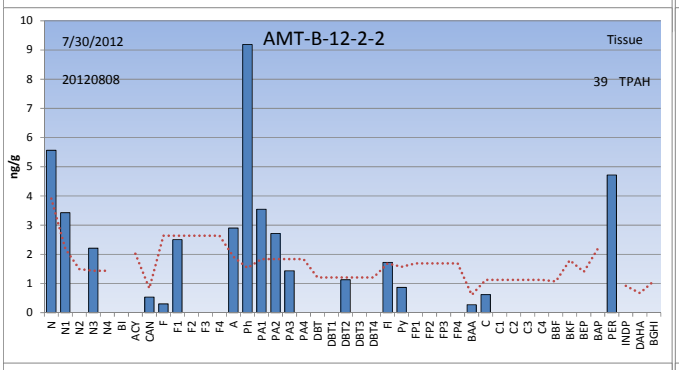
7/30/2012
AMT-B-12-2-2
Tissue
20120808
39 TPAH
ng/g

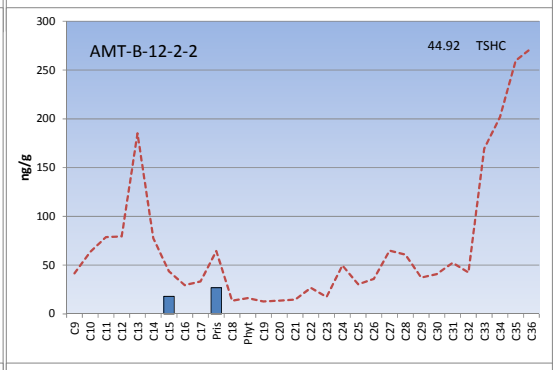
AMT-B-12-2-2
44.92 TSHC
ng/g

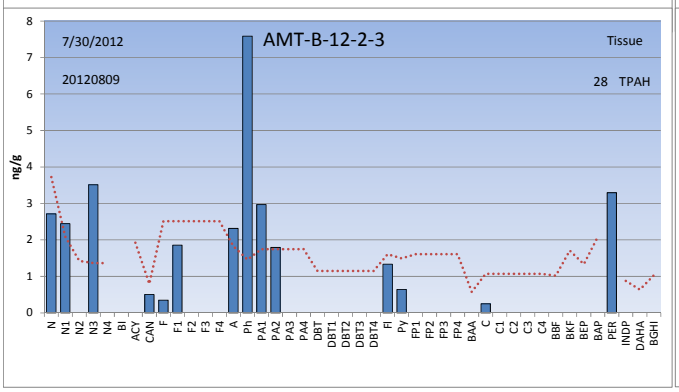
7/30/2012
AMT-B-12-2-3
Tissue
20120809
28 TPAH
ng/g

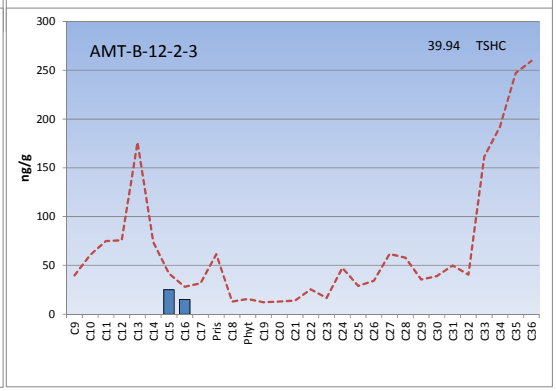
AMT-B-12-2-3
39.94 TSHC
ng/g

455

GOLD CREEK--GOC

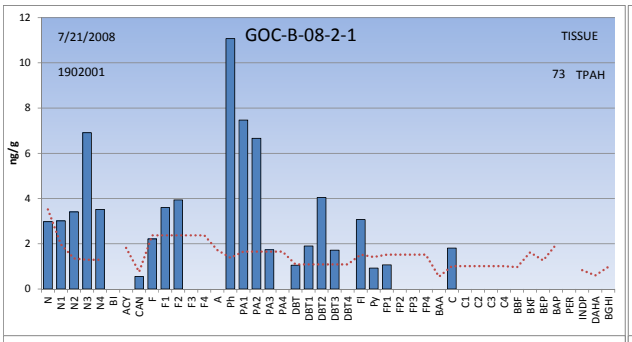

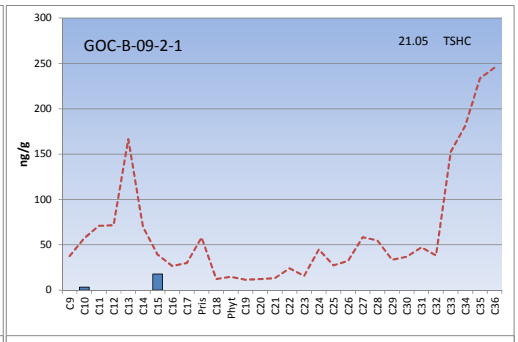

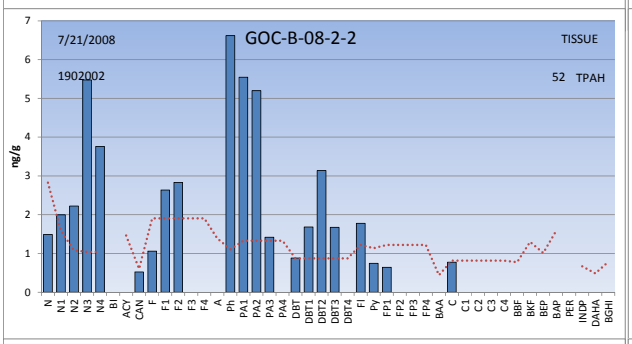

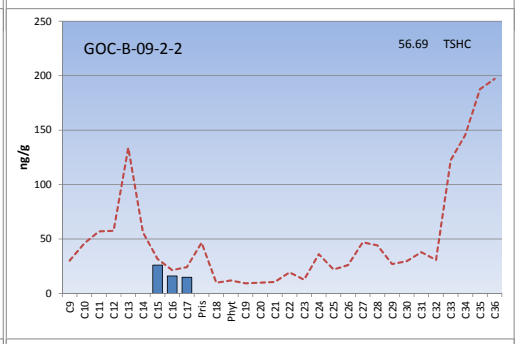

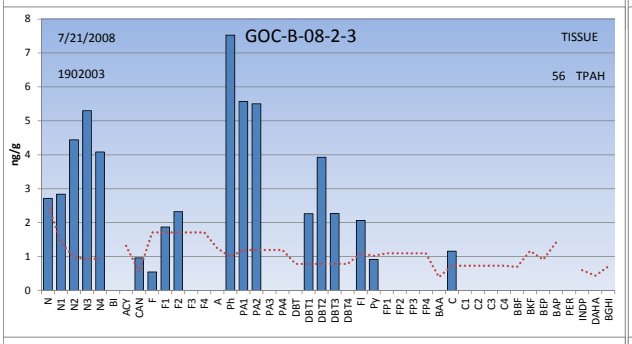

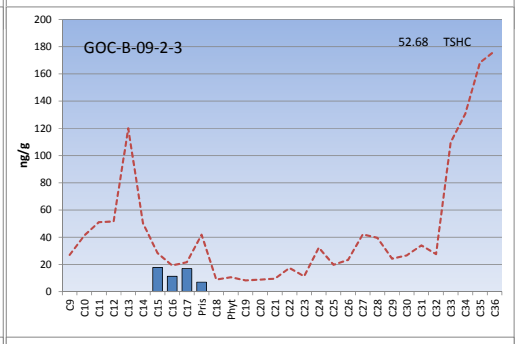

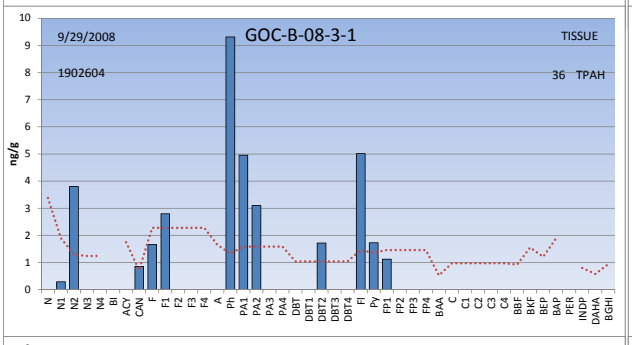

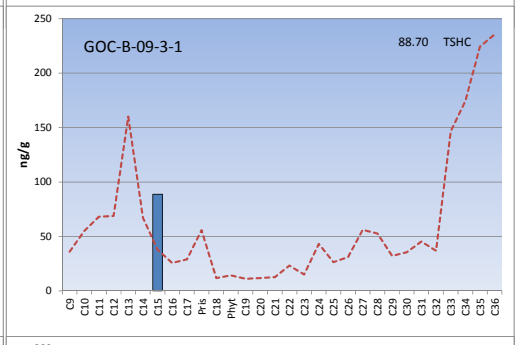

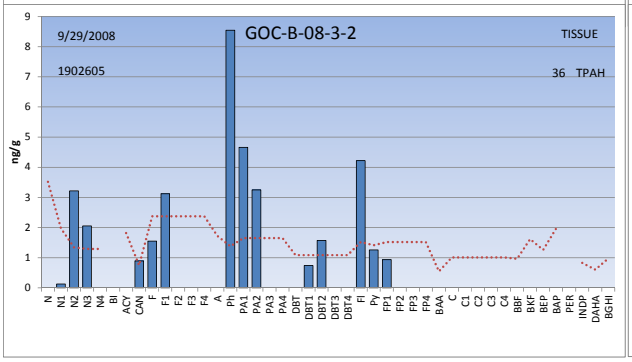

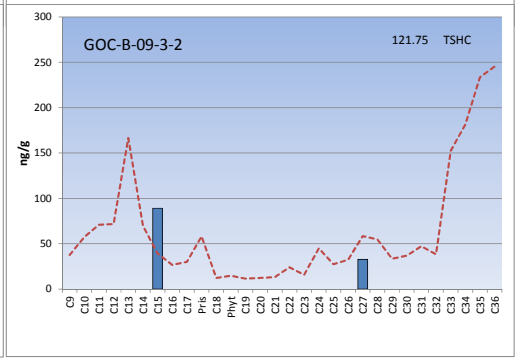

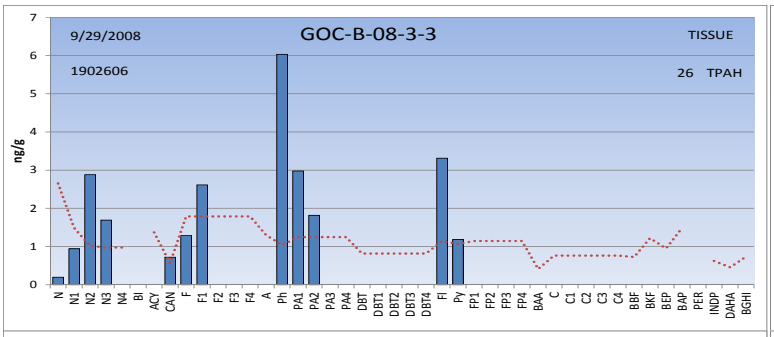
9/29/2008
GOC-B-08-3-3
TISSUE
1902606
26 TPAH
ng/g

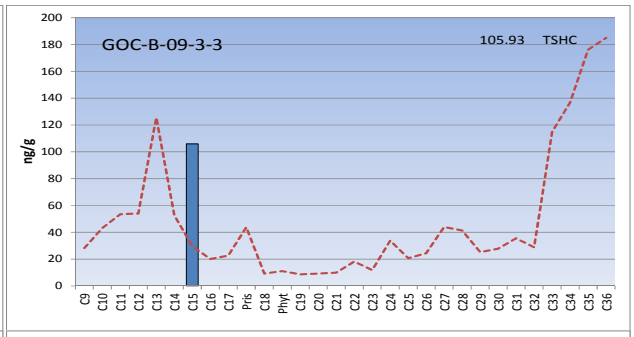
GOC-B-09-3-3
105.93 TSHC
ng/g

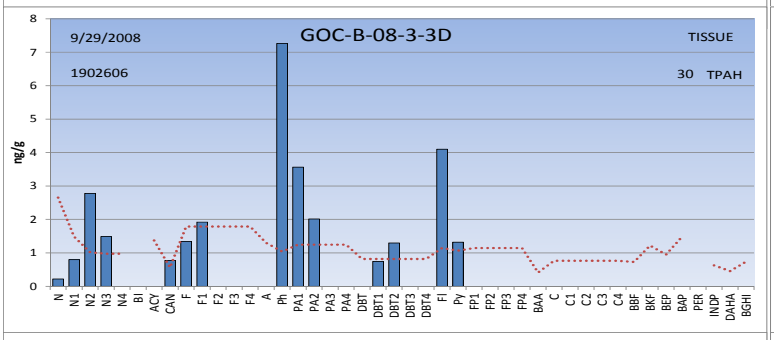
9/29/2008
GOC-B-08-3-3D
TISSUE
1902606
30 TPAH
ng/g

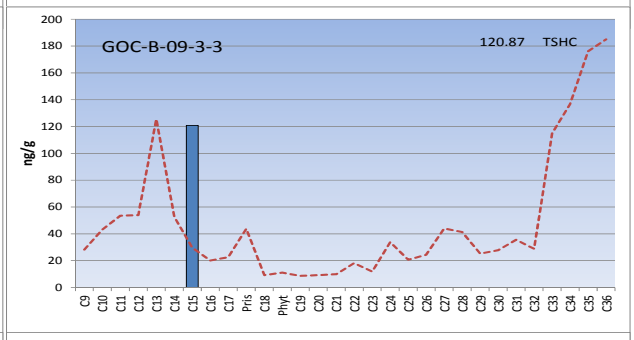
GOC-B-09-3-3
120.87 TSHC
ng/g

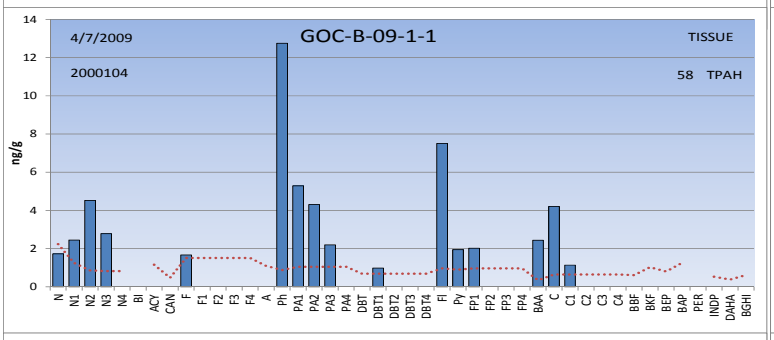
4/7/2009
GOC-B-09-1-1
TISSUE
2000104
58 TPAH
ng/g

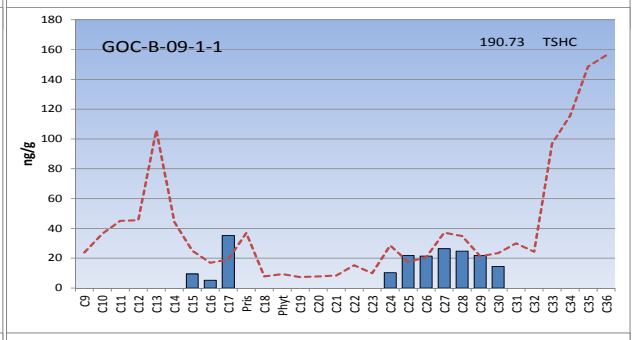
GOC-B-09-1-1
190.73 TSHC
ng/g

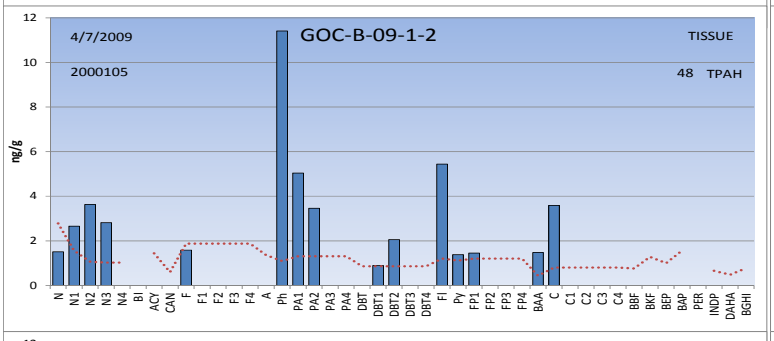
4/7/2009
GOC-B-09-1-2
TISSUE
2000105
48 TPAH
ng/g

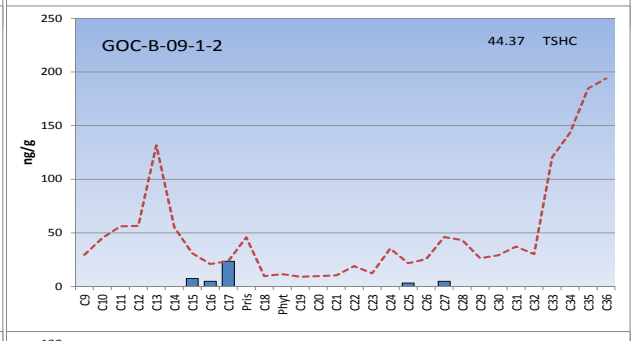
GOC-B-09-1-2
44.37 TSHC
ng/g

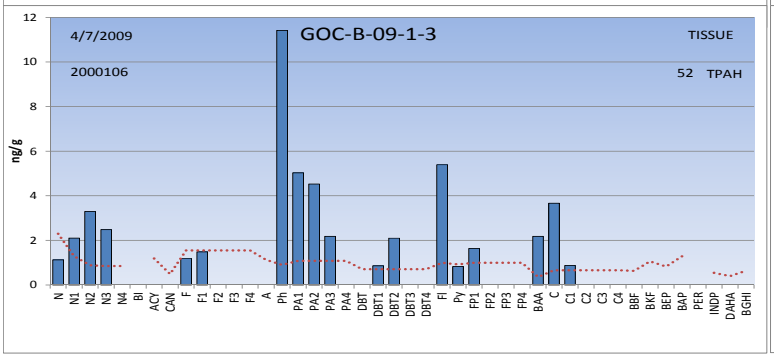
4/7/2009
GOC-B-09-1-3
TISSUE
2000106
52 TPAH
ng/g

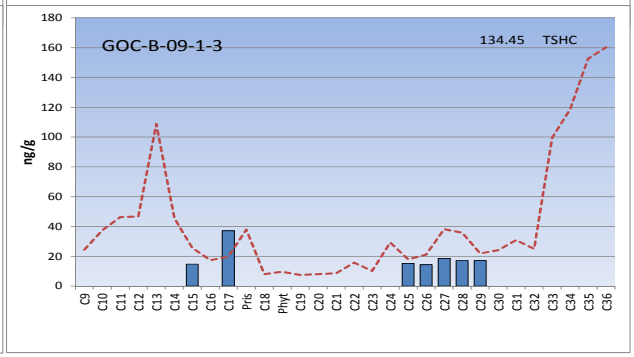
GOC-B-09-1-3
134.45 TSHC
ng/g

458

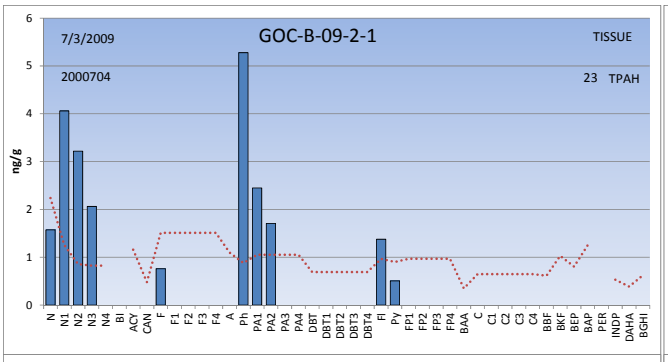
7/3/2009
GOC-B-09-2-1
TISSUE
2000704
23 TPAH
ng/g

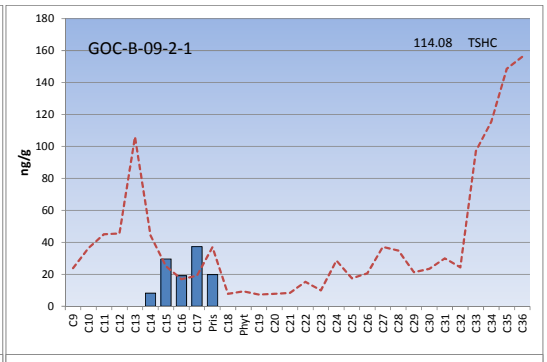
GOC-B-09-2-1
114.08 TSHC
ng/g

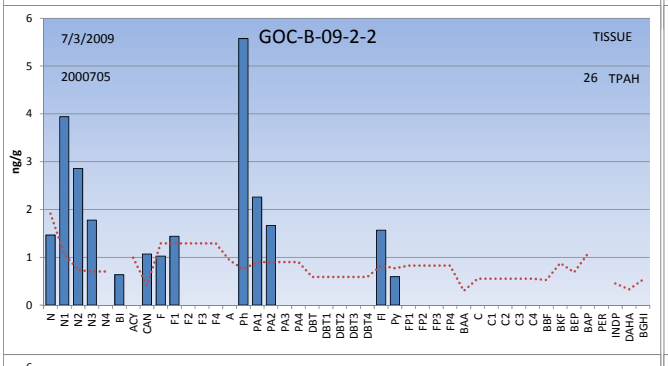
7/3/2009
GOC-B-09-2-2
TISSUE
2000705
26 TPAH
ng/g

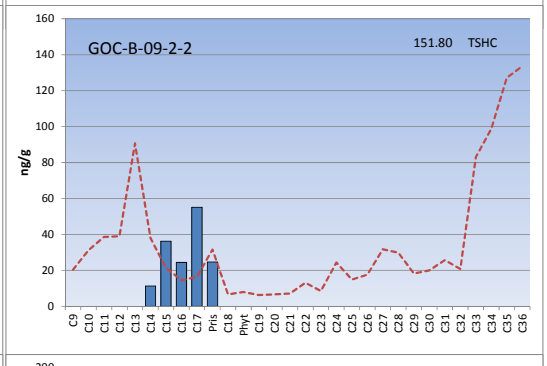
GOC-B-09-2-2
151.80 TSHC
ng/g

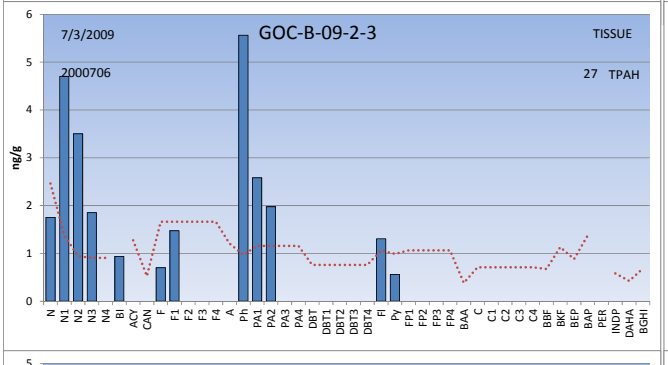
7/3/2009
GOC-B-09-2-3
TISSUE
2000706
27 TPAH
ng/g

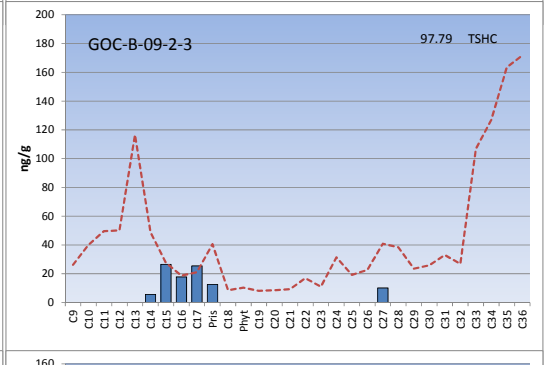
GOC-B-09-2-3
97.79 TSHC
ng/g

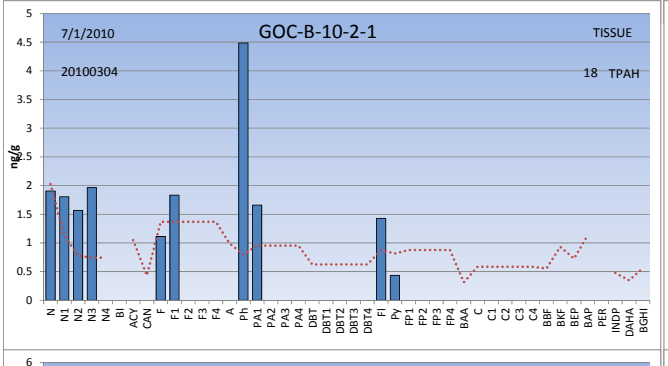
7/1/2010
GOC-B-10-2-1
TISSUE
20100304
18 TPAH
ng/g

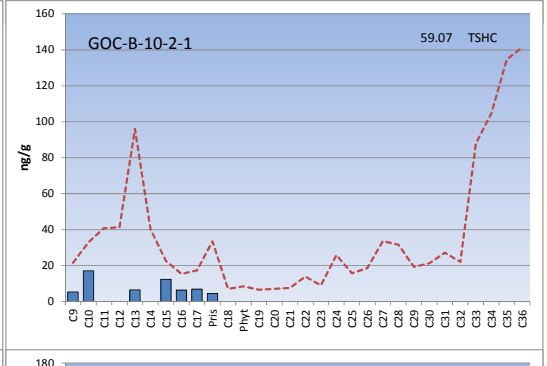
GOC-B-10-2-1
59.07 TSHC
ng/g

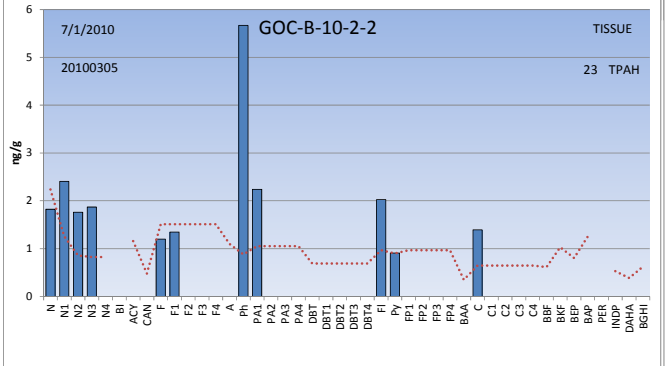
7/1/2010
GOC-B-10-2-2
TISSUE
20100305
23 TPAH
ng/g

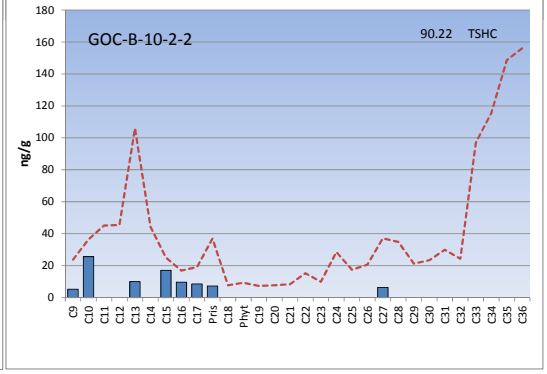
GOC-B-10-2-2
90.22 TSHC
ng/g

459

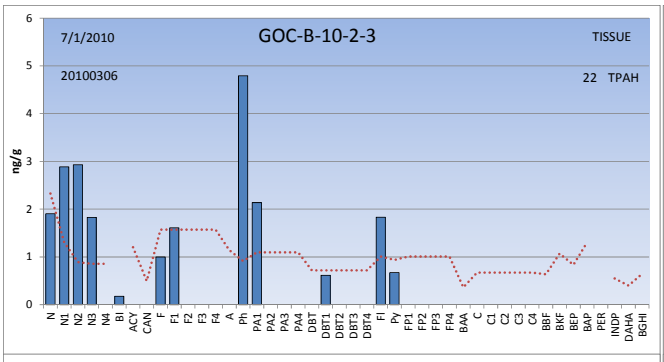
7/1/2010
GOC-B-10-2-3
TISSUE
20100306
22 TPAH
ng/g

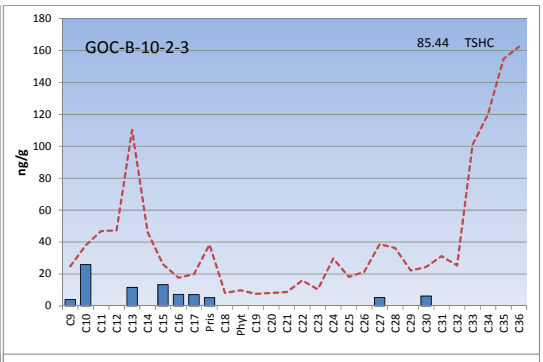
GOC-B-10-2-3
85.44 TSHC
ng/g

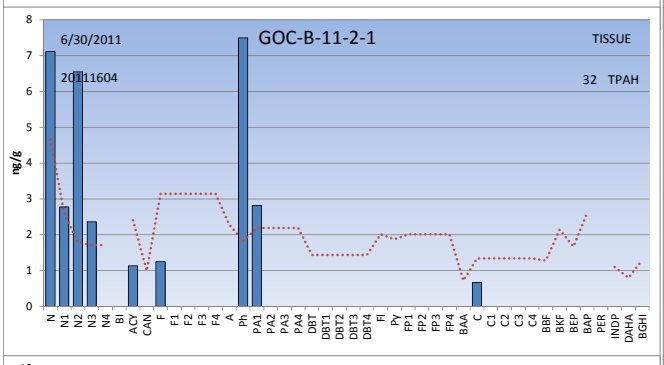
6/30/2011
GOC-B-11-2-1
TISSUE
20111604
32 TPAH
ng/g

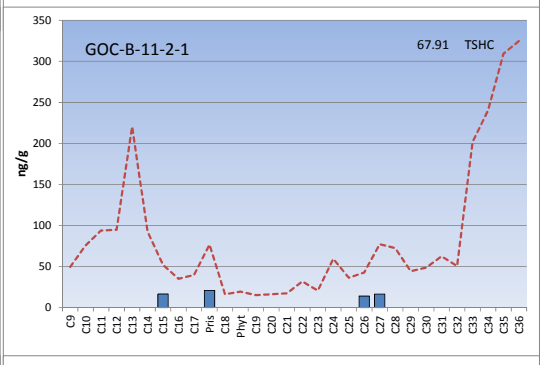
GOC-B-11-2-1
67.91 TSHC
ng/g

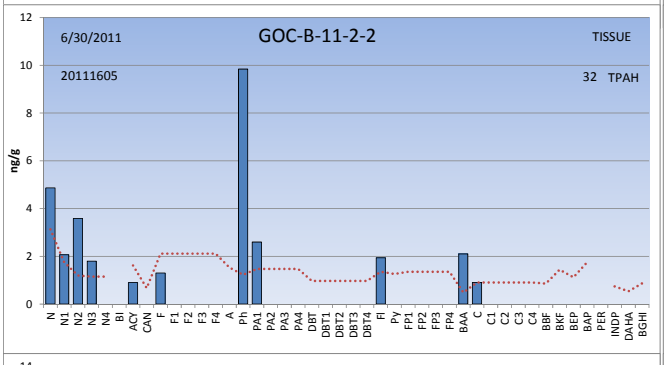
6/30/2011
GOC-B-11-2-2
TISSUE
20111605
32 TPAH
ng/g

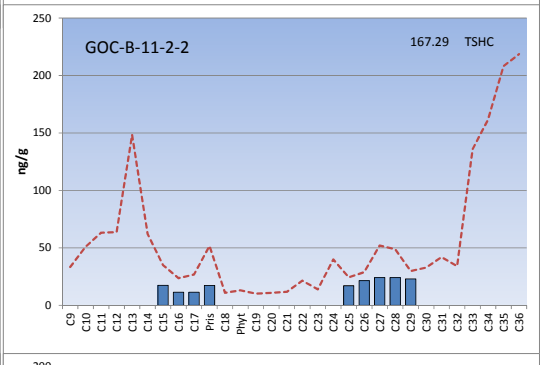
GOC-B-11-2-2
167.29 TSHC
ng/g

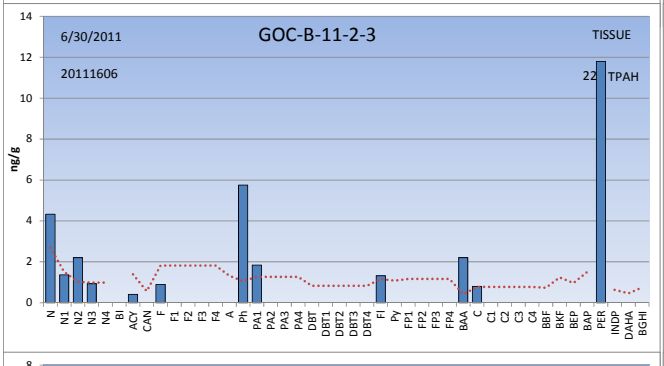
6/30/2011
GOC-B-11-2-3
TISSUE
20111606
22 TPAH
ng/g

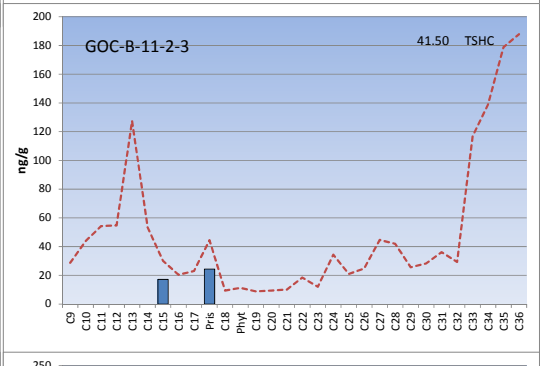
GOC-B-11-2-3
41.50 TSHC
ng/g

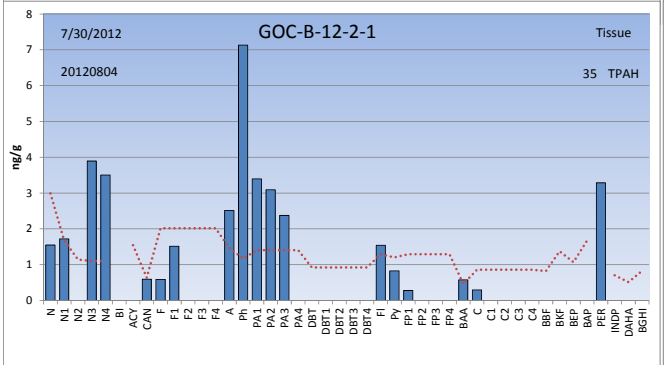
7/30/2012
GOC-B-12-2-1
Tissue
20120804
35 TPAH
ng/g

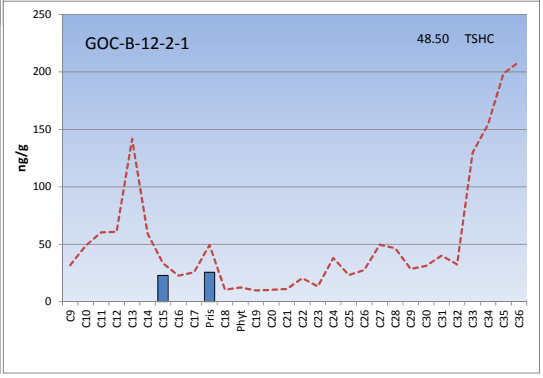
GOC-B-12-2-1
48.50 TSHC
ng/g

460

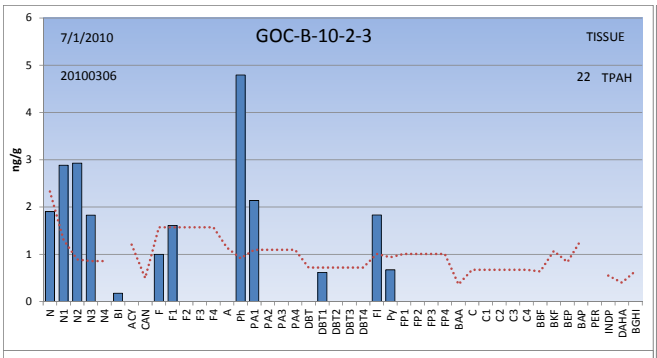
7/1/2010
GOC-B-10-2-3
TISSUE
20100306
22 TPAH
ng/g

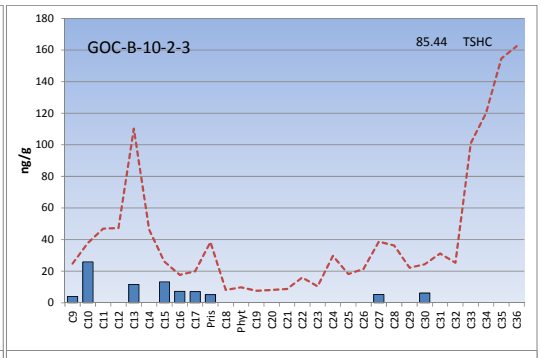
GOC-B-10-2-3
85.44 TSHC
ng/g

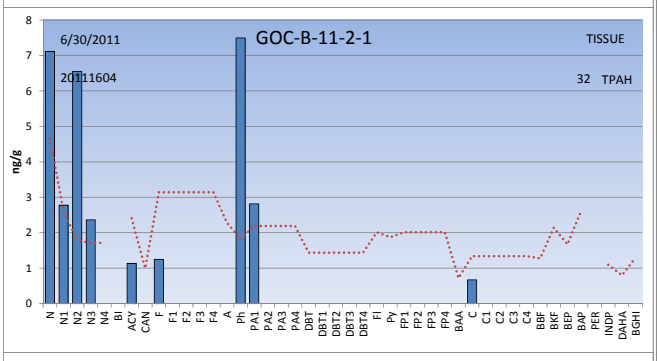
6/30/2011
GOC-B-11-2-1
TISSUE
20111604
32 TPAH
ng/g

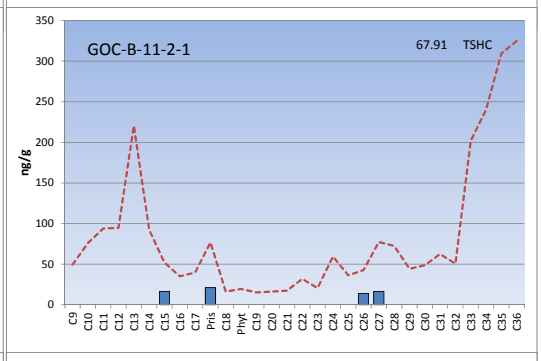
GOC-B-11-2-1
67.91 TSHC
ng/g

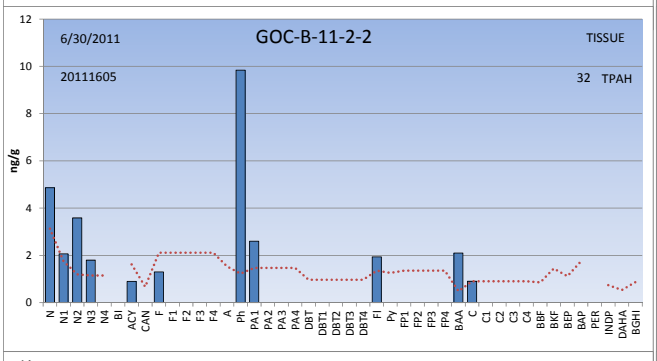
6/30/2011
GOC-B-11-2-2
TISSUE
20111605
32 TPAH
ng/g

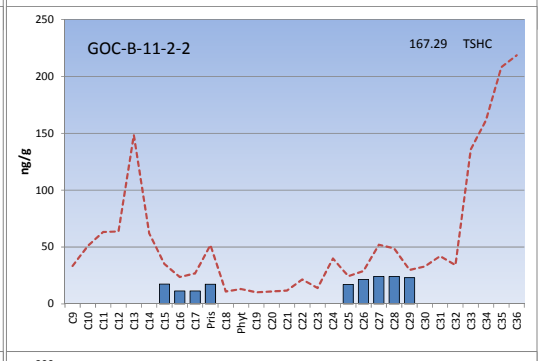
GOC-B-11-2-2
167.29 TSHC
ng/g

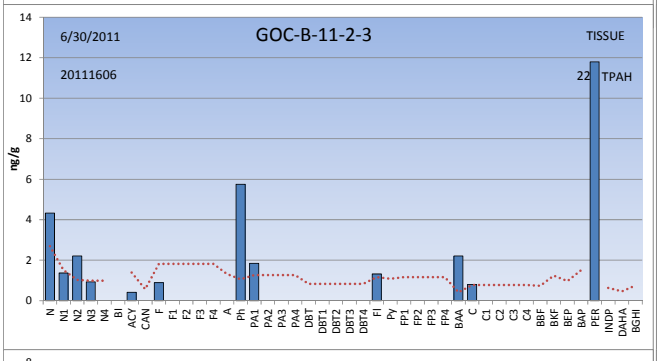
6/30/2011
GOC-B-11-2-3
TISSUE
20111606
22 TPAH
ng/g

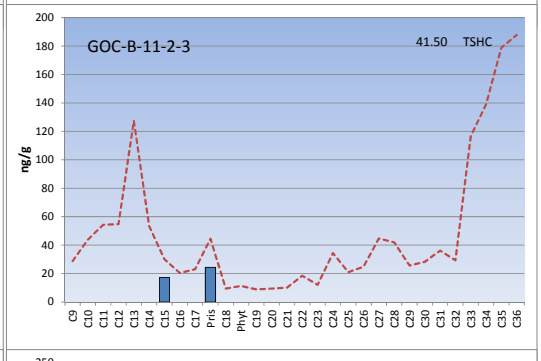
GOC-B-11-2-3
41.50 TSHC
ng/g

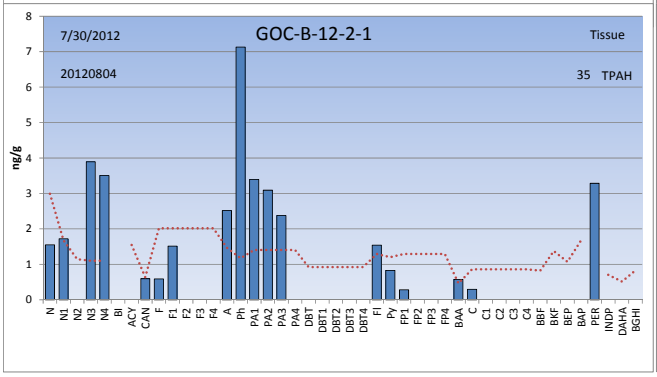
7/30/2012
GOC-B-12-2-1
Tissue
20120804
35 TPAH
ng/g

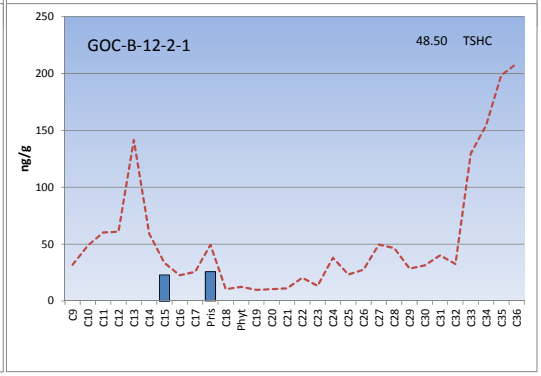
GOC-B-12-2-1
48.50 TSHC
ng/g

461

KNOWLES HEAD--KNH

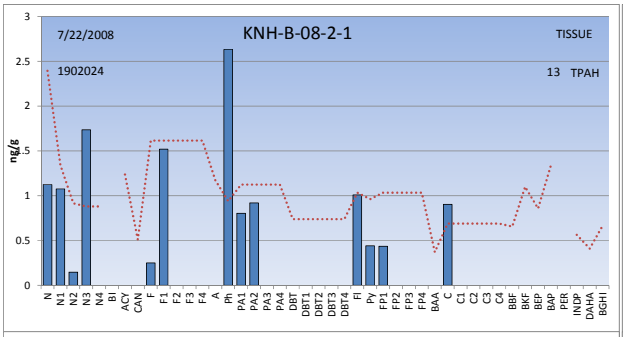

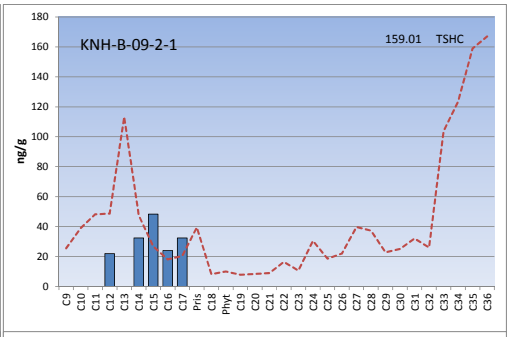

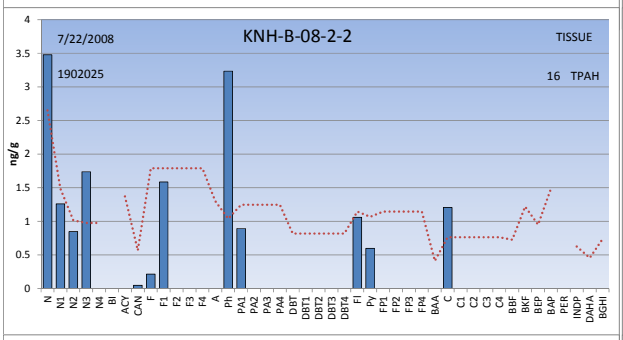

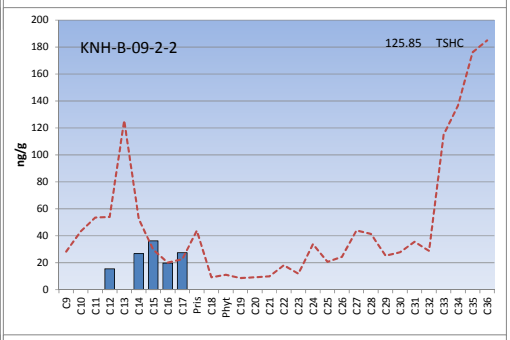

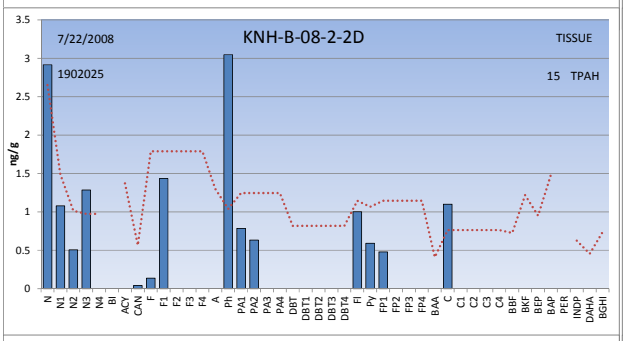

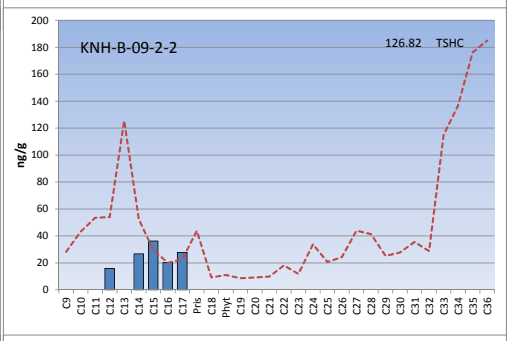

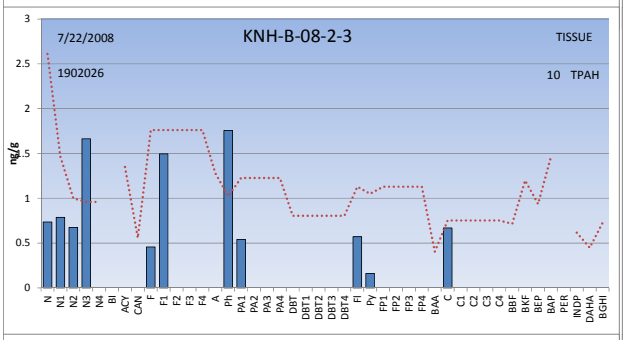

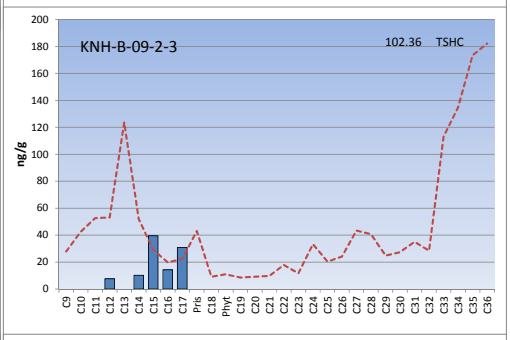

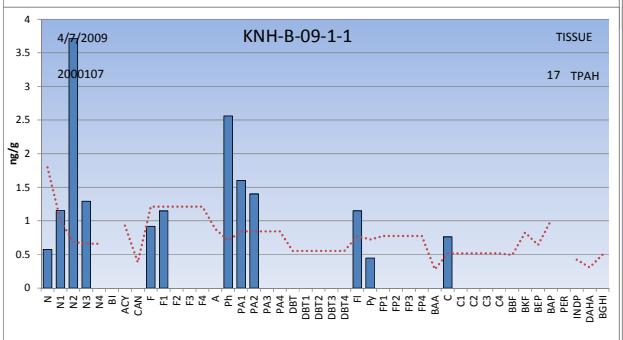

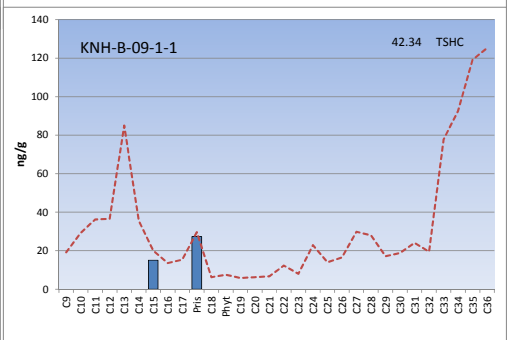

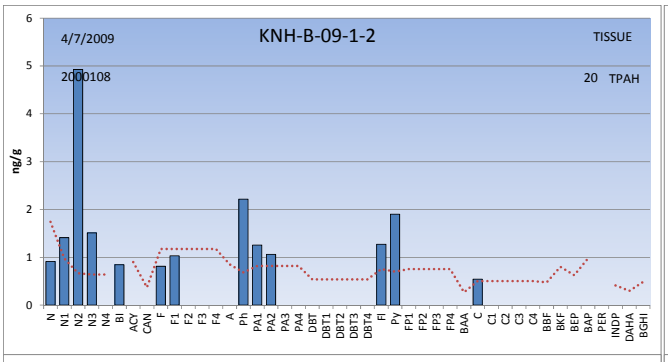
4/7/2009
KNH-B-09-1-2
TISSUE
2000108
20 TPAH
ng/g

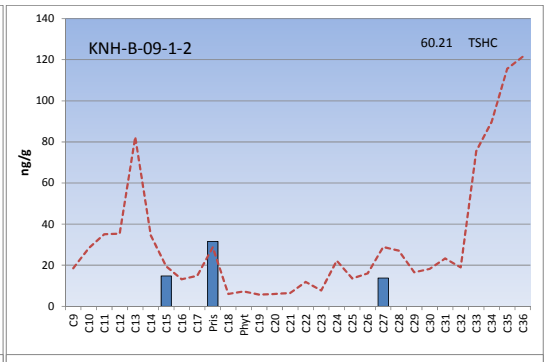
KNH-B-09-1-2
60.21 TSHC
ng/g

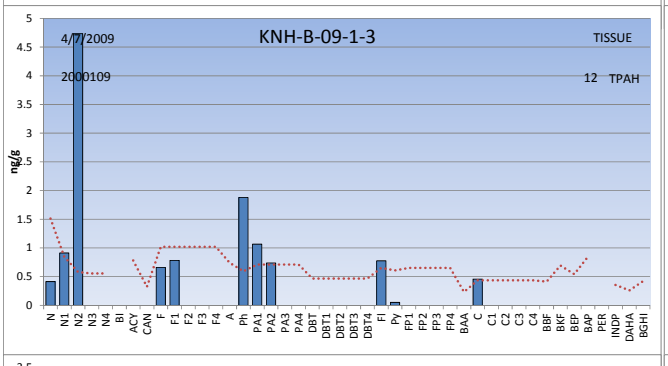
4/7/2009
KNH-B-09-1-3
TISSUE
2000109
12 TPAH
ng/g

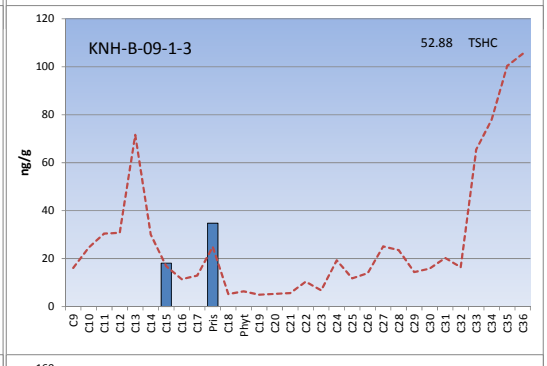
KNH-B-09-1-3
52.88 TSHC
ng/g

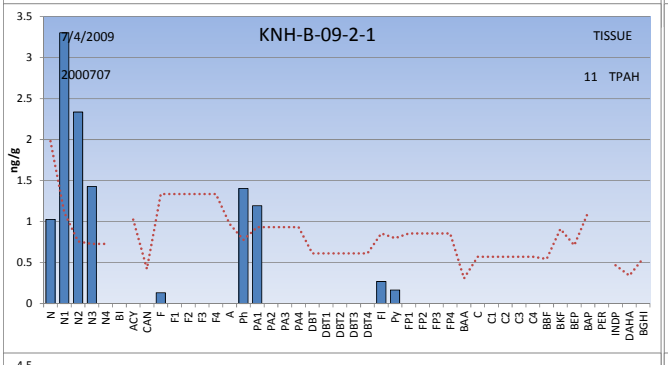
7/4/2009
KNH-B-09-2-1
TISSUE
2000707
11 TPAH
ng/g

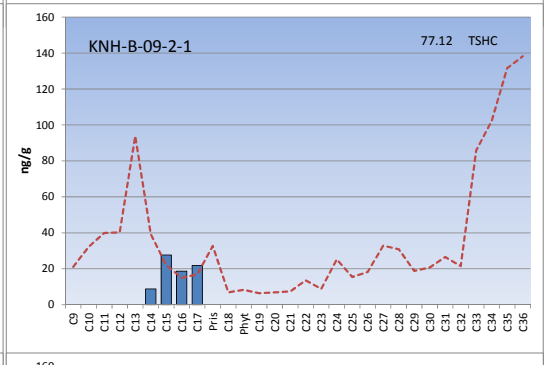
KNH-B-09-2-1
77.12 TSHC
ng/g

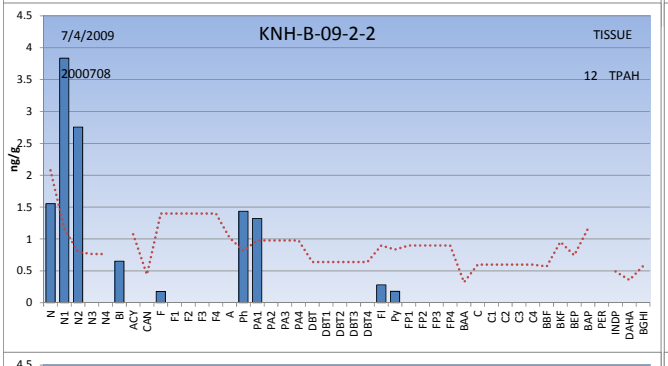
7/4/2009
KNH-B-09-2-2
TISSUE
2000708
12 TPAH
ng/g

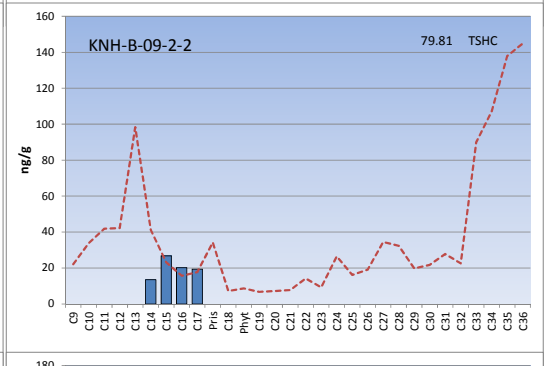
KNH-B-09-2-2
79.81 TSHC
ng/g

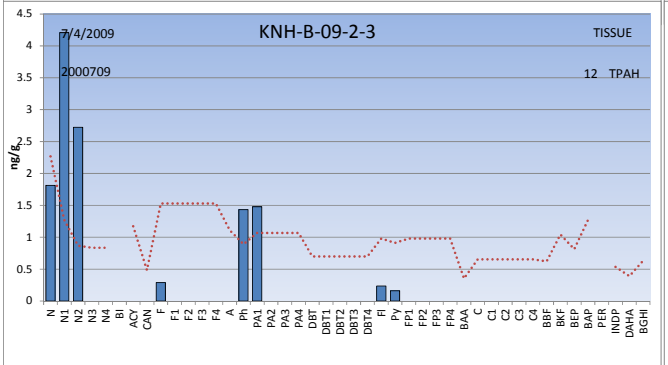
7/4/2009
KNH-B-09-2-3
TISSUE
2000709
12 TPAH
ng/g

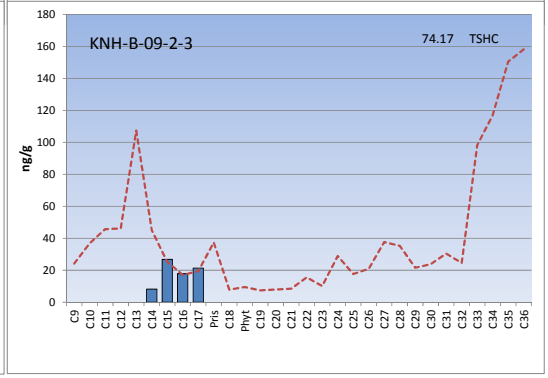
KNH-B-09-2-3
74.17 TSHC
ng/g

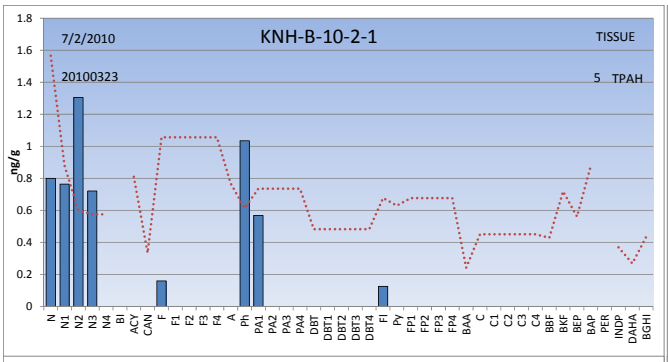
7/2/2010
KNH-B-10-2-1
TISSUE
20100323
5 TPAH
ng/g

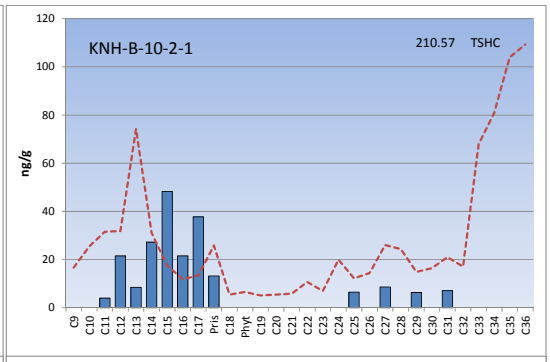
KNH-B-10-2-1
210.57 TSHC
ng/g

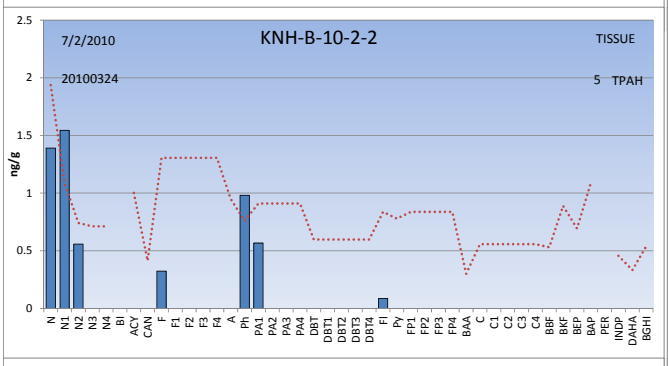
7/2/2010
KNH-B-10-2-2
TISSUE
20100324
5 TPAH
ng/g

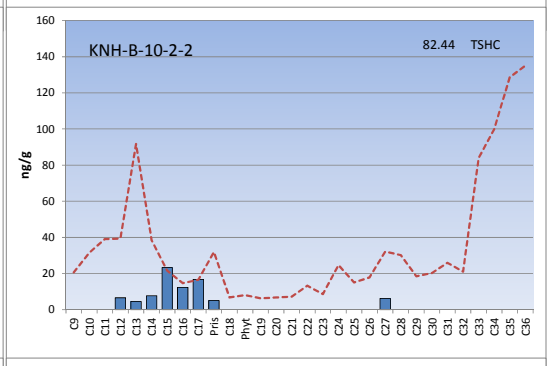
KNH-B-10-2-2
82.44 TSHC
ng/g

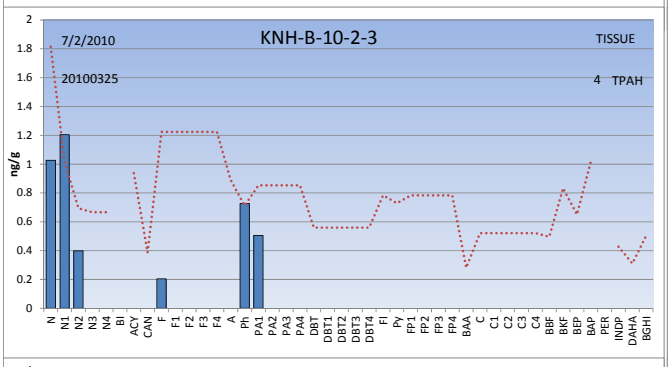
7/2/2010
KNH-B-10-2-3
TISSUE
20100325
4 TPAH
ng/g

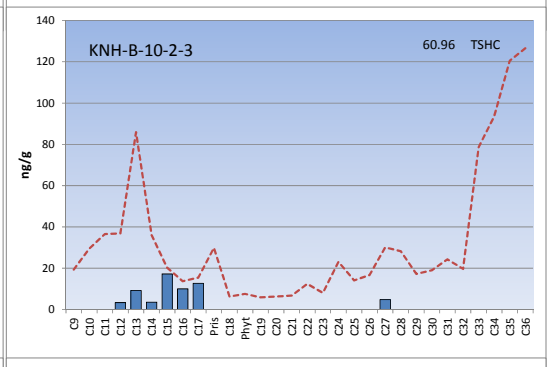
KNH-B-10-2-3
60.96 TSHC
ng/g

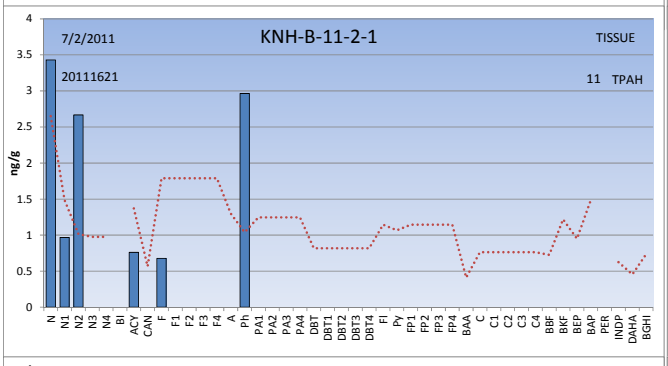
7/2/2011
KNH-B-11-2-1
TISSUE
20111621
11 TPAH
ng/g

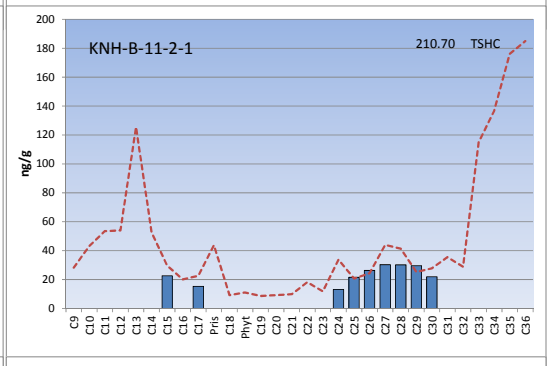
KNH-B-11-2-1
210.70 TSHC
ng/g

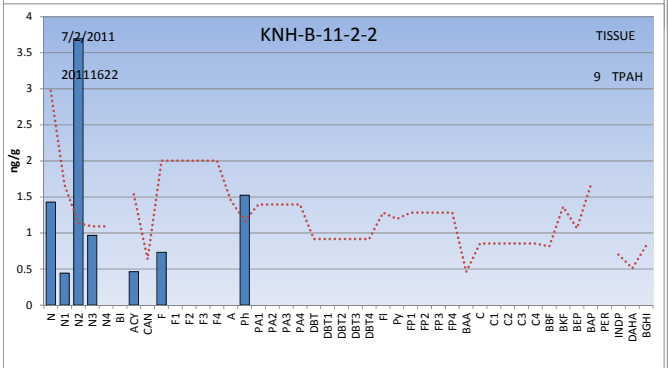
7/2/2011
KNH-B-11-2-2
TISSUE
20111622
9 TPAH
ng/g

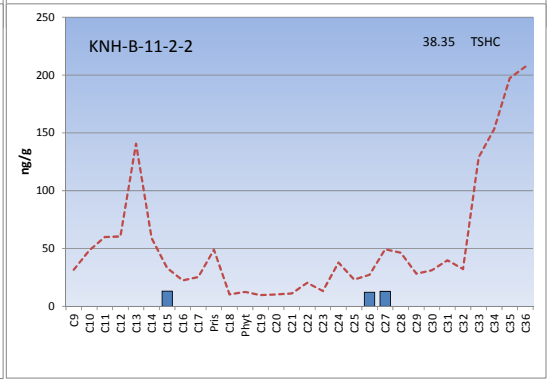
KNH-B-11-2-2
38.35 TSHC
ng/g

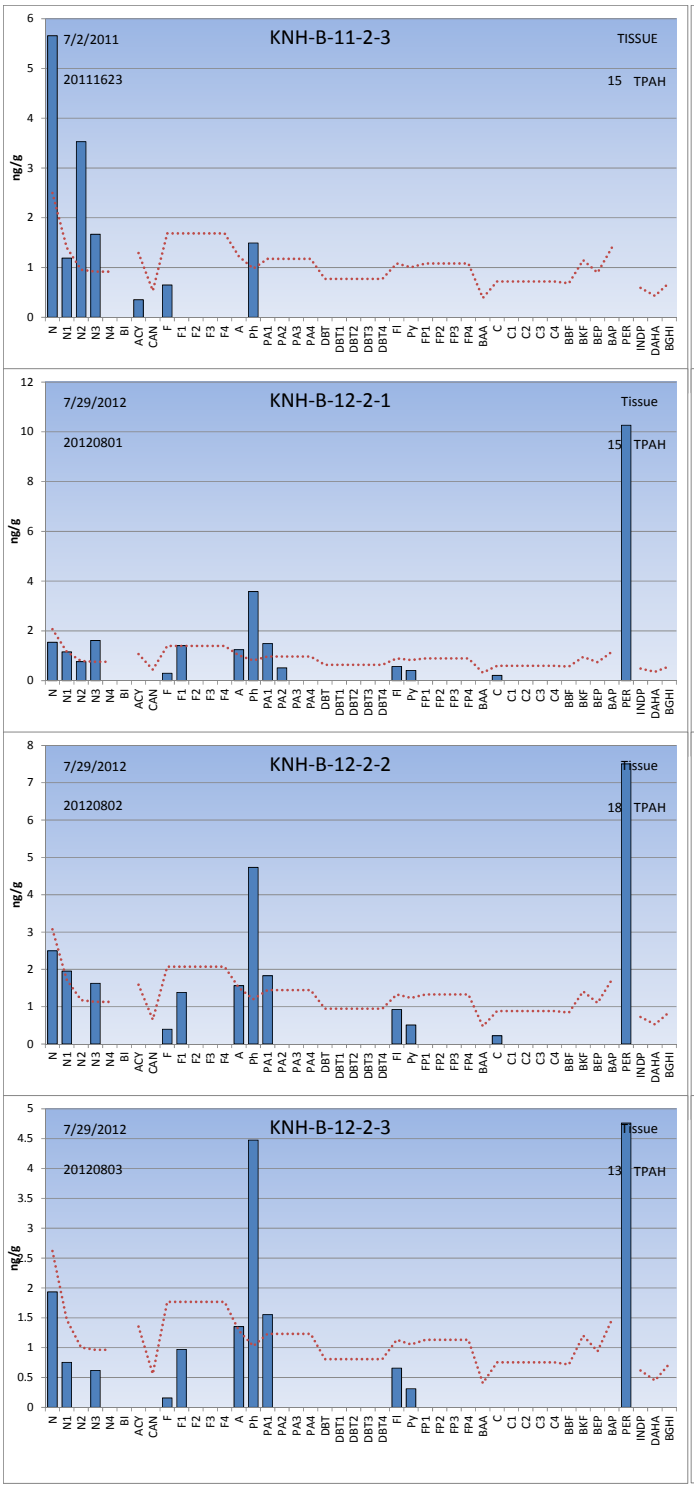
7/2/2011
KNH-B-11-2-3
TISSUE
20111623
15 TPAH
ng/g
KNH-B-11-2-3
96.05 TSHC
ng/g
7/29/2012
KNH-B-12-2-1
Tissue
20120801
15 TPAH
ng/g
KNH-B-12-2-1
50.06 TSHC
ng/g
7/29/2012
KNH-B-12-2-2
Tissue
20120802
18 TPAH
ng/g
KNH-B-12-2-2
48.27 TSHC
ng/g
7/29/2012
KNH-B-12-2-3
Tissue
20120803
13 TPAH
ng/g
KNH-B-12-2-3
20.53 TSHC
ng/g

466

SHEEP BAY--SHB

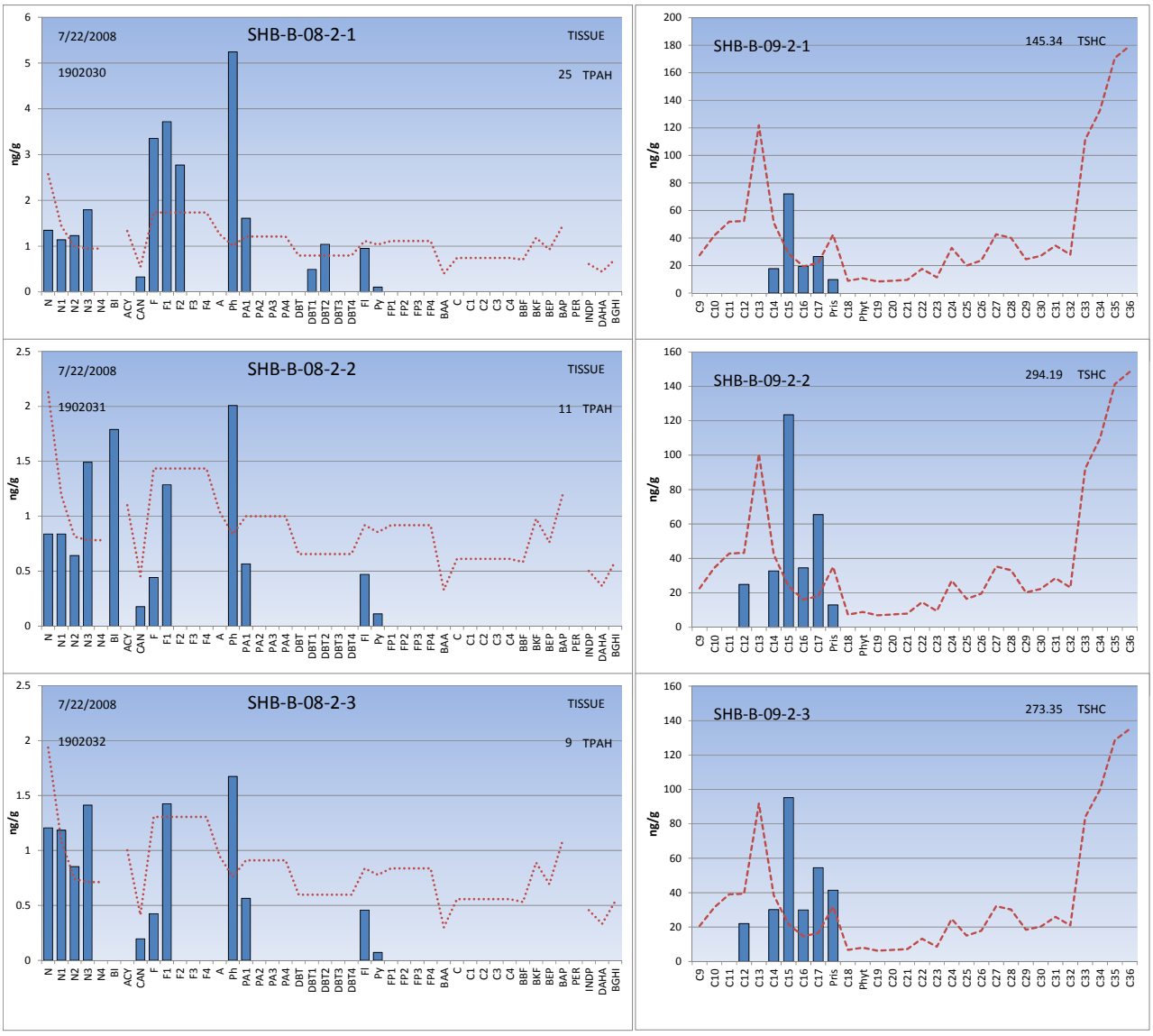

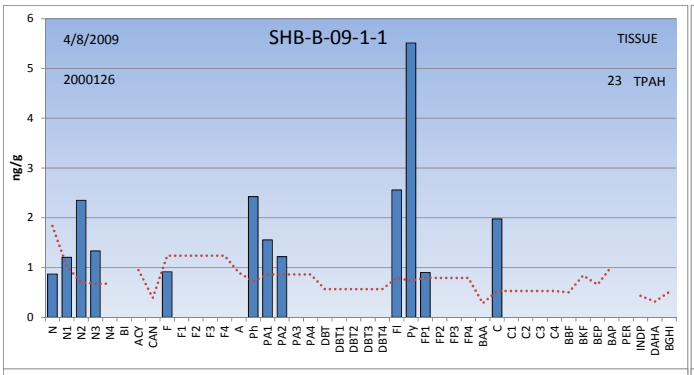
4/8/2009
SHB-B-09-1-1
TISSUE
2000126
23 TPAH
ng/g

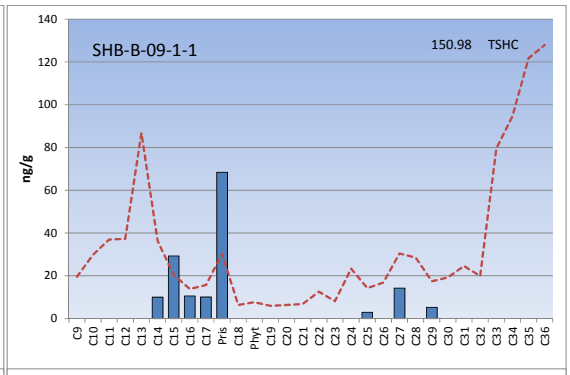
SHB-B-09-1-1
150.98 TSHC
ng/g

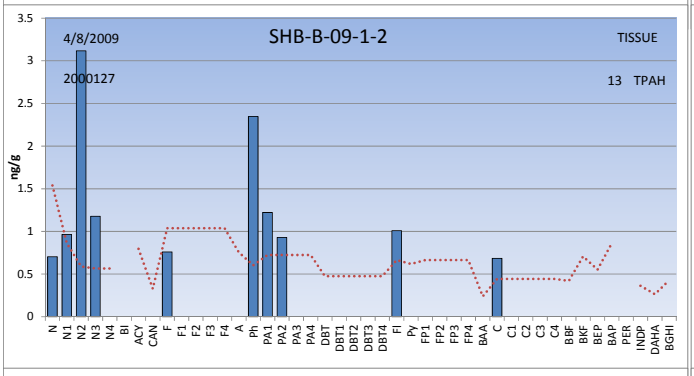
4/8/2009
SHB-B-09-1-2
TISSUE
2000127
13 TPAH
ng/g

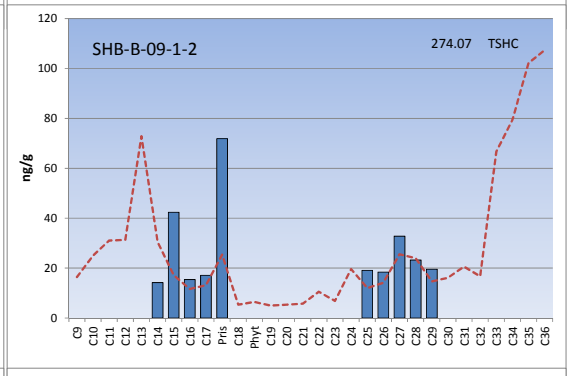
SHB-B-09-1-2
274.07 TSHC
ng/g

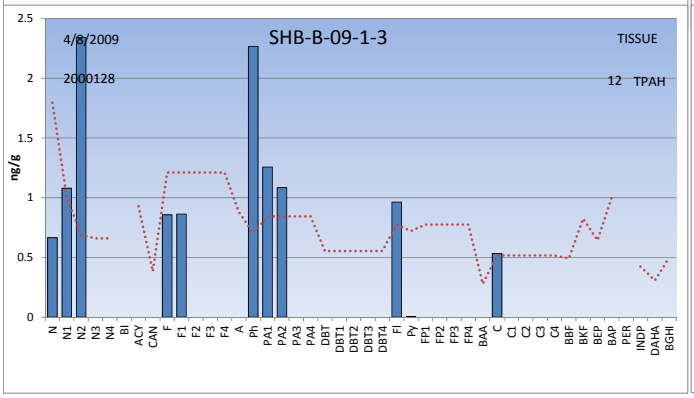
4/8/2009
SHB-B-09-1-3
TISSUE
2000128
12 TPAH
ng/g

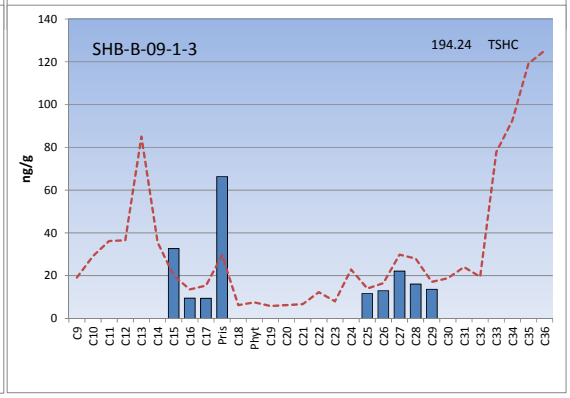
SHB-B-09-1-3
194.24 TSHC
ng/g

469

ZAIKOF BAY--ZAB

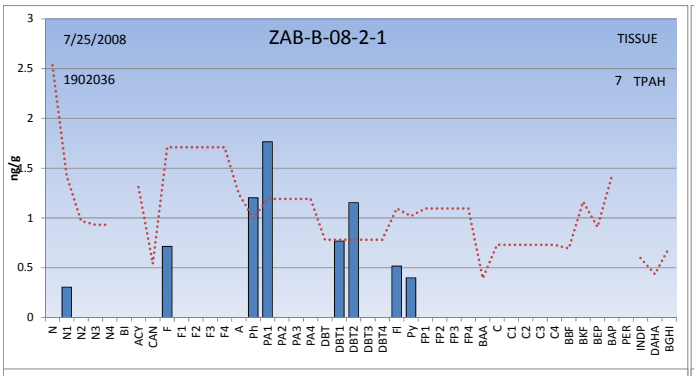

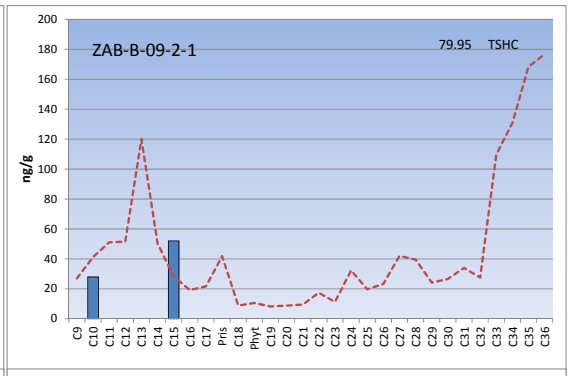

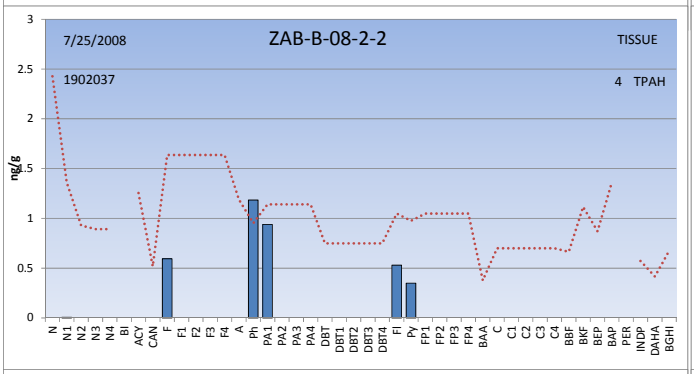

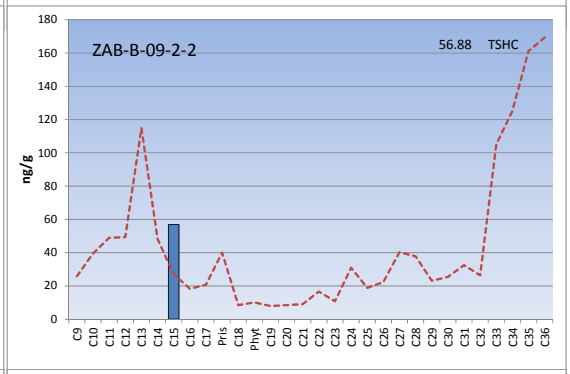

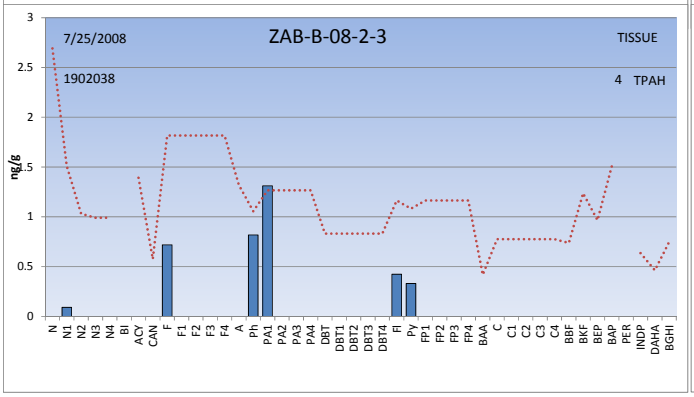

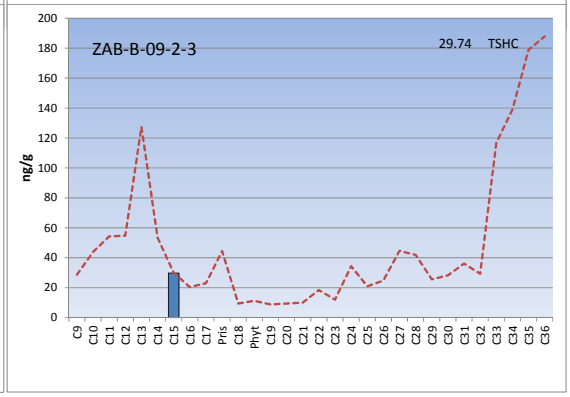

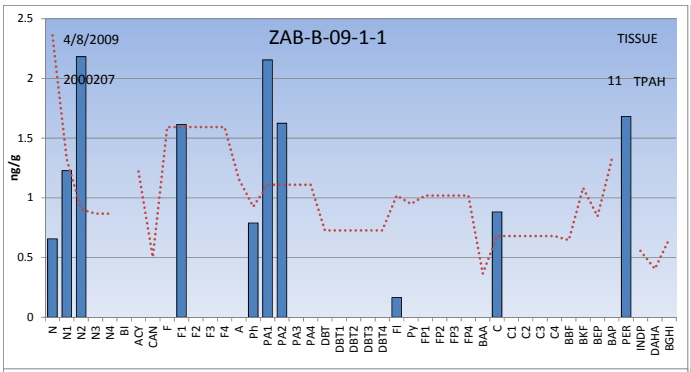
4/8/2009
ZAB-B-09-1-1
TISSUE
2000207
11 TPAH
ng/g

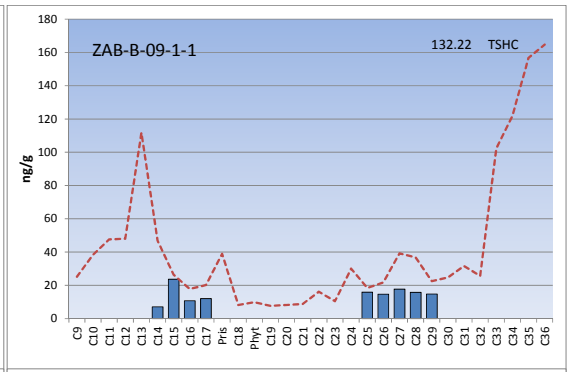
ZAB-B-09-1-1
132.22 TSHC
ng/g

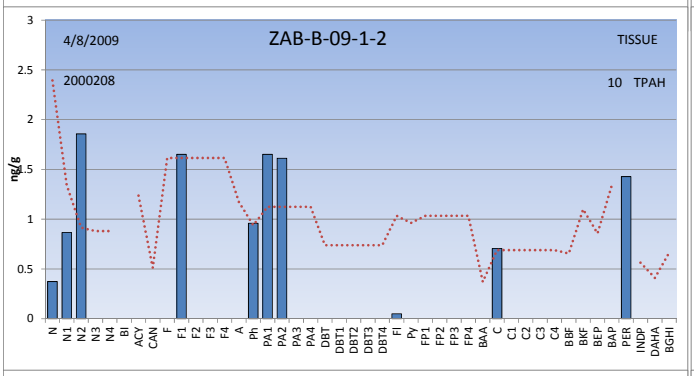
4/8/2009
ZAB-B-09-1-2
TISSUE
2000208
10 TPAH
ng/g

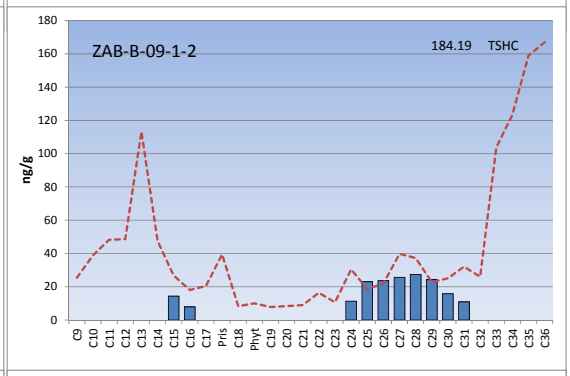
ZAB-B-09-1-2
184.19 TSHC
ng/g

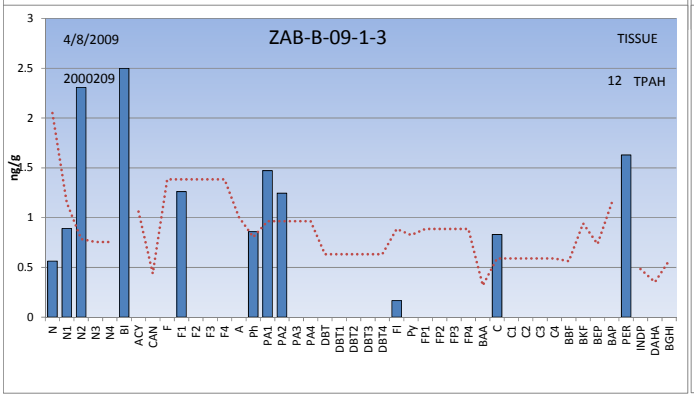
4/8/2009
ZAB-B-09-1-3
TISSUE
2000209
12 TPAH
ng/g

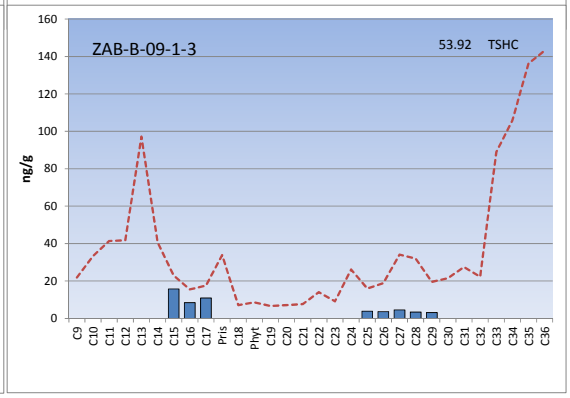
ZAB-B-09-1-3
53.92 TSHC
ng/g

472

SLEEPY BAY--SLB

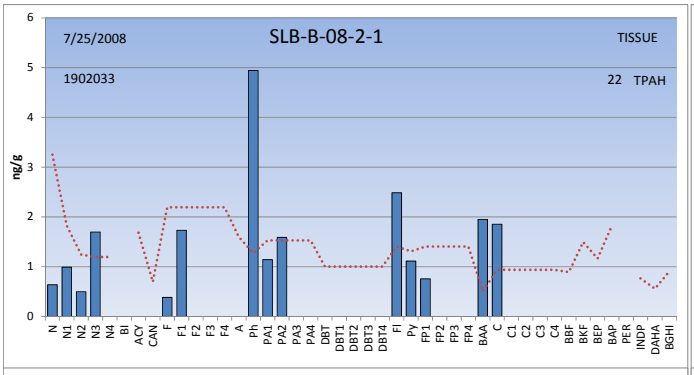

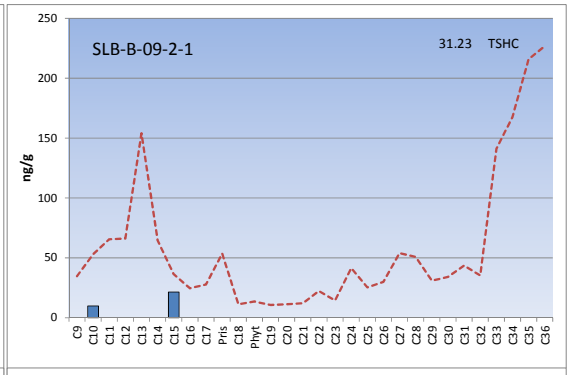

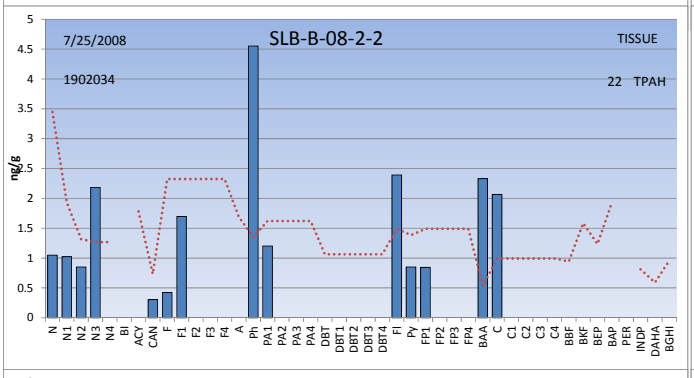

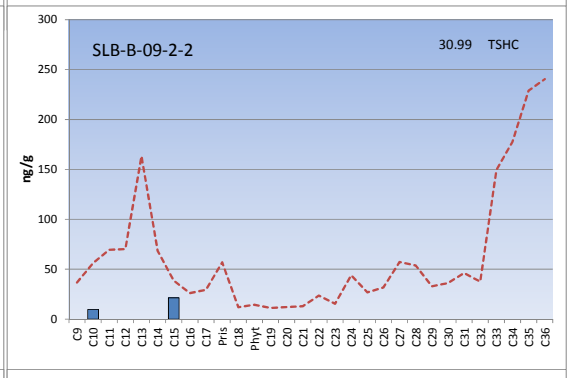

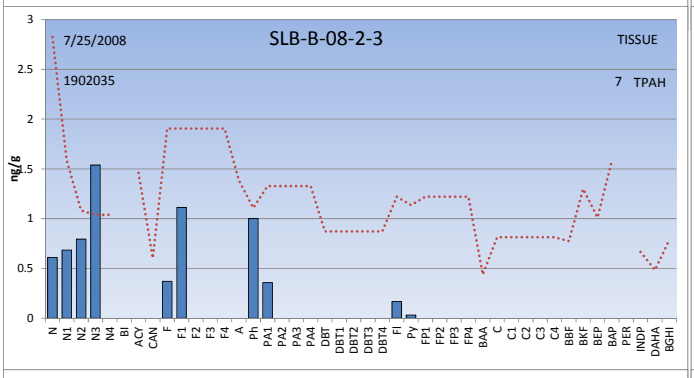

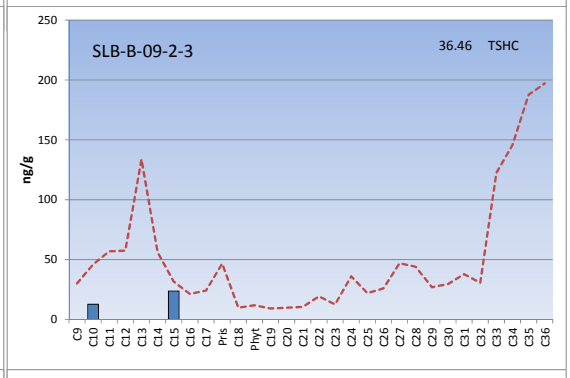

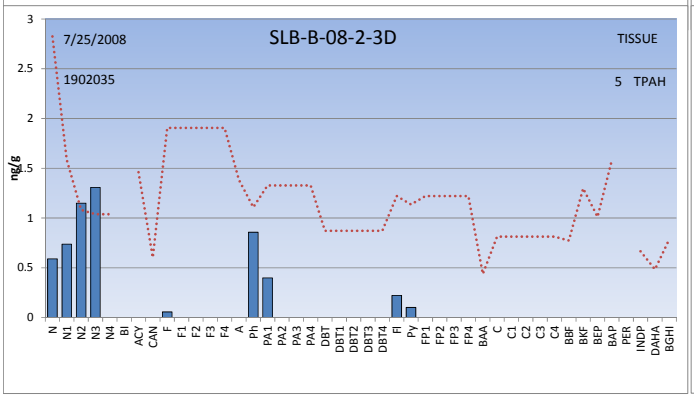

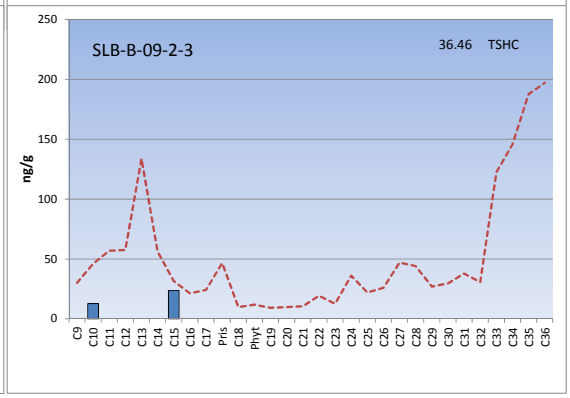

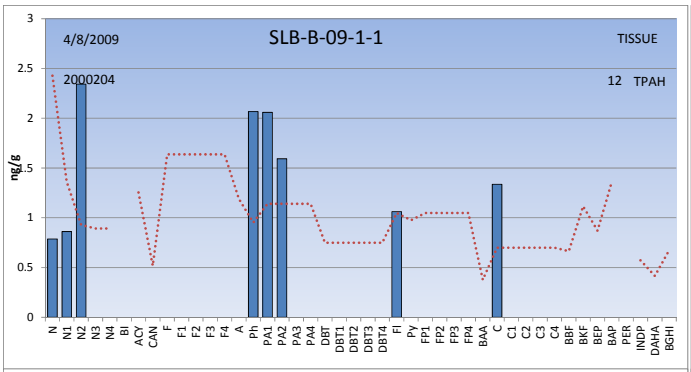
4/8/2009
SLB-B-09-1-1
TISSUE
2000204
12 TPAH
ng/g

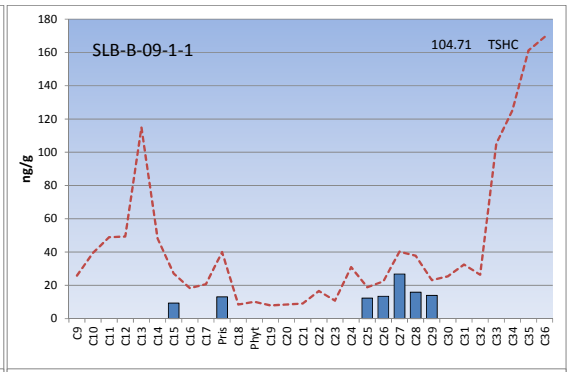
SLB-B-09-1-1
104.71 TSHC
ng/g

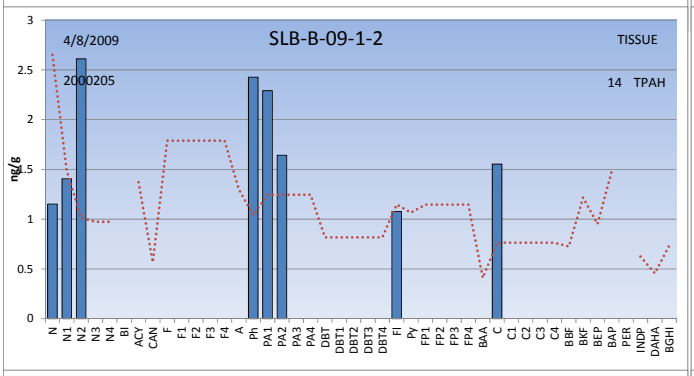
4/8/2009
SLB-B-09-1-2
TISSUE
2000205
14 TPAH
ng/g

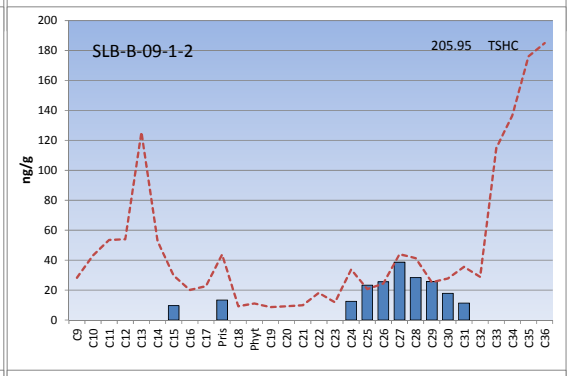
SLB-B-09-1-2
205.95 TSHC
ng/g

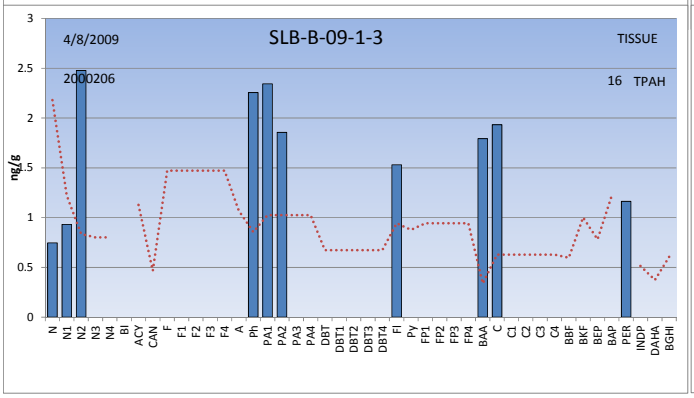
4/8/2009
SLB-B-09-1-3
TISSUE
2000206
16 TPAH
ng/g

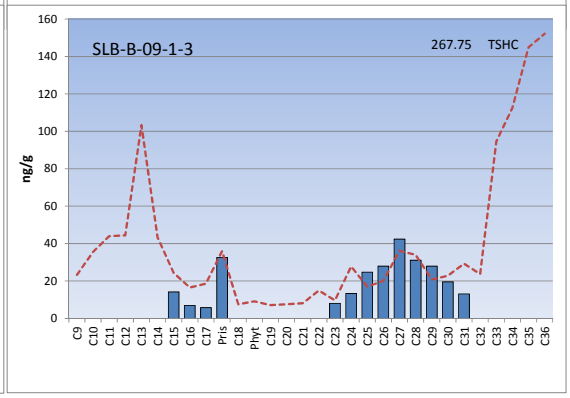
SLB-B-09-1-3
267.75 TSHC
ng/g

475

476 DISK ISLAND--DII

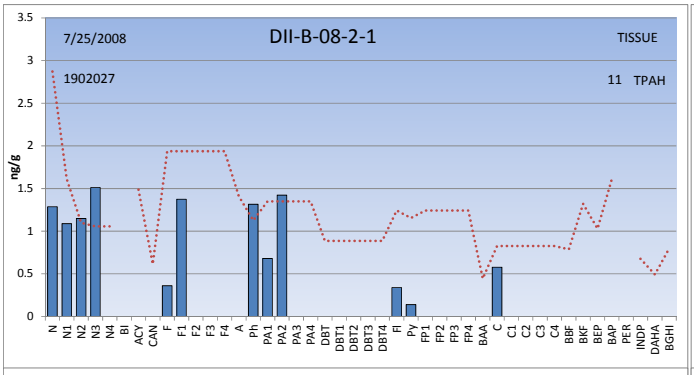

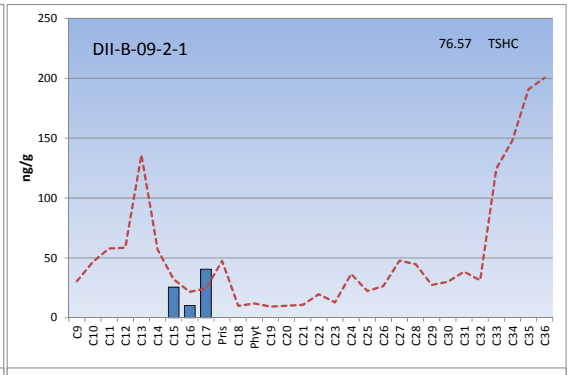

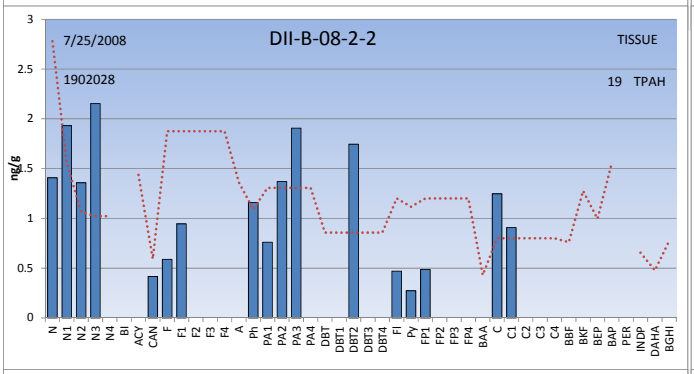

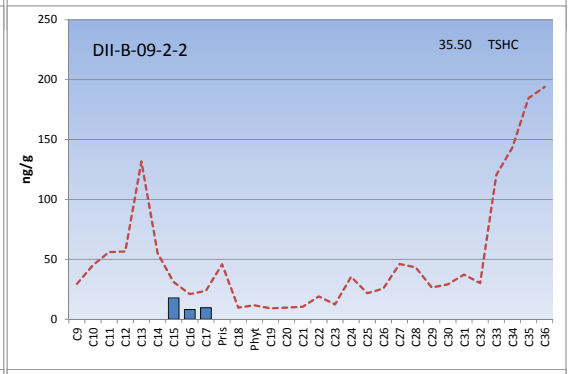

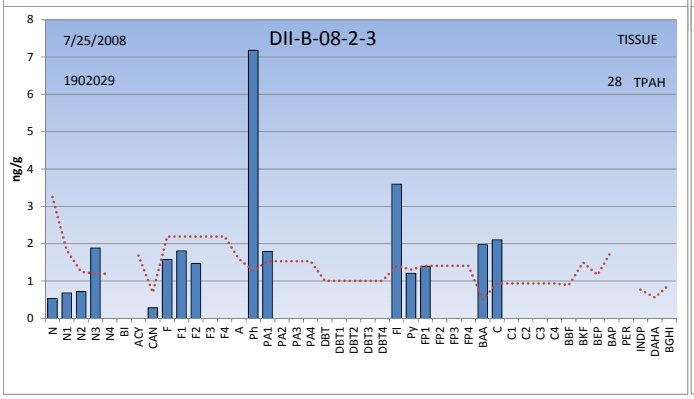

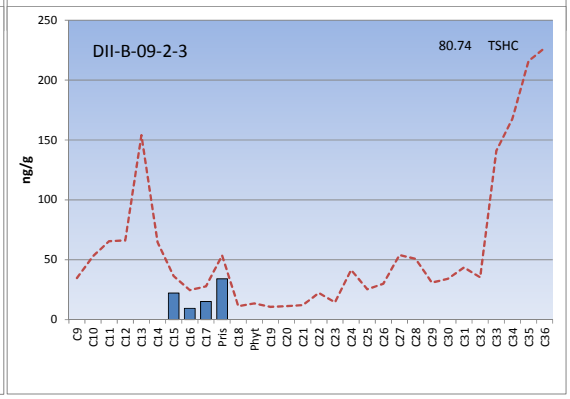

477

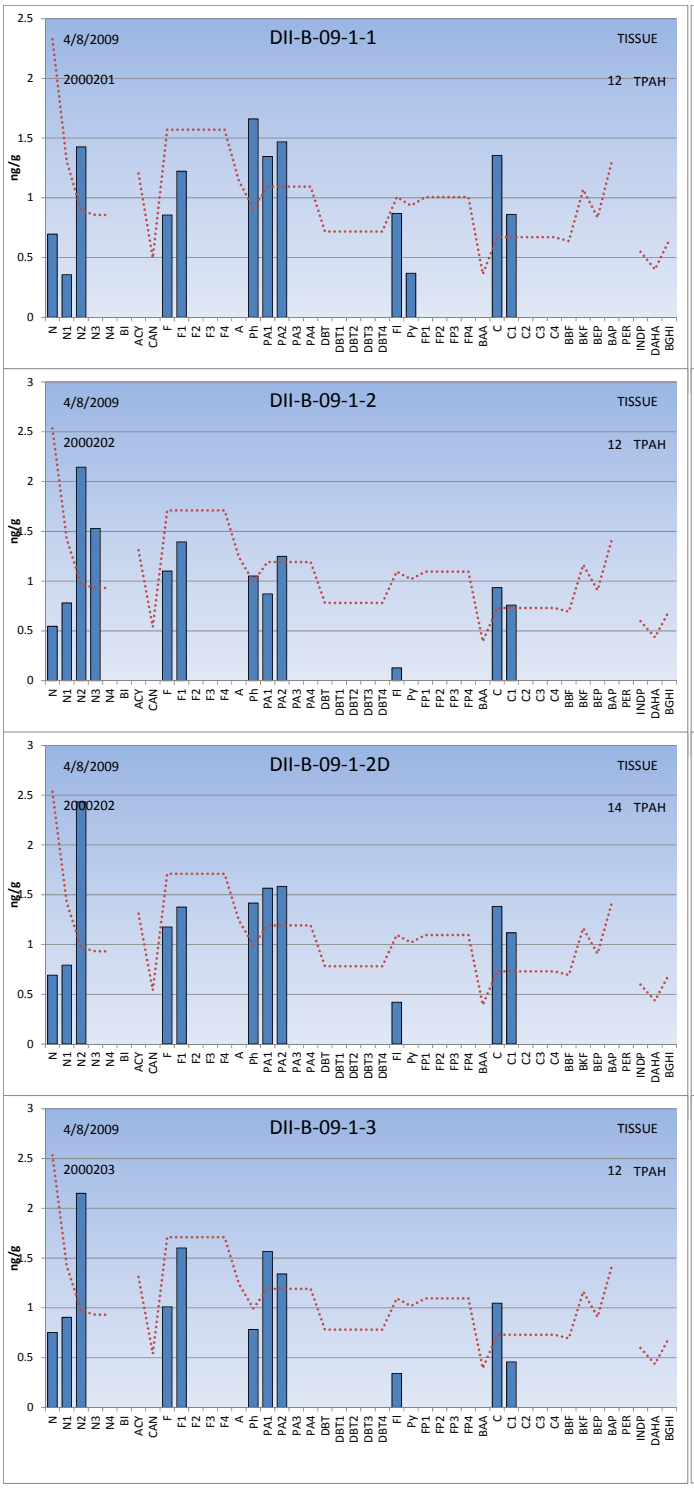
4/8/2009
DII-B-09-1-1
TISSUE
2000201
12 TPAH
ng/g
DII-B-09-1-1
164.17 TSHC
DII-B-09-1-2
96.97 TSHC
DII-B-09-1-2D
14 TPAH
DII-B-09-1-2
115.48 TSHC
DII-B-09-1-3
103.31 TSHC

478

AIALIK BAY--AIB

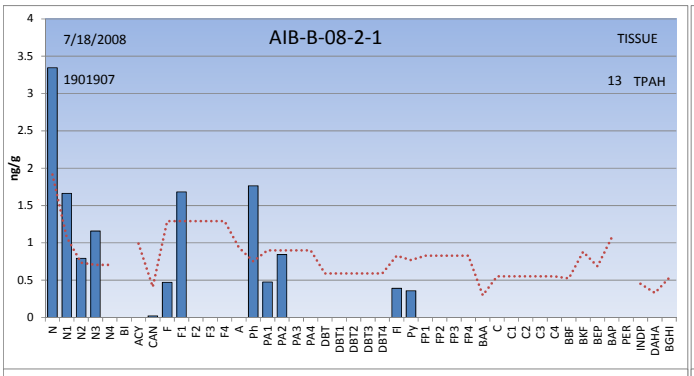

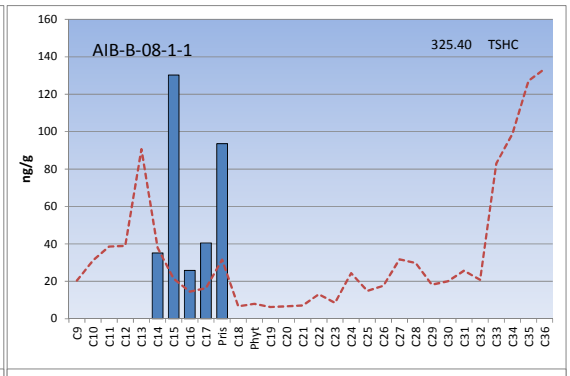

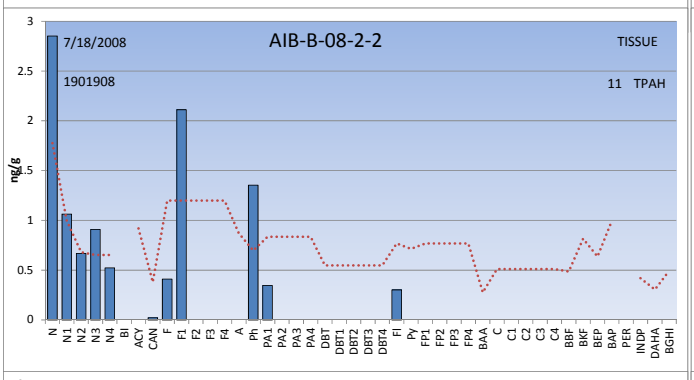

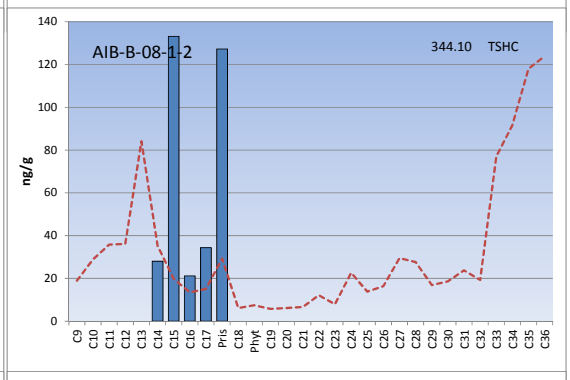

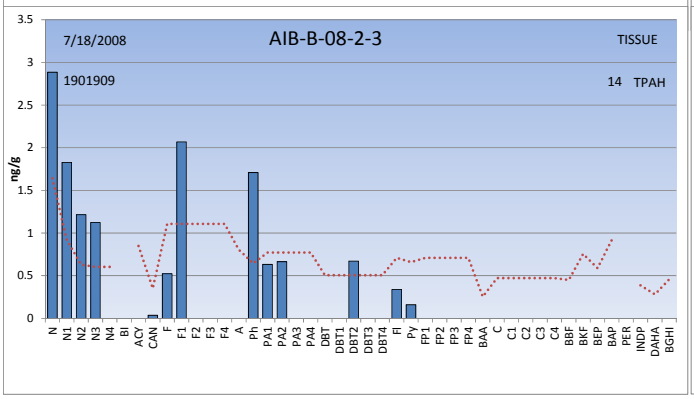

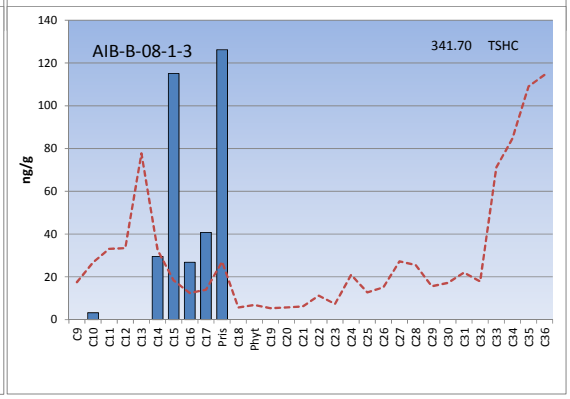

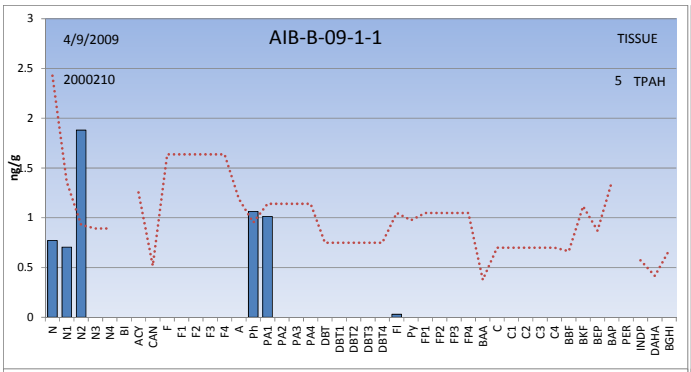
4/9/2009
AIB-B-09-1-1
TISSUE
2000210
5 TPAH
ng/g
N N1 N2 N3 N4 BI ACY CAN F F1 F2 F3 F4 A Ph PA1 PA2 PA3 PA4 DBT DBT1 DBT2 DBT3 DBT4 FI Py FP1 FP2 FP3 FP4 BAA C C1 C2 C3 C4 BBF BKF BEP BAP PER INDP DAHA BGHI

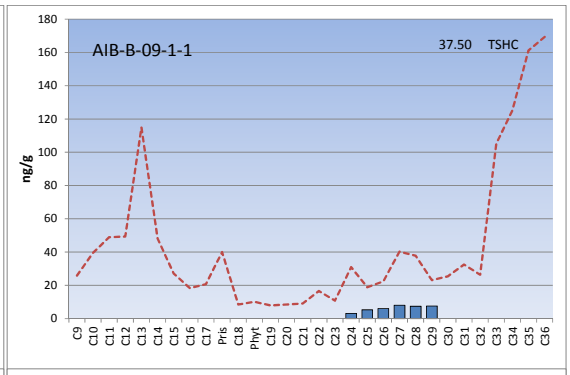
AIB-B-09-1-1
37.50 TSHC
ng/g
C9 C10 C11 C12 C13 C14 C15 C16 C17 Pr5 C18 Phyt C19 C20 C21 C22 C23 C24 C25 C26 C27 C28 C29 C30 C31 C32 C33 C34 C35 C36

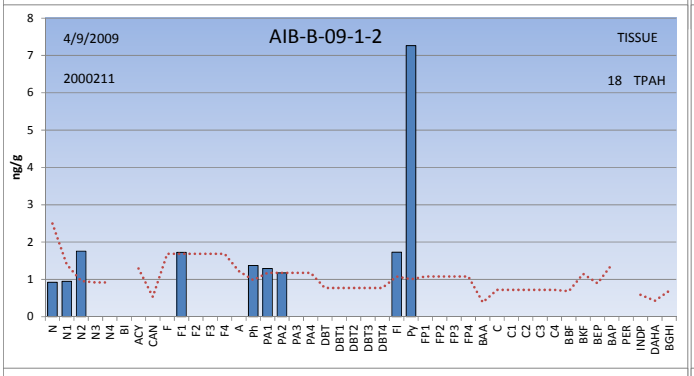
4/9/2009
AIB-B-09-1-2
TISSUE
2000211
18 TPAH
ng/g
N N1 N2 N3 N4 BI ACY CAN F F1 F2 F3 F4 A Ph PA1 PA2 PA3 PA4 DBT DBT1 DBT2 DBT3 DBT4 FI Py FP1 FP2 FP3 FP4 BAA C C1 C2 C3 C4 BBF BKF BEP BAP PER INDP DAHA BGHI

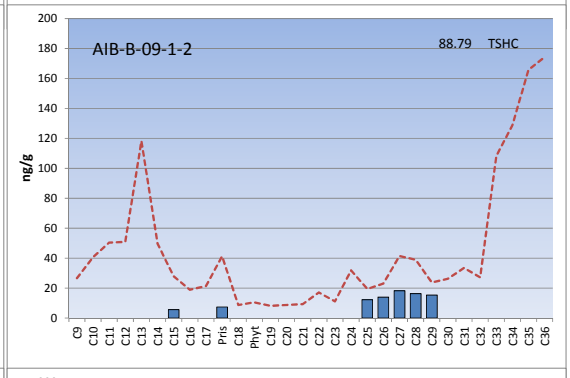
AIB-B-09-1-2
88.79 TSHC
ng/g
C9 C10 C11 C12 C13 C14 C15 C16 C17 Pr5 C18 Phyt C19 C20 C21 C22 C23 C24 C25 C26 C27 C28 C29 C30 C31 C32 C33 C34 C35 C36

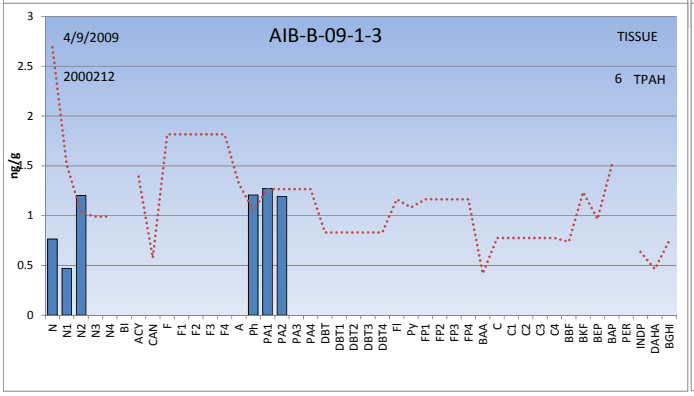
4/9/2009
AIB-B-09-1-3
TISSUE
2000212
6 TPAH
ng/g
N N1 N2 N3 N4 BI ACY CAN F F1 F2 F3 F4 A Ph PA1 PA2 PA3 PA4 DBT DBT1 DBT2 DBT3 DBT4 FI Py FP1 FP2 FP3 FP4 BAA C C1 C2 C3 C4 BBF BKF BEP BAP PER INDP DAHA BGHI

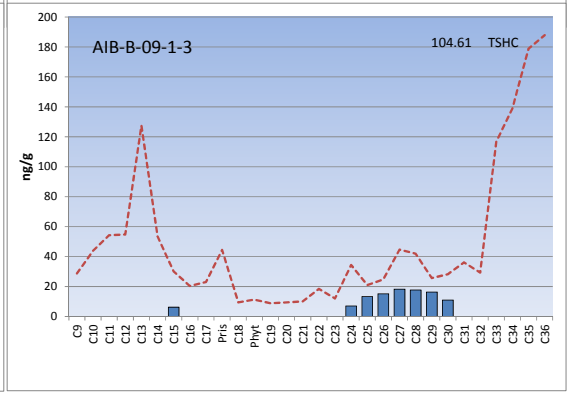
AIB-B-09-1-3
104.61 TSHC
ng/g
C9 C10 C11 C12 C13 C14 C15 C16 C17 Pr5 C18 Phyt C19 C20 C21 C22 C23 C24 C25 C26 C27 C28 C29 C30 C31 C32 C33 C34 C35 C36

481

WINDY BAY--WIB

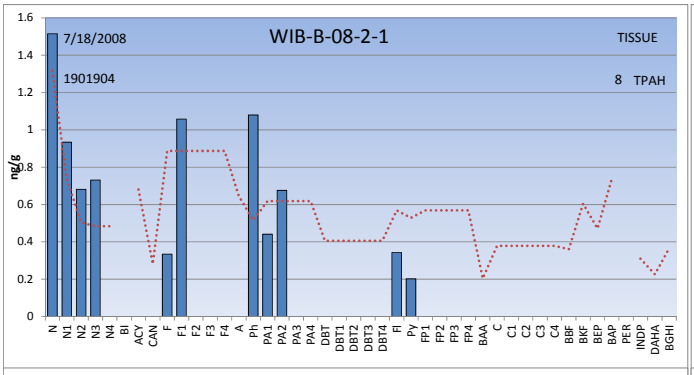

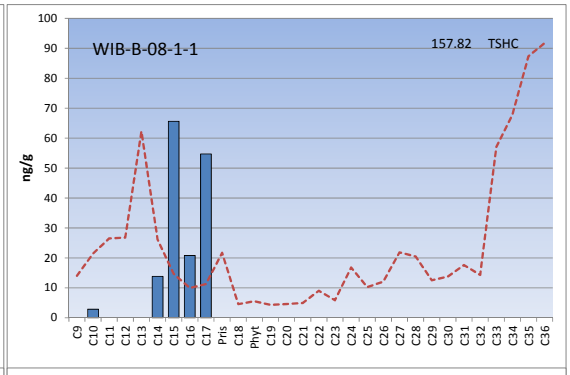

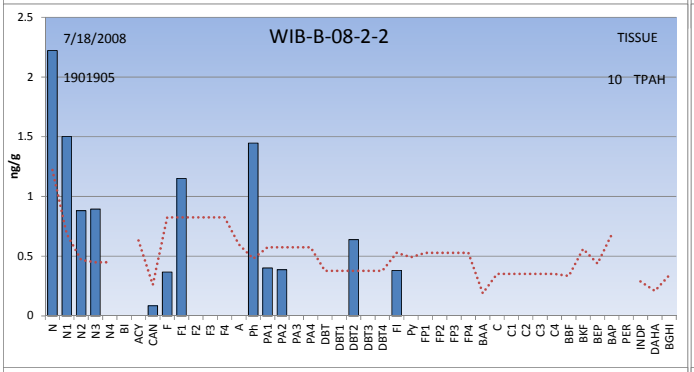

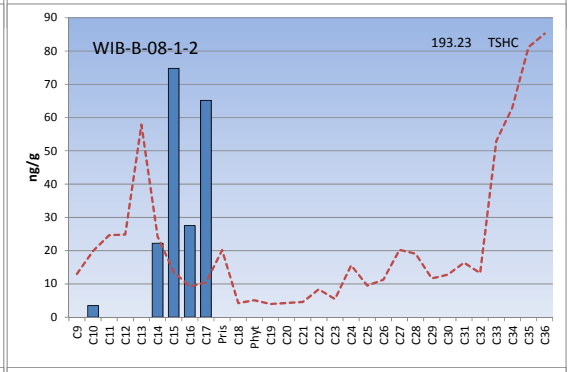

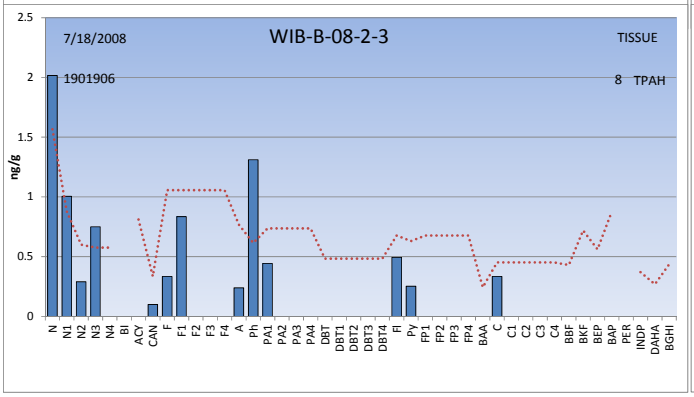

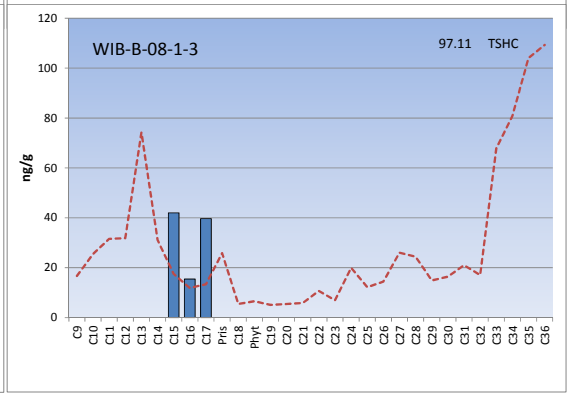

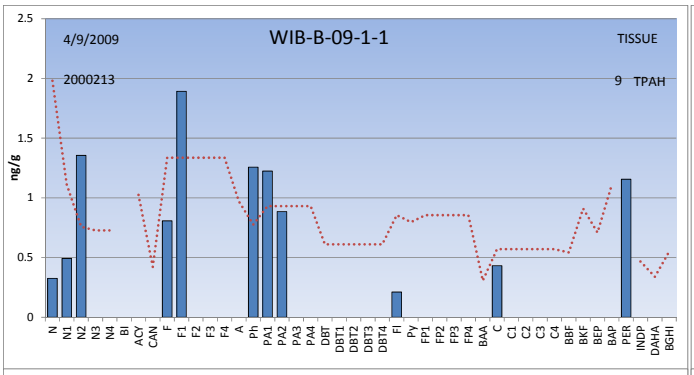
4/9/2009
WIB-B-09-1-1
TISSUE
2000213
9 TPAH
ng/g

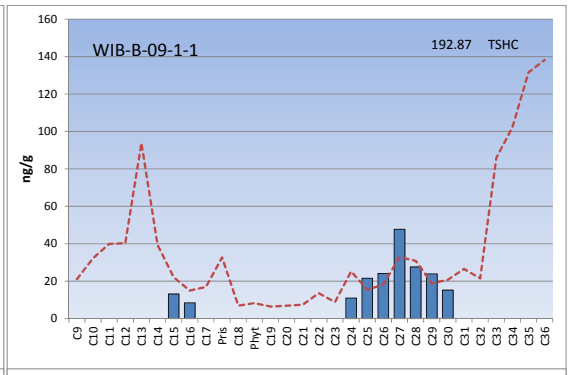
WIB-B-09-1-1
192.87 TSHC
ng/g

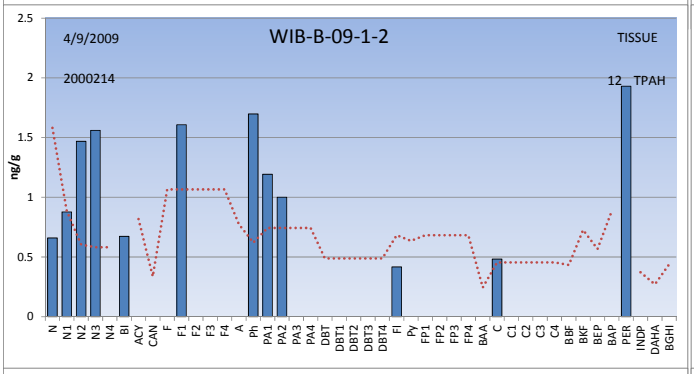
4/9/2009
WIB-B-09-1-2
TISSUE
2000214
12 TPAH
ng/g

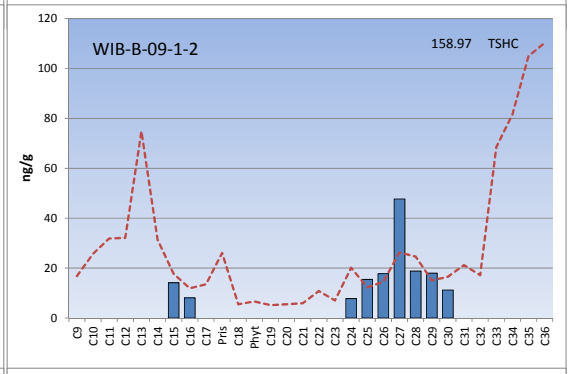
WIB-B-09-1-2
158.97 TSHC
ng/g

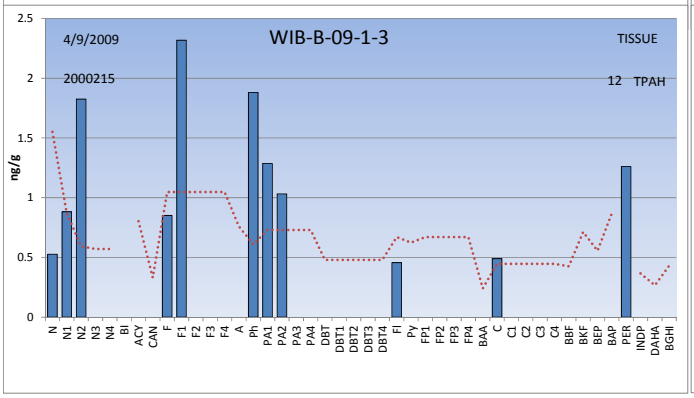
4/9/2009
WIB-B-09-1-3
TISSUE
2000215
12 TPAH
ng/g

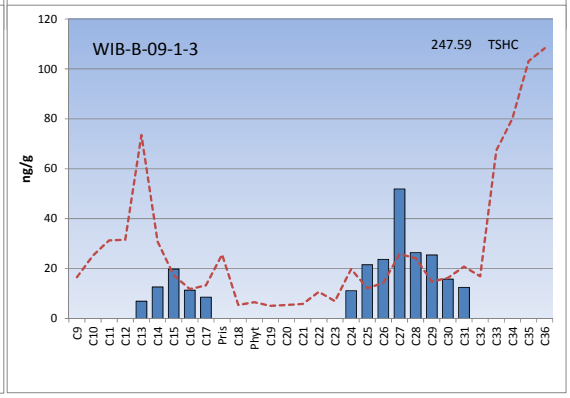
WIB-B-09-1-3
247.59 TSHC
ng/g

484

SHUYAK HARBOR--SHH

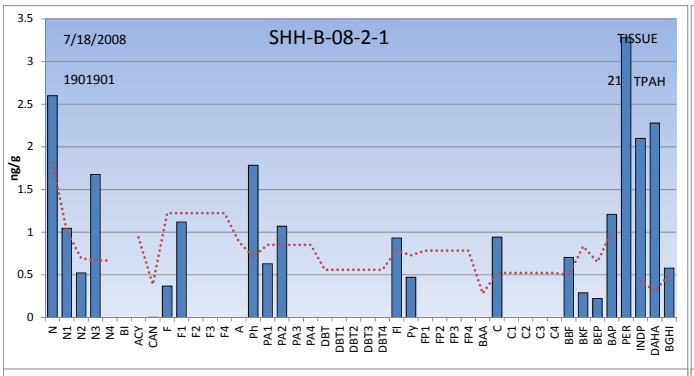

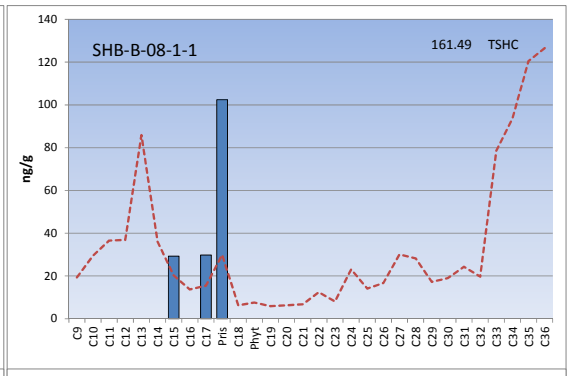

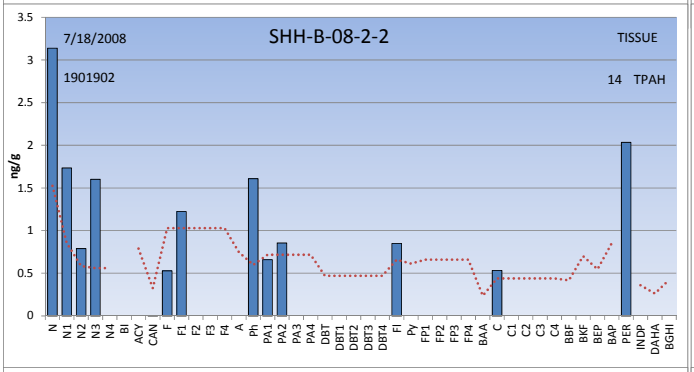

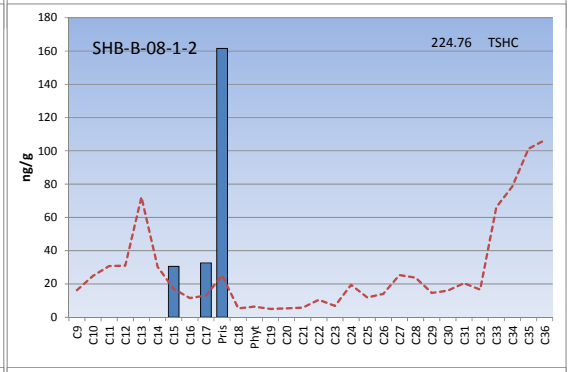

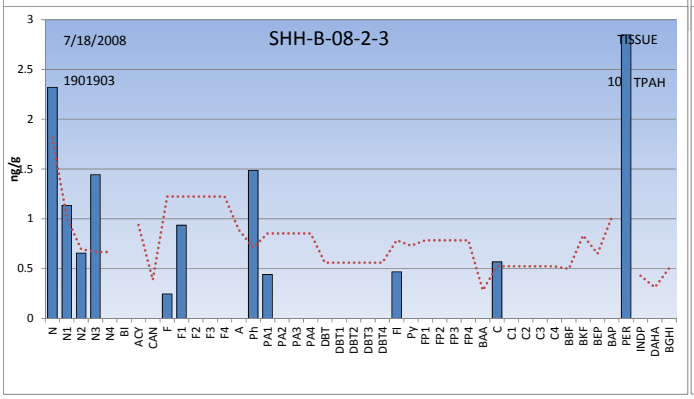

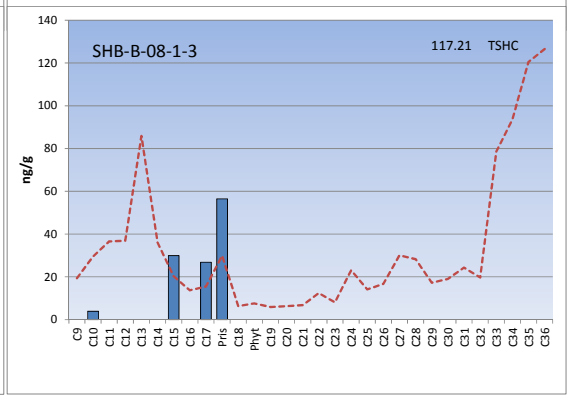

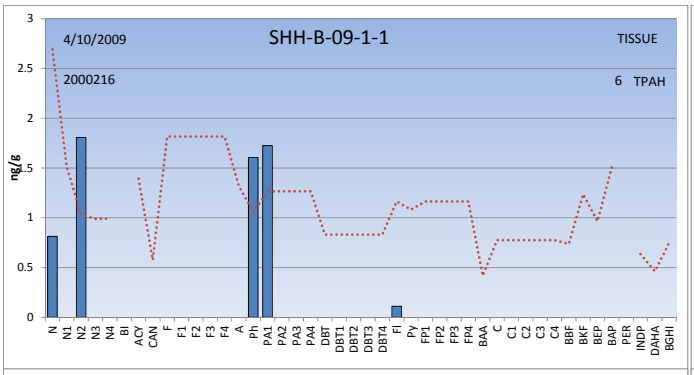
4/10/2009
SHH-B-09-1-1
TISSUE
2000216
6 TPAH
ng/g
N N1 N2 N3 N4 BI ACY CAN F F1 F2 F3 F4 A Ph PA1 PA2 PA3 PA4 DBT DBT1 DBT2 DBT3 DBT4 FI Py FP1 FP2 FP3 FP4 BAA C C1 C2 C3 C4 BBF BKF BEP BAP PER INDP DAHA BGHI

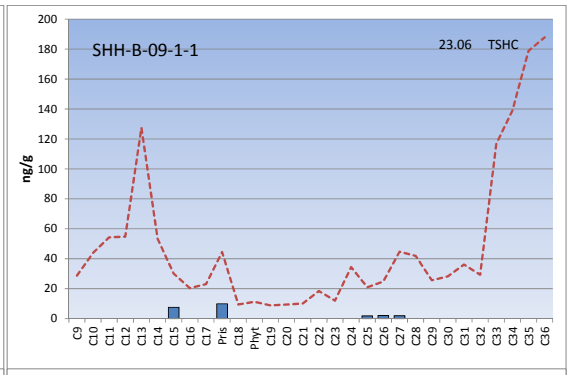
SHH-B-09-1-1
23.06 TSHC
ng/g
C9 C10 C11 C12 C13 C14 C15 C16 C17 Pr16 C18 Phyt C19 C20 C21 C22 C23 C24 C25 C26 C27 C28 C29 C30 C31 C32 C33 C34 C35 C36

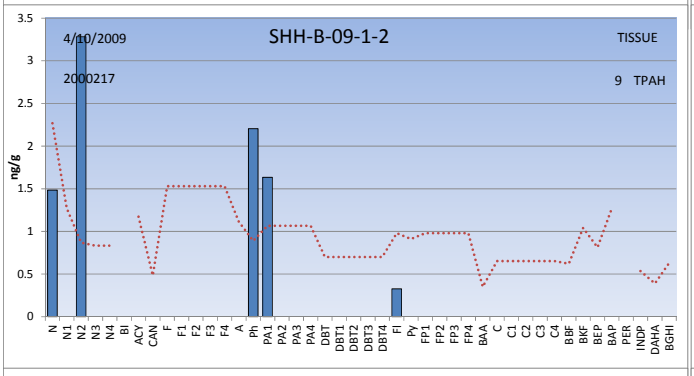
4/10/2009
SHH-B-09-1-2
TISSUE
2000217
9 TPAH
ng/g
N N1 N2 N3 N4 BI ACY CAN F F1 F2 F3 F4 A Ph PA1 PA2 PA3 PA4 DBT DBT1 DBT2 DBT3 DBT4 FI Py FP1 FP2 FP3 FP4 BAA C C1 C2 C3 C4 BBF BKF BEP BAP PER INDP DAHA BGHI

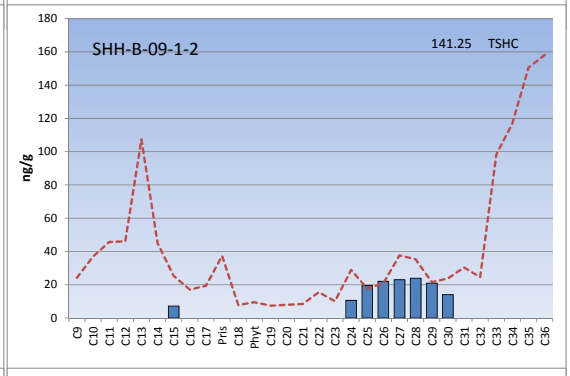
SHH-B-09-1-2
141.25 TSHC
ng/g
C9 C10 C11 C12 C13 C14 C15 C16 C17 Pr15 C18 Phyt C19 C20 C21 C22 C23 C24 C25 C26 C27 C28 C29 C30 C31 C32 C33 C34 C35 C36

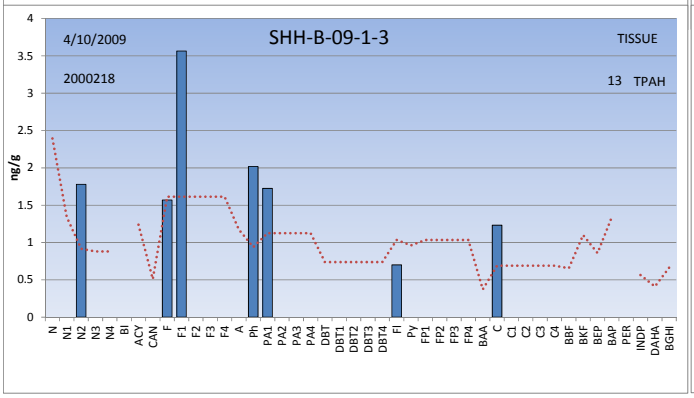
4/10/2009
SHH-B-09-1-3
TISSUE
2000218
13 TPAH
ng/g
N N1 N2 N3 N4 BI ACY CAN F F1 F2 F3 F4 A Ph PA1 PA2 PA3 PA4 DBT DBT1 DBT2 DBT3 DBT4 FI Py FP1 FP2 FP3 FP4 BAA C C1 C2 C3 C4 BBF BKF BEP BAP PER INDP DAHA BGHI

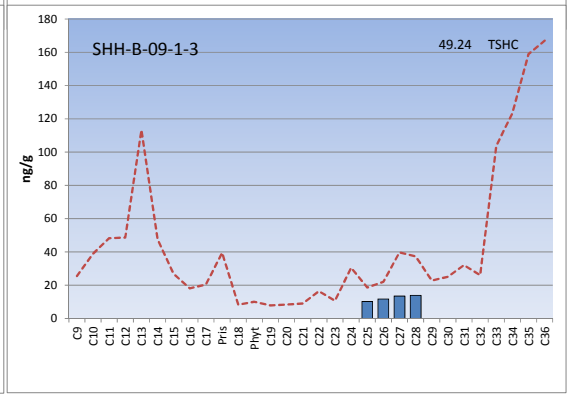
SHH-B-09-1-3
49.24 TSHC
ng/g
C9 C10 C11 C12 C13 C14 C15 C16 C17 Pr15 C18 Phyt C19 C20 C21 C22 C23 C24 C25 C26 C27 C28 C29 C30 C31 C32 C33 C34 C35 C36

487

APPENDIX 2 – BIOMARKER PLOTS

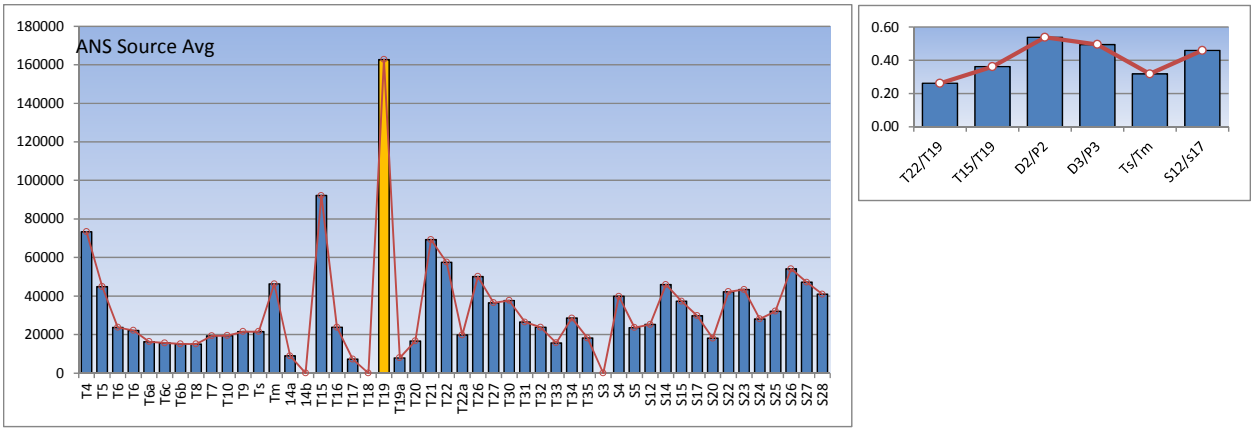

Quantified biomarkers for ABL's EVOS-era ANS reference oil (left). Hopane highlighted with gold fill. Selected diagnostic ratios (right). Red line in both plots represents ANS reference values, here matching the source sample values.

This section of the appendix contains the quantified biomarker plots and diagnostic ratios for all sediment samples from AMT and GOC 2011-2012. In each plot, the red line denotes ANS reference oil. In the left plots, the ANS profile is normalized to each sample's C30 hopane (T19).

ALYESKA MARINE TERMINAL--AMT JULY 2011

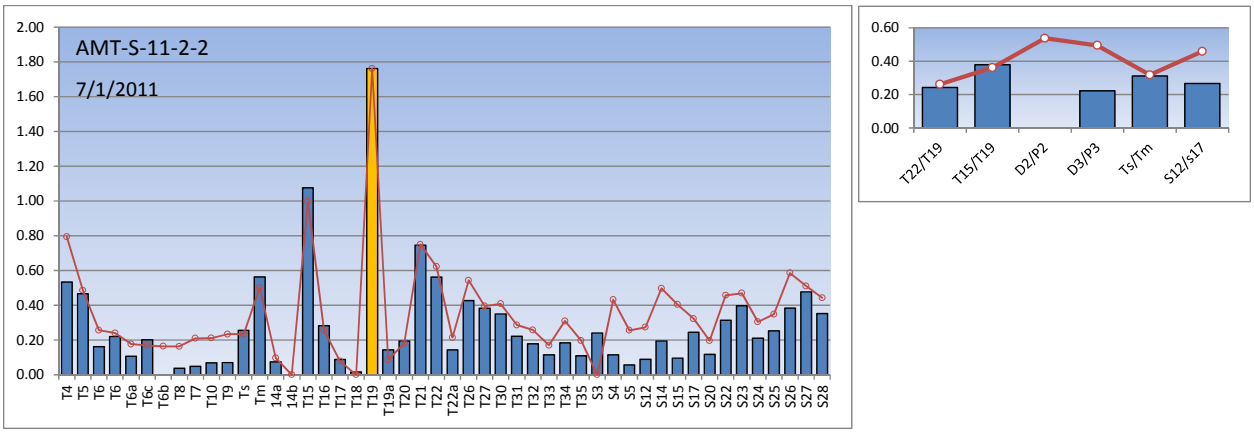

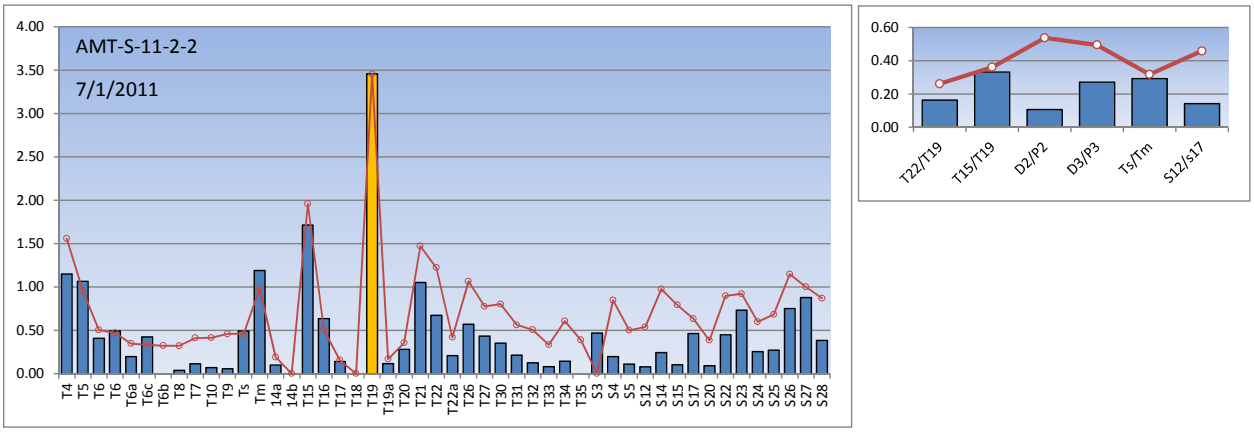

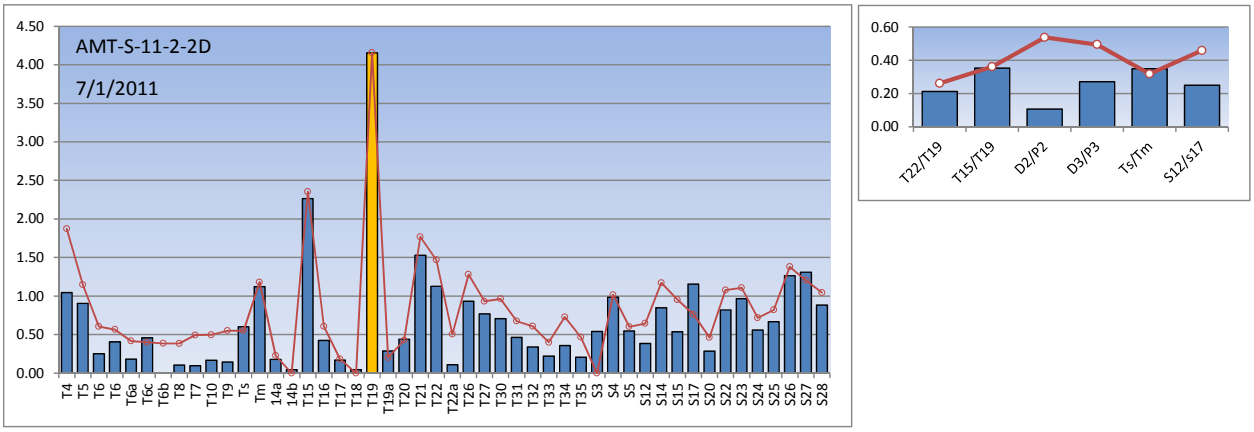

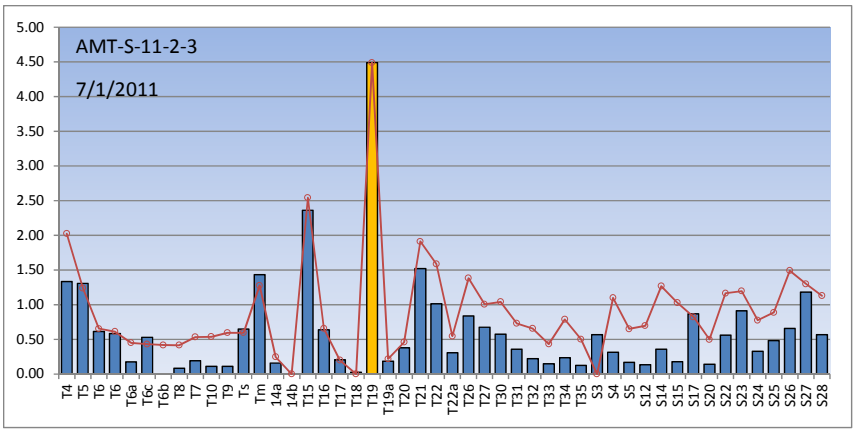

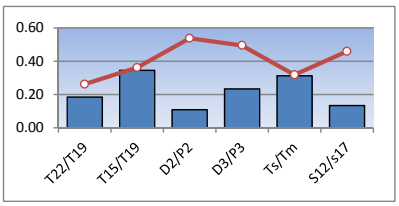

500

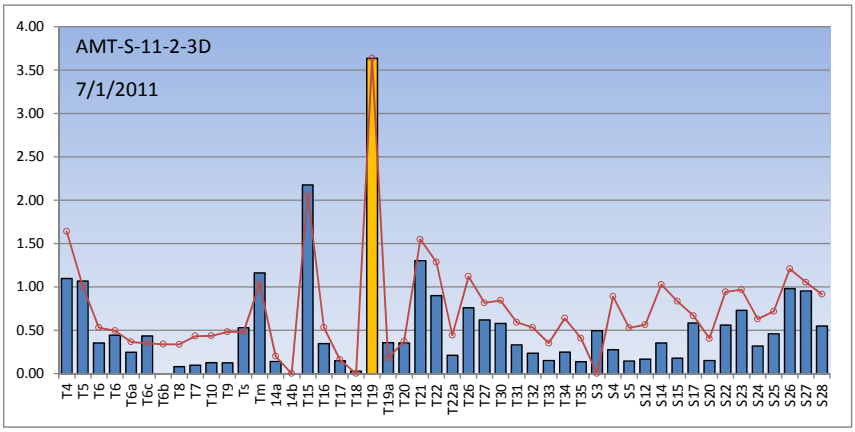

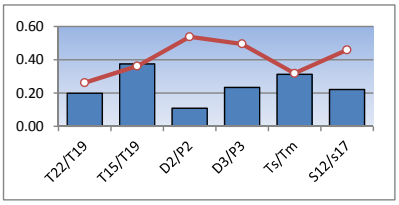

501

502 GOLD CREEK--GOC JULY 2011

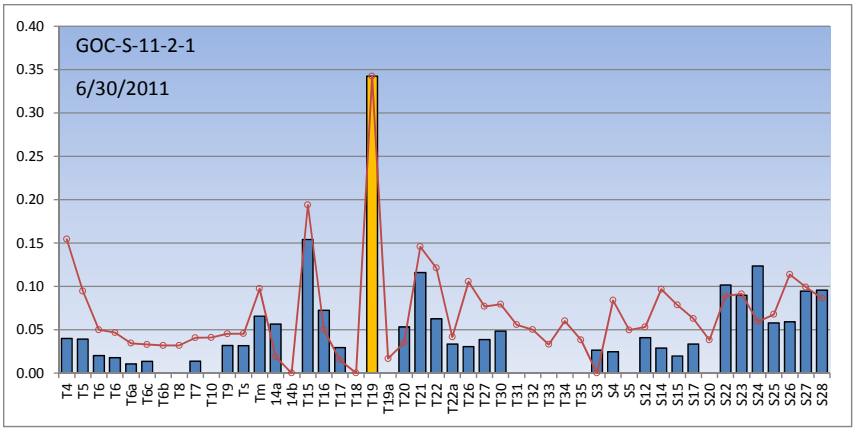

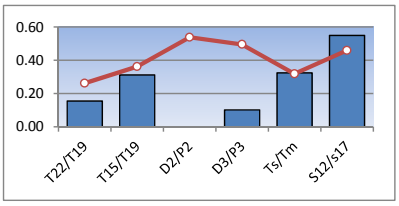

503

504

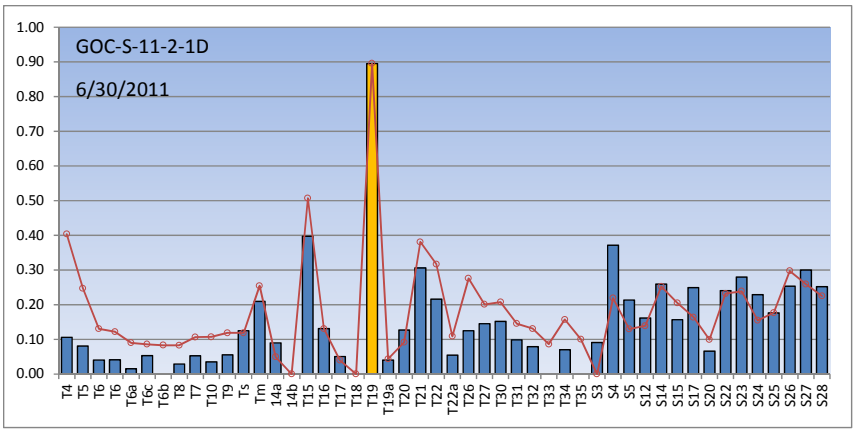
GOC-S-11-2-1D
6/30/2011
1.00
0.90
0.80
0.70
0.60
0.50
0.40
0.30
0.20
0.10
0.00
T4 T5 T6 T6 T6a T6c T6b T8 T7 T10 T9 Ts Tm 14a 14b T15 T16 T17 T18 T19 T19a T20 T21 T22 T22a T26 T27 T30 T31 T32 T33 T34 T35 S3 S4 S5 S12 S14 S15 S17 S20 S22 S23 S24 S25 S26 S27 S28

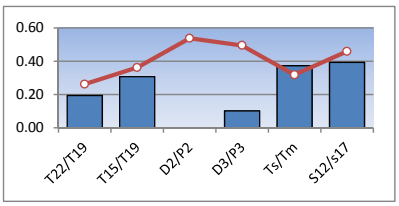
0.60
0.40
0.20
0.00
T22/T19 T15/T19 D2/P2 D3/P3 Ts/Tm S12/s17

505

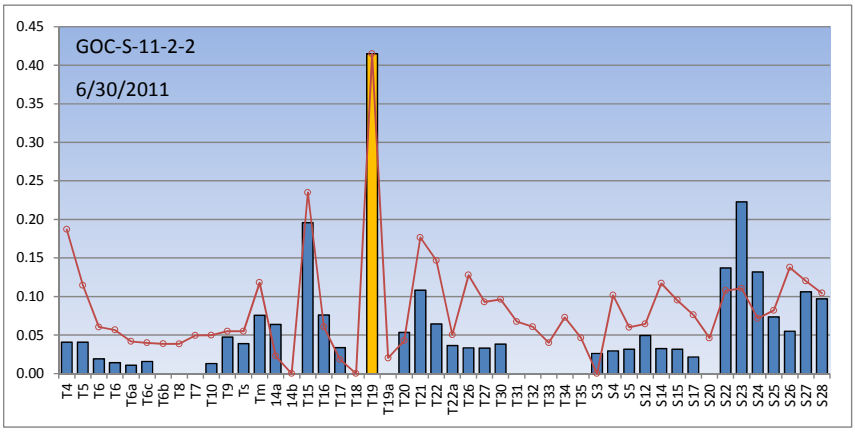
GOC-S-11-2-2
6/30/2011
0.45
0.40
0.35
0.30
0.25
0.20
0.15
0.10
0.05
0.00
T4 T5 T6 T6 T6a T6c T6b T8 T7 T10 T9 Ts Tm 14a 14b T15 T16 T17 T18 T19 T19a T20 T21 T22 T22a T26 T27 T30 T31 T32 T33 T34 T35 S3 S4 S5 S12 S14 S15 S17 S20 S22 S23 S24 S25 S26 S27 S28

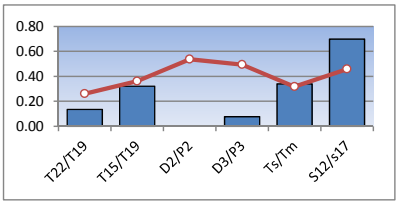
0.80
0.60
0.40
0.20
0.00
T22/T19 T15/T19 D2/P2 D3/P3 Ts/Tm S12/s17

506

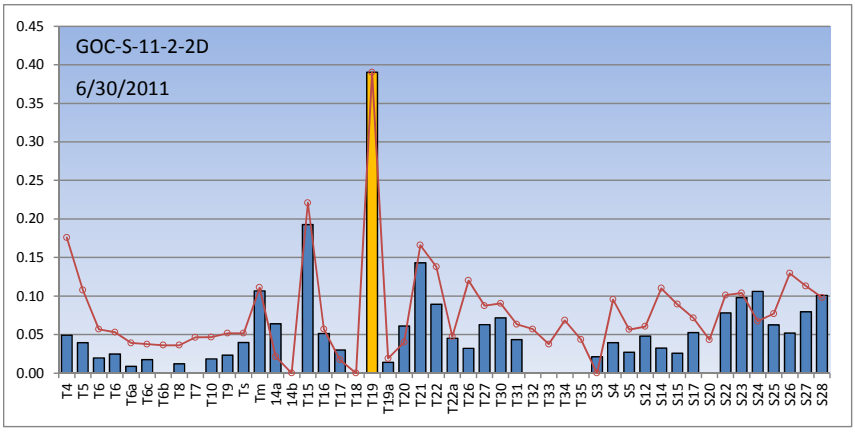
GOC-S-11-2-2D
6/30/2011
0.45
0.40
0.35
0.30
0.25
0.20
0.15
0.10
0.05
0.00
T4 T5 T6 T6 T6a T6c T6b T8 T7 T10 T9 Ts Tm 14a 14b T15 T16 T17 T18 T19 T19a T20 T21 T22 T22a T26 T27 T30 T31 T32 T33 T34 T35 S3 S4 S5 S12 S14 S15 S17 S20 S22 S23 S24 S25 S26 S27 S28

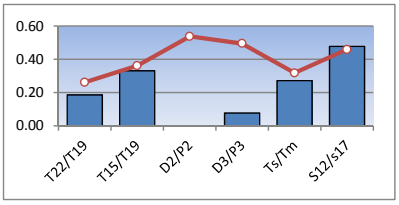
0.60
0.40
0.20
0.00
T22/T19 T15/T19 D2/P2 D3/P3 Ts/Tm S12/s17

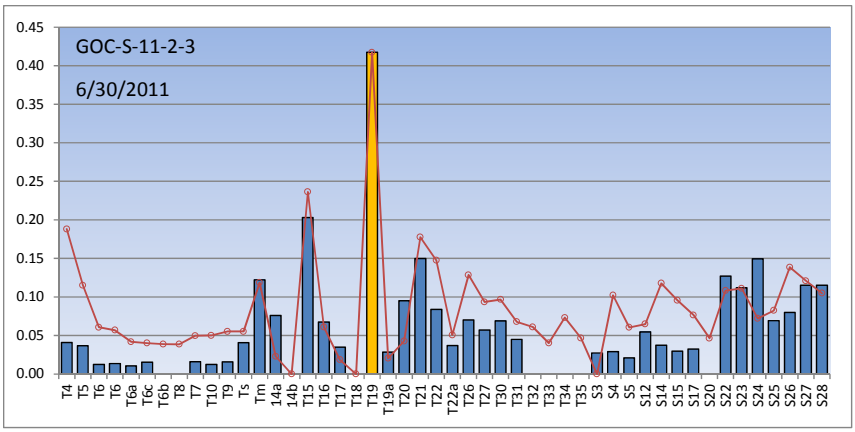

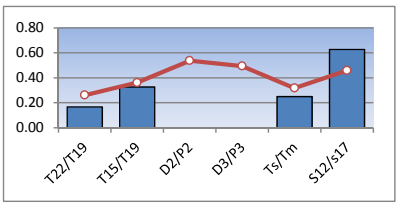

507

508 ALYESKA MARINE TERMINAL--AMT JULY 2012

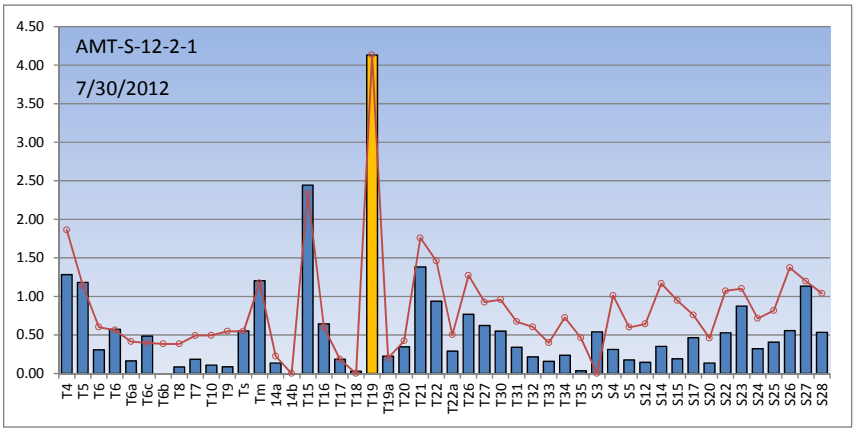

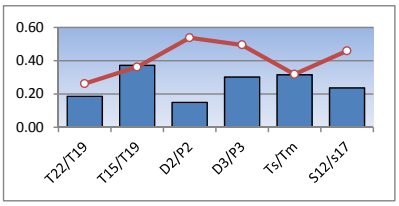

509

510

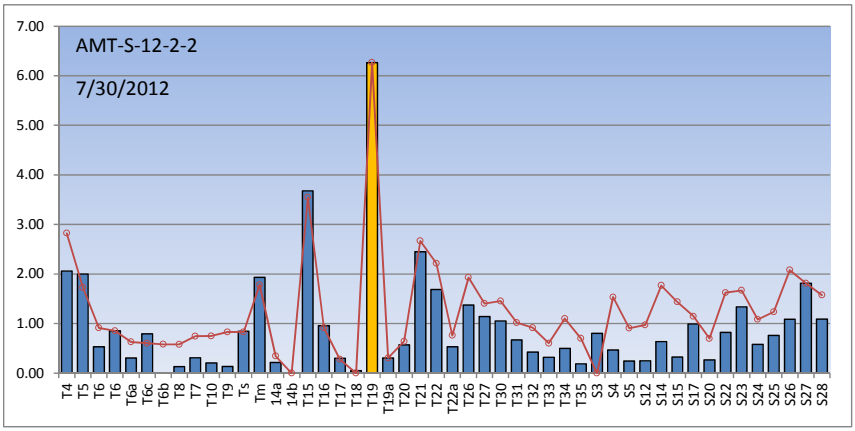

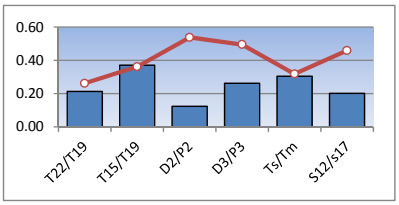

511

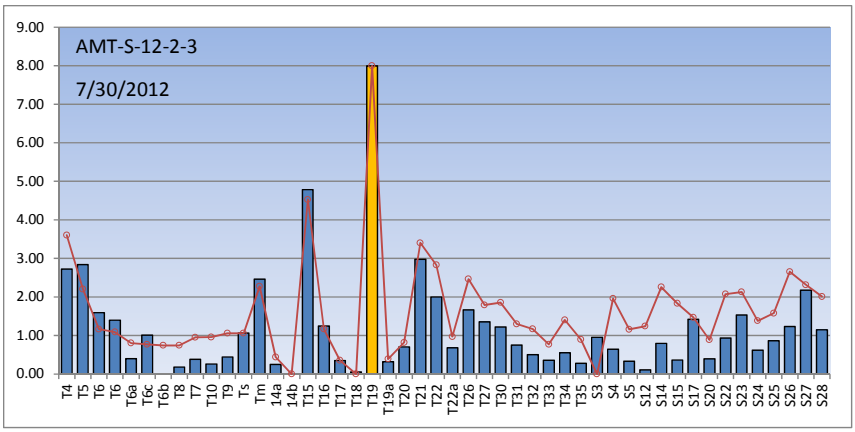

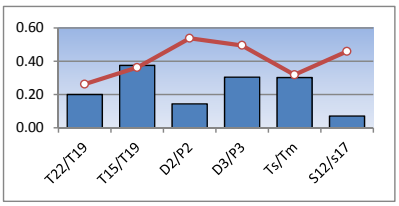

512

513 GOLD CREEK--GOC JULY 2012

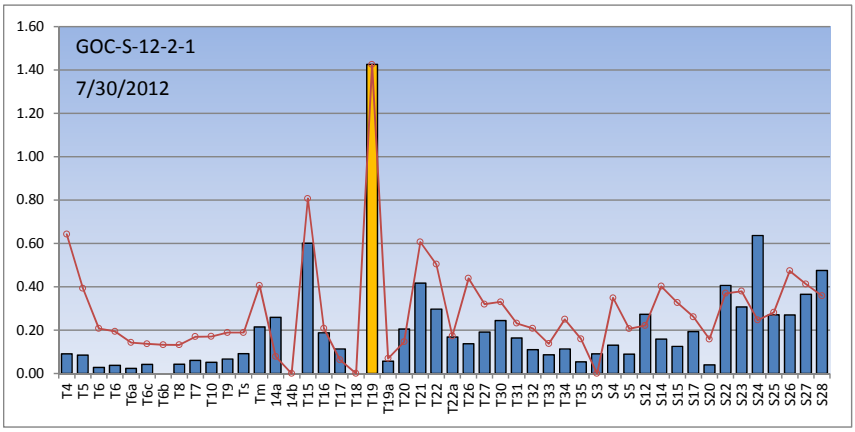

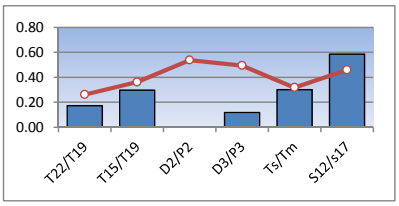

514

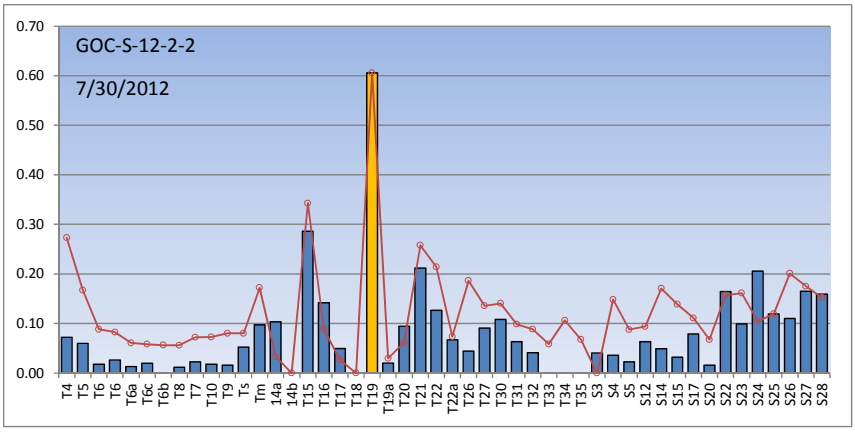

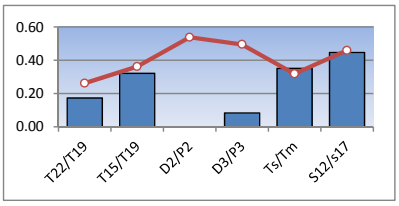

515

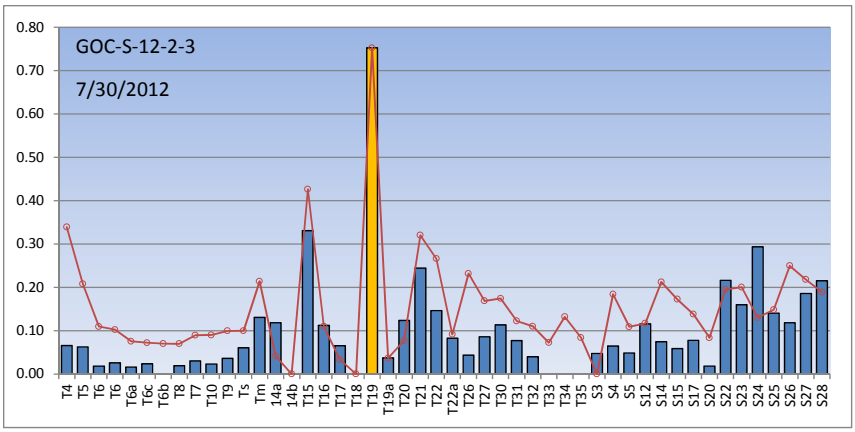
GOC-S-12-2-3
7/30/2012
0.80
0.70
0.60
0.50
0.40
0.30
0.20
0.10
0.00
T4 T5 T6 T6 T6a T6c T6b T8 T7 T10 T9 Ts Tm 14a 14b T15 T16 T17 T18 T19 T19a T20 T21 T22 T22a T26 T27 T30 T31 T32 T33 T34 T35 S3 S4 S5 S12 S14 S15 S17 S20 S22 S23 S24 S25 S26 S27 S28

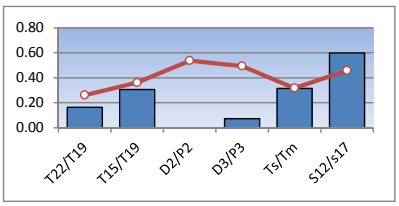
0.80
0.60
0.40
0.20
0.00
T22/T19
T15/T19
D2/P2
D3/P3
Ts/Tm
S12/s17

516

APPENDIX 3 – LTEMP PAH INTERPRETATION USING MULTIVARIATE SCORING METHODS

Preliminary report of LTEMP data, 2008 – 2012

Mark Carls, Auke Bay Laboratory, NMFS

Summary

Using nonparametric and multivariate methods described in Carls, 2006, oil is evident in Alyeska sediment based on PAH and alkanes. Hydrocarbons from the ballast treatment facility were not detected in tissues at any site. However, hydrocarbons from a probable diesel spill in 2008 were detected in tissue at Gold Creek (PAH only). There was also a hint of the diesel spill in sediment from Gold Creek – but only if it represents the dissolved fraction. Quality control samples were generally clean.

Water (rinsate) samples

PAH

Controls generally looked fine; TPAH range 0.3 to 21.4 ng.

Many PAHs in rinsate were below MDL

Alkanes

Calibrated alkanes were generally not detected in control samples

Alkane patterns are unusual in the last five samples collected (20111613, 20111620, 20120822-24); there was no discernible pattern, thus this is likely an artifact. Alkanes were generally not detected in these samples but C16, C18, and C25 alkanes were present.

Two samples (20100319-20) had distinct alkane patterns, C25-C32 and C22-C34 alkanes were present with no obvious odd-even preference

Sediment: PAH

TPAH concentration was least in blanks, intermediate at Gold Creek and highest at Alyeska (P_{ANOVA} = 0.000). There is a high outlier at Gold Creek and a low outlier at Alyeska. Nearly all detected analytes were above MDL in sediment.

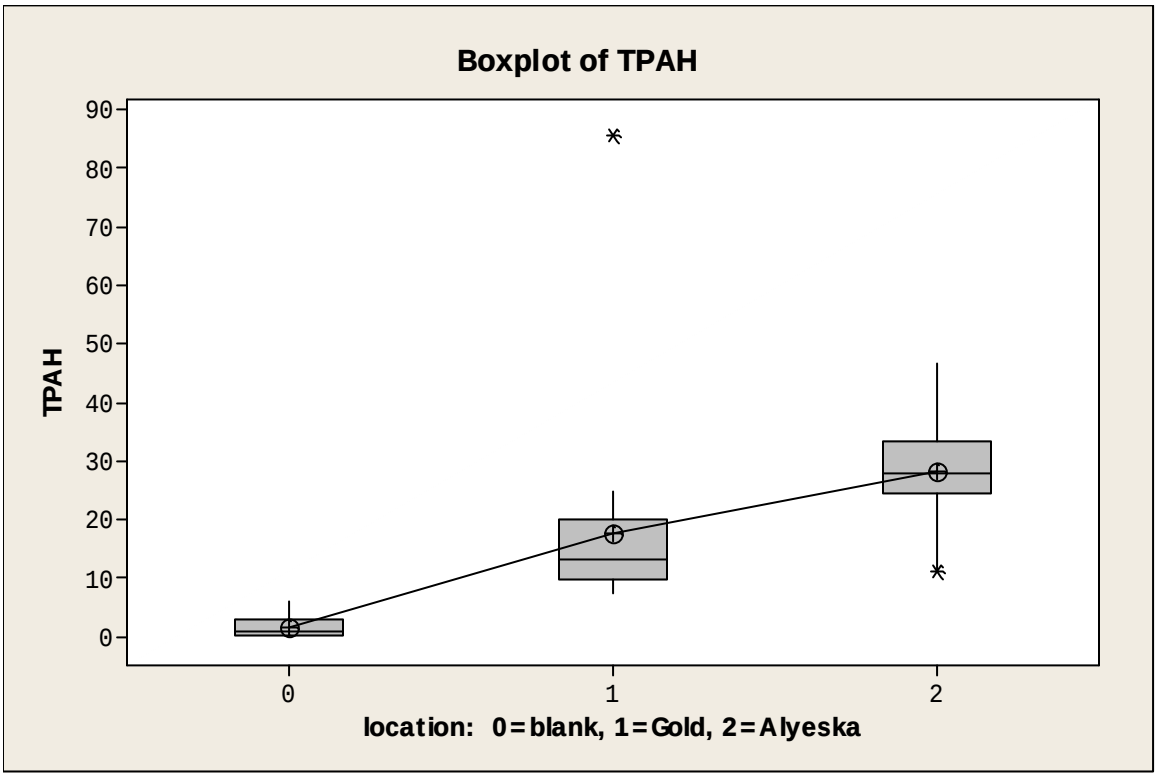

Alyeska Marine Terminal

Complex signal; weathering often estimable. The PAH source model finds oil sometimes – but signal is mixed and balance may be shifting towards more pyrogenic.

Gold Creek

Signal is consistently pyrogenic. The outlier concentration may have been caused by a diesel spill at Gold Creek about the time of sample collection (July 2008) but only if it represents the dissolved fraction because composition is pyrogenic.

All three locations were distinguishable by normalized PAH composition with principal components analysis. The blanks were completely separated (green triangles). The signal at Alyeska approached that at Gold Creek in some samples and was different in others, forming a gradient. This gradient (at Alyeska) is explained at least in part by weathering, a result consistent with weathering oil at other locations, such as Unalaska Island in the Aleutians (C1 is correlated with percent chrysenes, for example; percent chrysenes is a surrogate for weathering: r = 0.74).

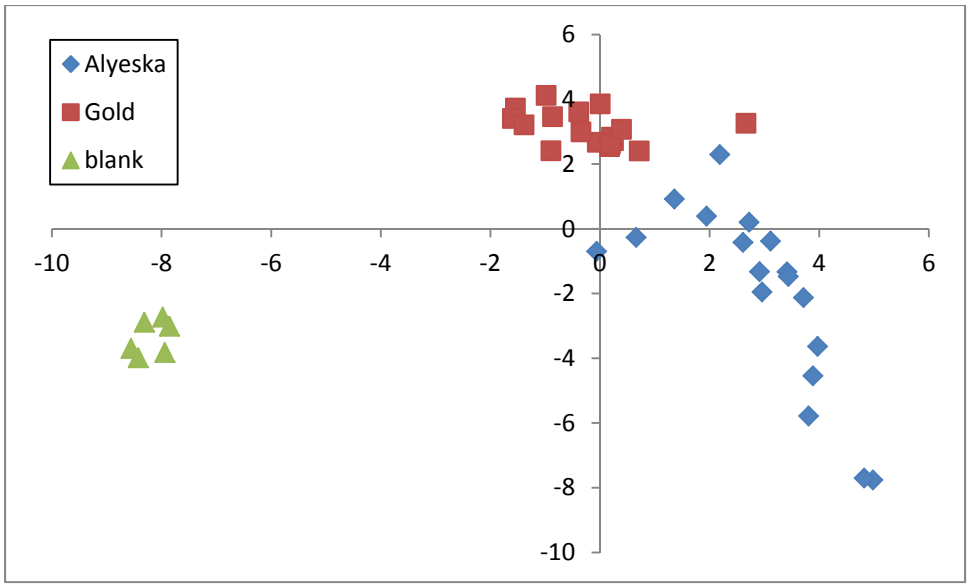

PCA results; x-axis is the first component, y-axis is the second component; these explain 61% of the variance

One sample from Gold Creek is separated from all other Gold Creek sediment samples in PCA space; it is the sample with an unusually high TPAH concentration at this site and may be contaminated with fuel oil. However, its PAH source score was -6.0, i.e., 100% pyrogenic. The only way this sample could represent oil is if it were the water-washed fraction. This merits more discussion.

Sediment, alkanes

Alkane and calibrated alkane concentrations were least in blanks, intermediate at Gold Creek and highest at Alyeska (P_{ANOVA} = 0.000). This result is consistent with the PAH pattern. Variance is greatest at the site most likely to be oiled (Alyeska); this is consistent with a range of samples, some clean, some contaminated. Most detected alkanes in sediment were above MDL.

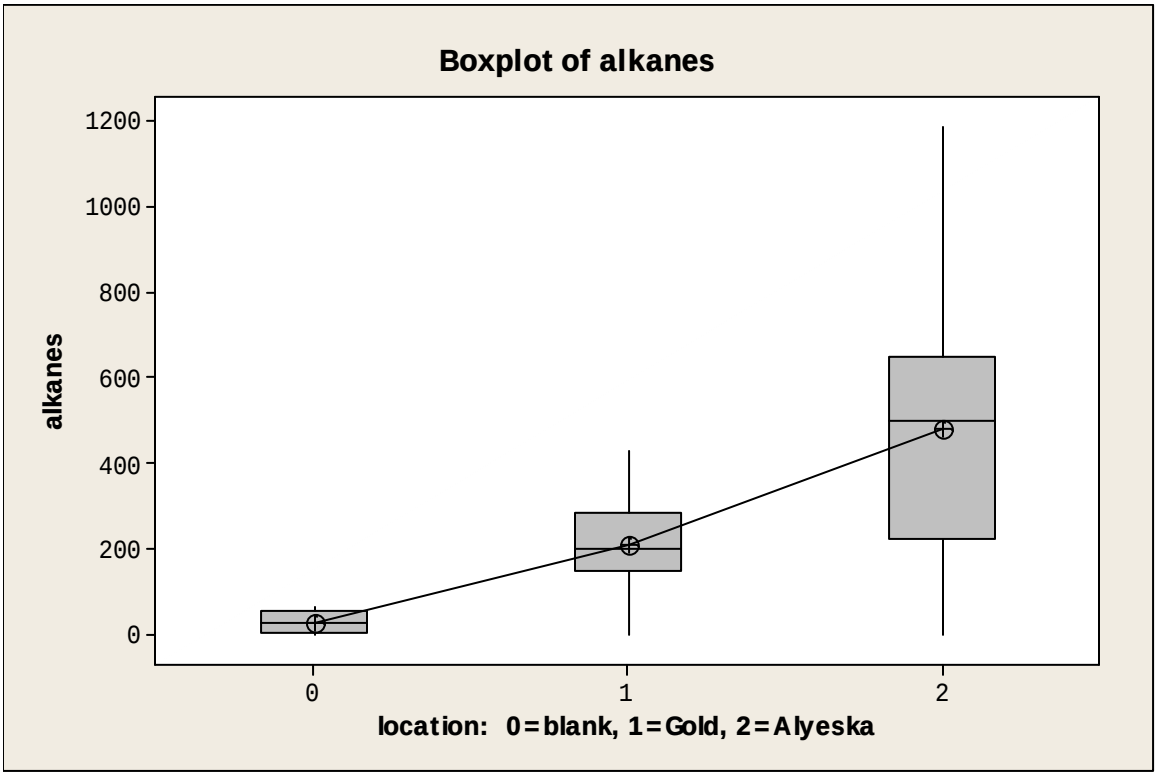

All three locations were distinguishable by normalized alkane composition with principal components analysis, consistent with the PAH PCA. The blanks were completely separated (green triangles). The signal at Alyeska approached that at Gold Creek in some samples and was different in others, forming a gradient.

573

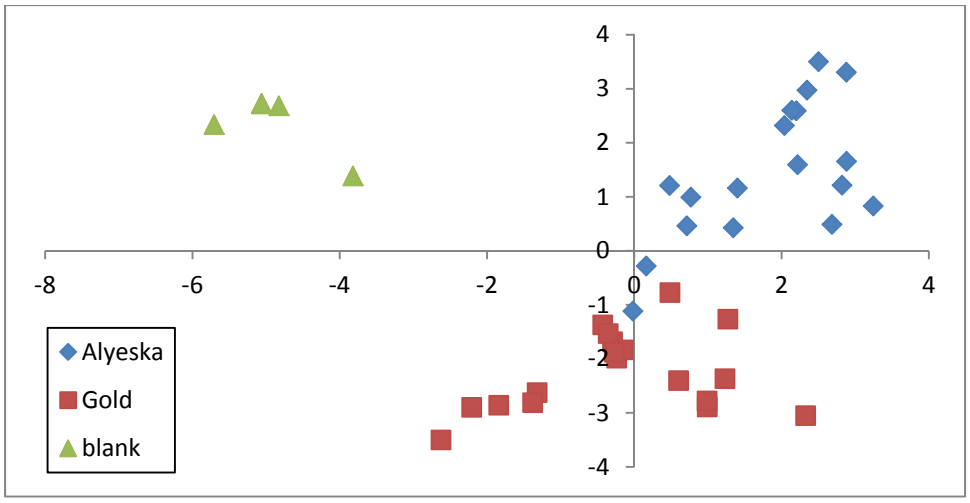

574

575 *PCA results; x-axis is the first component, y-axis is the second component; these explain 43% of the variance*

576

Tissue, PAH

PAH source modeling generally yielded mixed results (with both petrogenic and pyrogenic characteristics). Composition of PAH in tissue at the three sites monitored through 2012 closely overlapped except for three unusual Gold Creek samples and perhaps two Alyeska samples (see figure below). The general absence of separation suggests that most mussels did not accumulate petroleum hydrocarbons, or at least not in detectable quantities, but there were three notable exceptions. PAH concentrations in tissue were often below MDL.

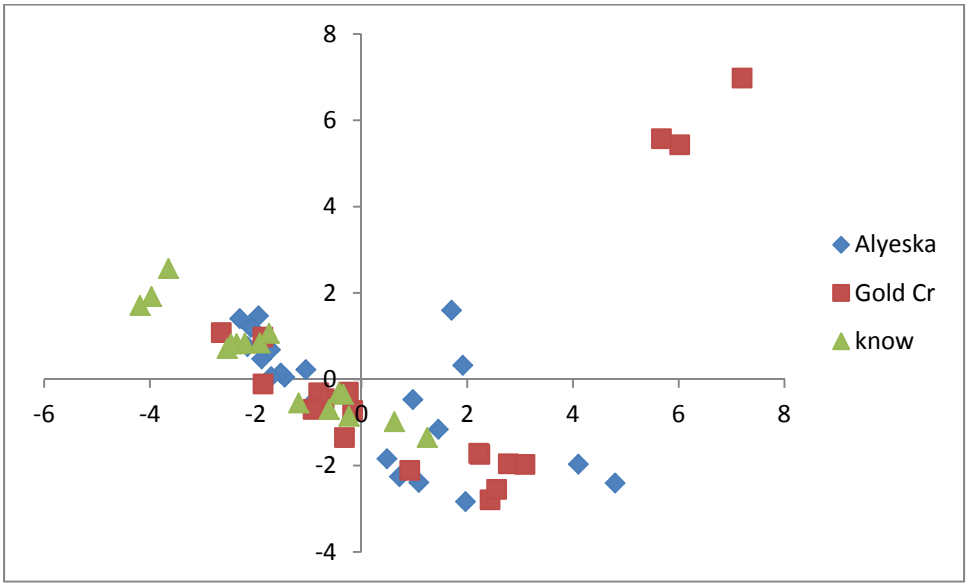

PCA results; x-axis is the first component, y-axis is the second component; these explain 38% of the variance

The three unusual Gold Creek tissues, collected in July 2008, had markedly different PAH source model scores (1.9) than all other Gold Creek samples (-0.5 to 1.0). They had significant dibenzothiophene concentrations, unlike the other Gold Creek tissues. Total PAH concentrations in the unusual samples were among the highest at this site. This is consistent with a diesel oil spill reported about this time (Payne et al. 2006; 2008).

The three unusual Gold Creek samples suggest where oiled tissue might fall in PCA space. Only two other tissue samples, both from Alyeska, had a proclivity in this direction. Their PAH source model scores, TPAH concentrations, and proportions of naphthalenes, fluorenes, dibenzothiophenes, phenanthrenes, fluoranthene/pyrenes, and chrysenes were within the range of other scores at Alyeska hence there were no obvious reasons to identify them as oiled.

Bottom line; most tissues do not have evidence of petroleum hydrocarbons. The exceptions were associated with a diesel spill.

Tissue, alkanes

Composition of alkanes in tissue at the three sites monitored through 2012 closely overlapped except for two unusual clusters (circled groupings in figure below). Most detected alkane concentrations in tissue were above MDL.

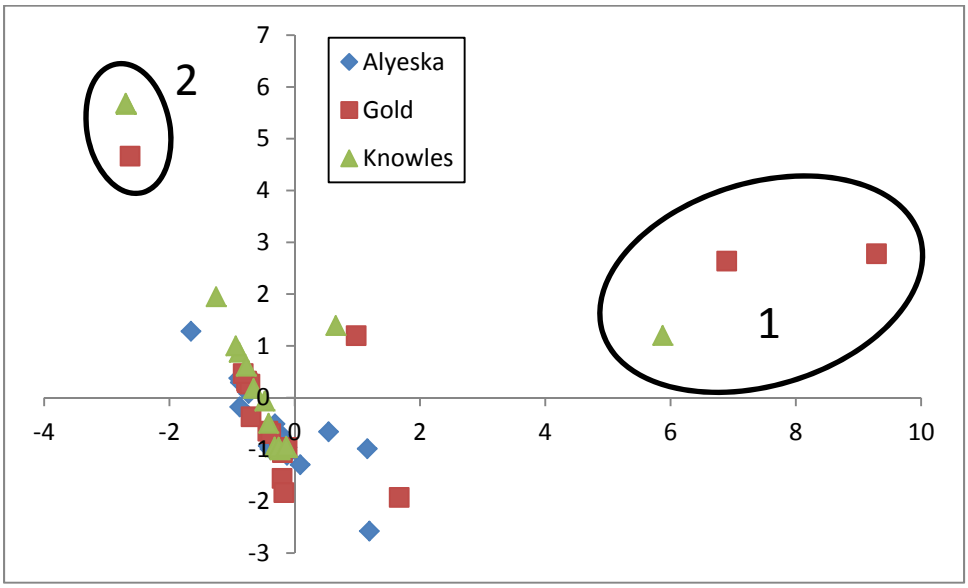

PCA results; x-axis is the first component, y-axis is the second component; these explain 37% of the variance

The exceptional alkane tissues in cluster 1 (lower right-hand quadrant) did not correspond to exceptional PAH composition. The two unusual Gold Creek tissues and single Knowles head tissue may be due to unusual approximately C_{23}-C_{29} alkanes generally not present in tissue at these sites. However, these mid-range alkanes were present in some tissues collected elsewhere and the same pattern occurred in a couple rinsate samples.

Exceptional tissue samples in cluster 2 (upper left-hand quadrant) are not consistent with oil. It contains a Gold Creek sample collected in July 2008 (1902002; post-diesel spill) but does not have an alkane pattern consistent with oil (only C_{14} –C_{16} biogenic alkanes were detected). Likewise, alkane composition in the Knowles Head tissue in cluster 2 has few detected alkanes and does not look like oil.

There is no obvious evidence of odd-even preference indicative of plant waxes.

We conclude that alkane composition does not provide evidence for oil contamination in tissue.